Budapest University of Technology and Economics

Department of Polymer Engineering

DEVELOPMENT OF CYCLIC BUTYLENE TEREPHTHALATE MATRIX COMPOSITES

– PHD THESIS –

Written by: Gábor Balogh

M.Sc. Mechanical Engineer

Supervisor: Dr. Tibor Czigány

Professor

- 2012 -

Nyilatkozat

Alulírott Balogh Gábor kijelentem, hogy ezt a doktori értekezést magam készítettem, és abban csak a megadott forrásokat használtam fel. Minden olyan részt, melyet szó szerint vagy azonos tartalomban, de átfogalmazva más forrásból átvettem, egyértelműen a forrás megadásával jelöltem.

Budapest, 2012. április 10.

Balogh Gábor

Acknowledgements

I would like to express my thanks to my supervisor, Professor Tibor Czigány for his help and support of my work and his guidance towards a deeper scientific way of thinking. Here, I also have to say thank you to my mentor, Pál Szaplonczay, who introduced me the exciting world of the high voltage technology and to Professor József Karger-Kocsis who foreshowed me reactive polyesters. I am grateful to all my colleagues and friends at the Department of Polymer Engineering for their help and the creative atmosphere. I would also like to express my thanks to my students (Márk Móró, Sándor Hajba, István Csákvári) who helped a lot with my work.

I am grateful to Sergiy Grishchuk and Markus Steeg at Institut für Verbundwerkstoffe (Kaiserslautern, Germany) and to Tobias Abt at Centre Català del Plàstic (Terrassa, Spain) for their generous help with regard to my work. I would like to say ‘thank you’ to Thorsten Hartmann (Cyclics Europe GmbH) for the GPC analyses; to Ralf Thomann (Universität Freiburg) for the TEM pictures; to Anton Apostolov for the X-ray spectra; to Balázs Ring for the heat and thermal conductivity examinations. I would like to express my thanks to Cyclics Europe GmbH for providing the necessary CBT160 for my work; to Perstorp Holding AB for supplying the polycaprolactone and to XG Ssciences Inc. for the graphene.

Last, but not least I would like to express my thanks to my family and friends for their unbroken support of my work.

The work reported in this thesis has been developed in the framework of the project "Talent care and cultivation in the scientific workshops of BME" project. This project is supported by the grant TÁMOP - 4.2.2.B-10/1--2010-0009.

This work is connected to the scientific program of the "Development of quality-oriented and harmonized R+D+I strategy and functional model at BME" project. This project is supported by the New Széchenyi Plan (Project ID: TÁMOP-4.2.1/B-09/1/KMR-2010-0002).

Table of contents

List of abbreviations and symbols

Abbreviations

ACSR	Aluminum conductor steel reinforced
AFM	Atomic force microscopy
BPADGE	Brominated bisphenol-A diglycidyl ether
CBT	Cyclic butylene terephthalate
CF	Carbon fiber
CNT	Carbon nanotube
CTE	Coefficient of thermal expansion
DC	Displacement control
DMA	Dynamic mechanical analysis
DSC	Differential scanning calorimetry
FBG	Fiber Bragg grating
FTIR	Fourier transform infrared spectroscopy
GE	General Electrics Corporation
GPC	Gel permeation chromatography
HDT	Heat distortion temperature
HFIP	Hexafluoro-2-propanol
HVTL	High voltage transmission line
IHP	Interval hot press
ILS	Interlaminar shear
IM	Injection molded (specimen)
ISP	In-situ polymerized (specimen)
MDSC	Modulated differential scanning calorimetry
MMT	Montmorillonite
MN	Number average of molecular weight
MP	Peak value of molecular weight
MW	Mean molecular weight
MWCNT	Multiwalled carbon nanotube
NMR	Nuclear magnetic resonance
o-DCB	Ortho-dichlorobenzene
OGTR	Tetrakis(2-ethylhexyl)titanate
PA	Polyamide
PAN	Polyacryl nitrile
PBT	Polybutylene terephtalate
PC	Pressure control
pCBT	Polymerized cyclic butylene terephtalate
PCL	Polycaprolactone
PDMS	Polydimethylsiloxane
PEEK	Polyether ether ketone
PEKK	Polyether ketone ketone
PPS	Polyphenylene sulfide

RIM	Reaction injection molding
ROP	Ring opening polymerization
RTM	Resin transfer molding
SAXS	Small angle X-ray scattering
SEM	Scanning electron microscope
SMA	Shape memory alloy
TBBPA	Tetrabromobisphenol-A
TEM	Transmission electron microscopy
TGA	Thermogravimetry
THF	Tetrahydrofuran
TiN	Titanium Nitride
UD	Unidirectionally aligned
UV	Ultraviolet radiation
VARTM	Vacuum-assisted resin transfer molding
WAXS	Wide-angle X-ray scattering
WGF	Woven glass fabric (reinforced specimen)
XB0, 1, 2 and 3	Experimental batches of CBT
α	Crystalline type of pCBT
β	Crystalline type of pCBT

Symbols

A_{comp}	[mm^2]	Cross section area of the composite in the pultruder
$A_{comp,m}$	[mm^2]	Matrix cross section area of the composite profile
A_{inj}	[mm^2]	Cross section area of the injector
b	[mm]	Specimen thickness
d	[m]	Lamellae distance
E	[J]	Energy
I	[A]	Electrical current
l	[m]	Length
L_{die}	[m]	Pultrusion die length
L_{inj}	[m]	Length of the injector system
n	[-]	Reflexion order (Bragg eq.)
Q	[g/min]	Mass flow
t_{die}	[s]	Time spent inside the pultruder die
T_g	[°C]	Glass transition temperature
T_{imp}	[°C]	Temperature of impregnation
t_{inj}	[s]	Time of injection
T_{inj}	[°C]	Temperature of injection
T_m	[°C]	Melting temperature
t_n	[mm]	Distance between the notches
T_{poly}	[°C]	Temperature of polymerization

t_{total}	[s]	Total time spent in molten state (pultrusion)
U	[V]	Voltage
V	[cm^3]	Volume
V_f	[-]	Fiber volume fraction
v_{inj}	[m/min]	Flow speed in the injector
V_m	[-]	Matrix volume fraction
v_{proc}	[m/min]	Process speed
W_i	[-]	Mass fraction
α_{heat}	[W/mK]	Coefficient of thermal conductivity
α_r	[-]	Primary thermal relaxation
β_r	[-]	Secondary thermal relaxation
ΔH_c	[J]	Crystallization enthalpy
ε	[%]	Deflection
$\dot{\varepsilon}$	[1/s]	Deformation speed
Θ	[°]	Bragg angle
λ	[m]	Wavelength
ρ_f	[g/cm^3]	Density of the fibers
ρ_m	[g/cm^3]	Density of the matrix
ρ_s	[Ohm/cm]	Specific resistivity
σ_c	[S/m]	Conductivity
τ_{din}	[kJ/m^2]	Dynamic interlaminar strength
χ_c	[%]	Crystalline fraction
ω	[rad/s]	Angular velocity

1. Introduction

Nowadays electricity-usage is increasing extremely fast due to globalization, and widespreading of household utilities such as air conditioning devices (Table 1). Production possibilities of this energy is given (by water, gas or nuclear power plants) but transmitting this faces problems – remember the northeastern US blackout in August 2003 which was caused by the obsoleting high voltage transmission lines (HVTL) and their sagging [1].

	Electrical energy consumption [TWh]					
Year	**1990**	**2000**	**2005**	**2009**	**2010**	**2011**
Hungary	35	33	35	37	38	42
European Union	1803	2528	2661	2926	2906	3037
USA	2923	3356	3660	3829	3873	3873
China	580	1014	1630	3428	3438	3503

Table 1. World electrical energy consumption between 1990 and 2011 [2]

The transmission technology utilized nowadays that applies only metallic parts has faced its frontiers because only a given amount of electrical energy can be transferred through a cross section unit due to the temperature rise in the wires (the limit is 80°C) [3]. Another problem is wire sagging between the poles. This phenomenon is caused by thermal expansion and material structure: the wire gets warm and elongate and is capable to deform elastically and as a consequence of this its own weight bends the wire, so it gets closer to the ground. To minimize sag, low pole distances and high poles are utilized. Sagging is to be avoided because a strong electromagnetic field is generated around the wire and if it gets too close to the ground it may cause health problems. According to earlier studies inhabitants living close to HVTLs have problems like leucosis and sleep disorders more likely [4]. A further problem with metallic parts is corrosion due to the presence of water mainly in the inner steel core.

A possible solution for the problems described above is replacing some metal parts with polymeric composite materials. Their main application in HVTLs may be the load-carrying inner core. Suitable composite materials have much higher stiffness-to-weight ratio than steel [5, 6] so sagging would be reduced which results in a reduction in the above mentioned problems.

For high-tech composites nowadays mostly thermosetting materials (generally epoxy resins) are used. Epoxy resins have excellent mechanical properties that make them

suitable for being used as the inner core of a HVTL cable but they are problematic to recycle and tend to micro-crack. Moreover, these resins have to be cured which makes production times longer. To solve these problems a new generation of thermoplastic matrices can be utilized, like the *in-situ* polymerizable cyclic butylene terephtalate (CBT) oligomer system. It is in solid state at room temperature and has water-like melt viscosity (below 0.1 Pas) above its melting point which makes fiber wet-out easy and polymerizes fast among the reinforcing fibers. Since this is a brand new matrix material no industrially applicable processing technology is developed yet. To process CBT new low pressure technologies may be utilized, which consume much less energy than the currently applied thermoplastic processing technologies. Composite materials with this new CBT matrix are capable to replace the conventional steel cores of HVTLs.

Since CBT is a low viscosity thermoplastic semi-finished composite parts, such as sheets or preforms and tapes may easily be processed with this matrix system. Such materials are highly desired by the composite industry, especially for automotive applications.

The aim of this PhD thesis is to develop composites with CBT matrix which possesses appropriate properties to serve as an inner core of a HVTL. It is also desired to develop technologies for processing CBT into a proper composite matrix material.

2. Literature overview

In this chapter the main elements of high voltage transmission lines are introduced as well as polymeric composites are also discussed extensively. Polymeric matrices, especially thermoplastic ones, their modifiers, fillers and reinforcing fibers are described here.

2.1. High voltage overhead transmission lines (HVTL)

Electrical energy transmission systems consist of three main parts: the wires themselves, poles and insulators. *Utility poles* are the base holder elements of the HVTL system and from the technical point of view they are truss grudgers. Their main task is to ensure the appropriate distance between the ground and the wire. Their sizes are mainly defined by the wire voltage and ground characters [7]. Wires are held on the poles by *insulators*. Their main task is to ensure insulation and to avoid short-circuit between poles and wires. Nowadays most of the insulators are made of glass-fiber reinforced composite and silicone, but some ceramic and glass ones are also in use [7]. Main task of *wires* is to transfer electricity. Normally wires are made of metallic materials as they have the best electrical conductivity properties among the suitable materials. These wires consist of an inner and an outer layer. The inner core carries most of the mechanical load and is made of steel, while the outer layer transmits most of the electricity due to skin effect. However, the inner core still has to be conductive [7]. This steel-aluminum system is called ACSR (Aluminum Conductor Steel Reinforced).

Due to high electrical load these wires get warm, and which causes elongation due to thermal expansion, so they get closer to the ground. This phenomenon is called sagging and should be avoided. This sagging is a mechanically problematic effect and causes other problems: The so called electrosmog, an electromagnetic field surrounding the wire [8] can cause health problems like leucosis and sleep disorders reported by Varga [4], other psychological effects are reported by Beale *et al.* [9]. Sagging is a function of coefficient of thermal expansion (CTE), the distance between the poles and the sag itself (the equation for describing sag is not discussed here as it does not belong to this work) and the higher these values are, especially CTE, the higher the sag is. To avoid sag, utilization of low CTE materials or reduction of transferred electricity is necessary. As the latter is not a viable route low-CTE solutions will be discussed hereinafter.

2.2. Solutions for HVTLs

As mentioned already, low CTE materials should be applied in the high voltage field. Such materials may be special metals, or composites.

In HVTLs some composite parts are already applied, such as glass fiber reinforced composite based insulators. This insulating technology was developed in the 1960s [10], became widespread in the 1970s and 80s and by nowadays it is used all around the world even above 700 kV [11]. The advantage of using glass fiber reinforced composite materials in insulation technology is their light weight compared to ceramic ones, non-conductivity, high strength and outdoor-resistivity.

Utility poles may also be made of composites. These poles were first used in Hawaii to replace wooden poles because composites have much better corrosion resistance [12]. These poles have an extreme long service life of up to 80 years if appropriate UV protection is applied [13].

Apart from poles, composites are also necessary in wires. As it was mentioned above, HVTLs are composed of an inner core and an outer coating, and composites are suitable replacement for steel inner cores as it was reported by Alawar *et al*. [14, 15]. However, only carbon fibers are appropriate reinforcements because other fibers do not transmit electricity [16]. Another problem arises if carbon fibers are utilized, namely galvanic corrosion between the carbon and the aluminum interface so these two materials have to be galvanically separated. This problem is described in the literature much more detailed, for example in [17]. This issue will not be discussed since the solution is simple; an insulating layer has to be applied.

Special low CTE wires were developed by several companies and research groups:

A nickel-containing wire system was developed by VISCAS Corp. (Japan) under the trade name of INVAR®. In this wire the inner core is made of nickel-steel alloy wires and the outer layer is made of aluminum-zirconium alloy. Due to similar strength properties and ~60% less thermal expansion these wires can operate at up to 230°C. Their only drawback is the price, which is approximately ten times more than conventional wires (Figure 1/a) [18].

3M Corp. (USA) has developed a metal matrix composite inner core with alumina fibers in alumina matrix. The outer layer is an Al-Zr alloy. This system also ensures low sag at high temperatures and higher tensile strength than conventional ACSR systems (Figure 1/b). Widespreading of this system is hindered by its price, which is approximately ten times higher also than that of ACSR [19].

Carbon fibers are already utilized in HVTLs. In this case the inner core is made of a pultruded carbon and glass fiber reinforced rod with a special heat resistant epoxy matrix [20]. Electricity-transmitting aluminum wires are twisted around this rod (Figure 1/c). Glass fibers are necessary to avoid galvanic corrosion [17] which comprises the functionality of the wire. This system was developed by Composite Technology Corporation (CA, USA) in the early 2000s and has been used in several countries in the world [21]. This technology is protected by patents [22, 23]. However, these composites may have critical bending loads leading to cable failure according to Burks *et al.* [24, 25]. Such bending loads occur if the cable is bent for example over mandrels and showing that apart from epoxy resins other matrix materials should be investigated. Note, that due to thermal expansion the aluminum outer core loosens around the inner composite core during peak loads. If the cable cools down, the outer core re-fastens. This is a complicated issue from the point of the transmission lines, but out of scope of his thesis.

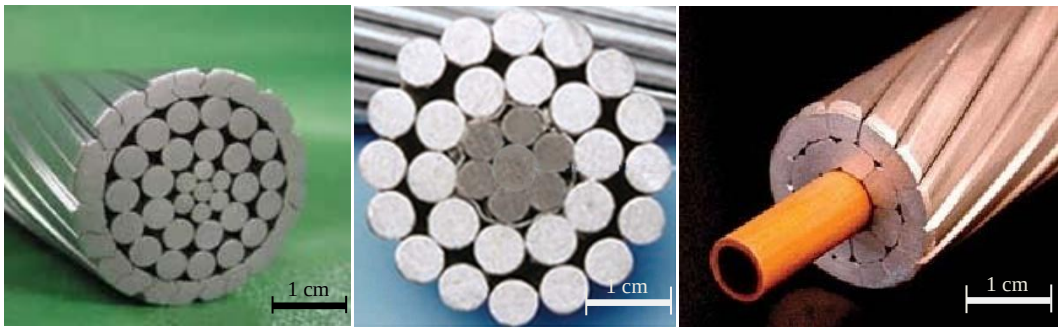

a) *b)* *c)*

Figure 1. Wire systems with low CTE: special steel wire (a), metal matrix composite system (b), polymer composite system (c). Core diameters are 9.53 mm – these samples are Drake cables [18, 19, 26]

High voltage insulators and conductors are fixed with fittings which are crimped onto them. An example of this is shown in Figure 2/a. This so-called crimping technology is critical and has to be carried out with care. A strong contact has to be present between the rod and the fitting during the whole service lifetime of the insulator or conductor which is at least 30 years. The crimping should not affect tensile properties during this timeframe. Crimping is carried out with special presses with usually 8 or 8+8 dies (Figure 2/b) with a pressure that does not break the composite part inside. Once a conductor is developed based on polymeric materials this problem has to be dealt with [27].

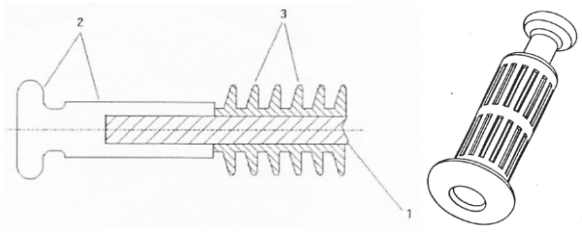

a) *b)*

Figure 2. a) End fitting of a high voltage composite insulator: 1 – glass fiber/epoxy composite rod; 2 – metal end fitting; 3 – silicone weather sheds; b) Crimped end-fitting with 2x8 + 2x8 pressing dies [27]

2.3. Polymeric composites

Polymer composites are multi-phase materials where strong adhesion bonds the tough matrix to the high strength reinforcement. This adhesive contact remains stable in high stress conditions [6]. In this chapter general properties and base element of composites will be introduced.

The advantage of applying composites is utilizing the synergy of matrix toughness and fiber strength. If adhesive connection is achieved between them the positive properties of both materials can be used.

As reinforcements usually fibrous structures are applied due to their high surface-to-volume ratio. This is important because in composites the higher the surface the higher the area for adhesion [28, 29]. In this work only carbon fibers are studied as this type of fibers have the highest electrical and heat conductivity among reinforcing fibers. This conductivity is so high that carbon fibers are applied even in sensor technology [30]. Do not forget, that these fibers possess also low, even almost zero thermal expansion, which helps to avoid sagging [31].

Carbon fiber production starts with a precursor fiber which is carbonized and then graphitized throughout the manufacturing process. Different surface treatments are applied after graphitization. Finally the fiber is wound up [26]. Fiber precursors may be made of poly acryl-nitrile (PAN), viscose, pitch, rayon or even Kevlar®. Properties of different precursor-based fibers are listed in Table 2. In this study only PAN-based carbon fibers are used as these fibers are available in Hungary (Zoltek has a plant in Nyergesújfalu) and they are the the most widespread in the industry. These PAN fibers are produced via wet spinning (Figure 3) and then stabilized in oxygen atmosphere at 200-300°C under tension.

The next step is carbonization where the heated fiber is also under tension but an inert atmosphere is applied. The whole process is presented in Figure 4. Properties of the fibers are set by the temperature of this phase: above 2000°C a high modulus fiber with lower

strength is produced, below 2000°C the situation is vice-versa. A commonly used PAN based carbon fiber, Panex 35 by Zoltek has a Young's modulus of 242 GPa with a tensile strength of 3800 MPa, for properties of some high-performance polymer based ones see Table 2 [26, 31-33].

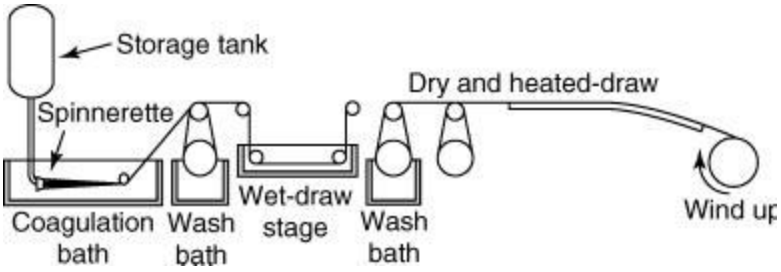

Figure 3. Wet spinning of PAN precursor fibers [34]

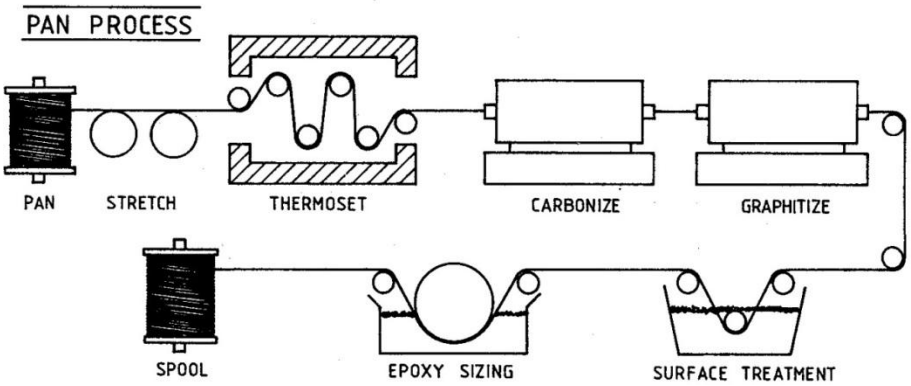

Figure 4. Schematics of carbon fiber production [35]

Precursor	Product designation	Tensile strength [GPa]	Young's modulus [GPa]	Electrical resistivity [μΩm]
Kevlar-29	1600°C	0.94	143	23
PAN	T-300	3.66	231	18
Pitch	P-55	1.90	415	9

Table 2. Properties of high performance polymer based carbon fibers [26, 36]

Beside fibrous reinforcements, nano-scaled reinforcements or modifiers are also used in polymer composites. These materials mainly change the matrix-dominated properties like compressive strength and flexural strength, energy absorbing properties, heat and electrical conductivity and creeping properties [37, 38]. Among HVTLs most of these properties are critical: bending – because the conductor is between two poles and is bent by its weight; conductivity – this material has to transmit electricity; creeping and compressive strength – fittings have to be crimped onto the conductor.

According to the above written, nano modifiers are also investigated in this work to improve mechanical and conductivity properties which may be increased by carbon

nanotubes [39, 40] or graphene [41]. Other properties may also be changed by other materials like toughening agents or chemical modifiers – these will be discussed later in Chapter 2.4.3.

In this thesis only graphene will be discussed owing to its low price compared to carbon nanotubes and in production of a conductor core low price materials should be applied.

Graphene can be simply described as a carbon monolayer (Figure 5/d) with outstanding mechanical and electrical properties. Graphene, according to Geim and Novoselov, may also be considered as a building material of all other carbon structures – see Figure 5/a, b, c [42].

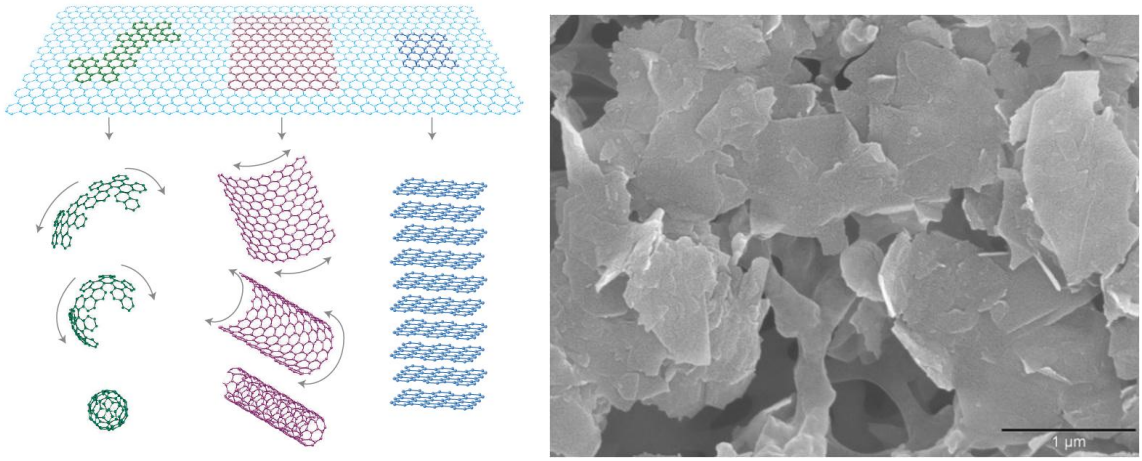

Figure 5. Graphene as a building material of all other dimensionalities: a – fullerenes; b – carbon nanotube; c – graphite; d – graphene nanoplatelets, SEM image [42]

Graphene was discovered in 2004 [43] and before that time it was believed that such a structure cannot thermodynamically exist. Graphene was reported to show reinforcing effect in nanocomposites with both thermosetting and thermoplastic matrices. According to these results graphene causes a Young's modulus increase with some decrease in strain at break [44]. These nanocomposites can get additional carbon fiber reinforcement. Hybrid systems are producible for example by *in-situ* polymerization (this method is discussed later) in one step. The problem is graphene dispersion in the matrix which is similar to carbon nanotube or any other nanoparticle dispersion. Possible dispersion solutions were widely examined and three routes were described: *in-situ* polymerization, melt intercalation and exfoliation in solvents [38]. According to these results graphene can be dispersed in any kind of polymeric matrix.

Nowadays mainly thermosetting resins are used as matrices in high-tech composites. However in this work these resins will not be discussed because thermoplastics are

believed to be the next generation of high tech matrices. Thermoplastics are also more environmentally friendly as they are much easy to recycle because they can be reprocessed [45].

2.4. Cyclic butylene terephthalate (CBT)

Cyclic butylene terephthalate is a cyclic oligomer system in powder or pellet form designed to be a thermoplastic matrix material for composites. This CBT is capable to polymerize into pCBT *in-situ* via ring-opening polymerization (ROP). The resulting polymer is chemically identical to PBT with different molecular weight and crystalline fraction, so it is designated as pCBT for clarity.

For impregnating long-fiber reinforced composites a resin of dynamic viscosity below 1 Pas is necessary. Conventional thermoplastics have much higher viscosity value (~10^2-10^4 Pas) and are mainly used with short fibers in injection molded products. So in this thesis only low-viscosity materials will be discussed. According to Steeg's work [46], who examined thermoplastic materials, CBT has the lowest melt viscosity among the available thermoplastic raw materials on the market (Figure 6, 'classic' thermoplastics mean materials polymerized before usage, while 'reactive' thermoplastics are polymerized *in-situ*). This CBT polymerizes through ROP and prior to ROP the low molecular weight results in the water-like (~10^{-2} Pas) viscosity. For further work CBT was chosen due to this low viscosity value and only this material will be discussed in the followings.

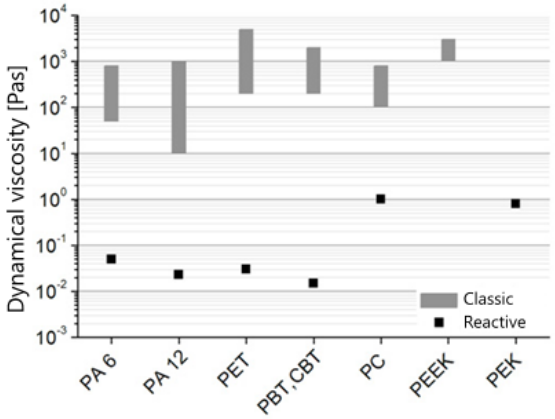

Figure 6. Dynamic viscosity of classic and reactive thermoplastic polymers [46]

Generally, ROP means that monomers or oligomers have a ring form prior to polymerization. During the polymerization process these rings open and in the presence of a suitable catalyst form a linear polymer. If this process happens in the timeframe of manufacturing, than it means *in-situ* polymerization. An advantage of this is the low melt viscosity prior to polymerization because the melt consists of only small monomers or

oligomers. So impregnation should be completed before polymerization starts, and in this case no high pressures are needed. From a chemical point of view it is much easier to ‘assemble’ the molecules *in-situ*, than produce them, then ‘degrade’ them with high pressure as they are pressed though a reinforcing system [47, 48].

In case of CBT all of this means that this material is built up by cyclic oligomers, which are capable to polymerize into a linear polymer (for the whole process see Figure 7 and Figure 9) [47, 49].

CBT belongs to the family of polyesters and this group is proven to be excellent matrix materials for composites as described by Czigány and Karger [50].

Cyclic oligomers of polyesters were first reported by Ross *et al.* [51]. Starting from that time until the 1990s there was only academic interest in these cyclic structures as they were produced during conventional polyester processing in a concentration of ~1-3% and there was no use of them [52]. Later, it became clear that these molecules polymerize through ROP, form no by-product and have low melt viscosities which makes reinforcement impregnation easy. This makes it possible to use these cyclic oligomers for thermoplastic resin transfer molding (RTM), pultrusion or other hot melt impregnation processes.

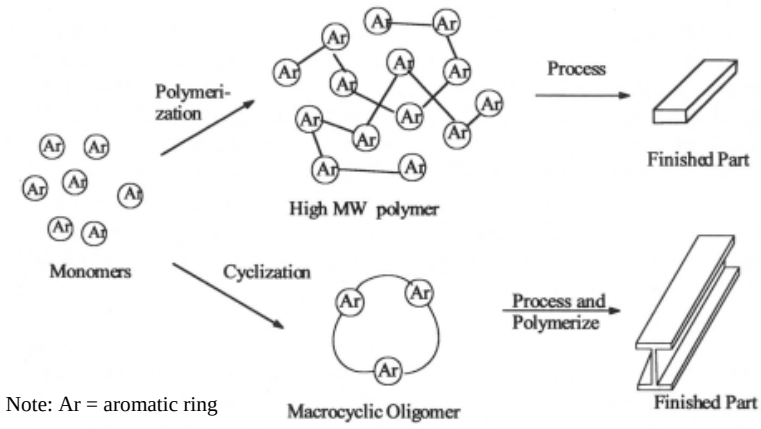

Figure 7. Conversion of monomers to low viscosity macrocyclics (bottom side) allows *in-situ* polymerization during processing and produce more structured parts [49]

In the 1990s efforts were made at General Electric Corp. to develop a preparation method for cyclic oligomers of polyesters based on the above described processing methods. Most of this work was done by Brunelle [48] with the result of dissolving commercial PBT in dry ortho-dichlorobenzene (o-DCB) at reflux, then adding the equilibration catalyst [53] (see Figure 8). These cyclic oligomers were then polymerized via ring-opening

polymerization into conventional polyesters with unusually long chains, also by Brunelle *et al.* [52].

Parallel to Brunelle, another research group led by Semlyen also developed a method for synthesizing and polymerizing cyclic ester oligomers and published a series of articles about their work [54-62] including a patent [63]. He also applied high dilution condensations and ring-chain equilibrium methods and the latter seemed to be more productive.

As the proper technology was developed, production of cyclic PBT oligomers started at General Electric Corp., and then the technology was acquisited by Cyclics Corporation. From this time on cyclic butylene terephthalate oligomers are available on the global market under the trade name of CBT - as an abbreviation of Cyclic Butylene Terephthalate. Cyclics Corporation has two manufacturing plants, one in the USA (Schenectady, NY) and one in Europe (Schwarzheide, Germany).

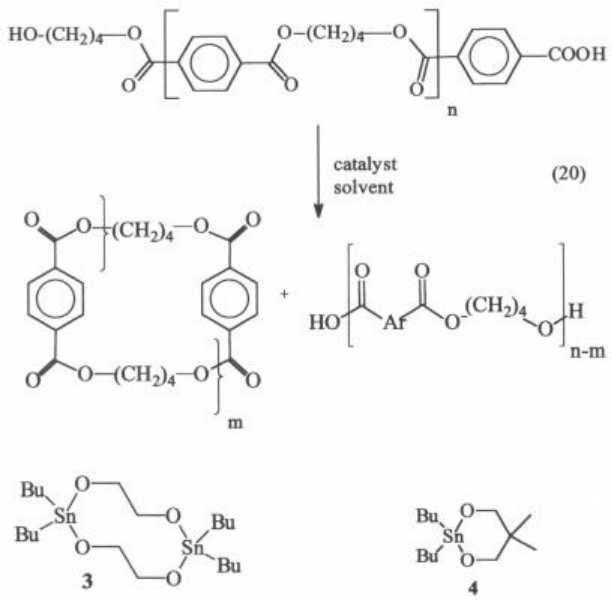

Figure 8. Processing of cyclic ester oligomers [49, 53]

In Schwarzheide the base material for CBT production is ULTRADUR 6505 by BASF. This PBT is cyclo-depolymerized, catalyst is added then it is ready for further processing.

Polymerization of CBT is the already mentioned ROP where the rings are opened by heat in the presence of a suitable catalyst. For commercial use, a TiN based catalyst (butyl chlorotin dihydroxide), Fascat 4101, is used which is manufactured by Arkema.

Polymerization method is as follows (Figure 9): in the initiation phase cyclic oligomers are opened by heat and initiator and start to polymerize (in this case the initiator is butyl chlorotin dihydroxide) into linear pCBT. pCBT refers to polymerized CBT and considered

to be chemically identical to conventional PBT [64, 65] with higher molecular weight [66]. The propagation phase is similar to chain-growth polymerization processes. Initiators are believed to operate by Lewis acid activation of the ester group and then transferring a ligand and forming a new ester bond and an active chain end (Figure 9). Propagation continues until most cyclic oligomers are depleted and the ring-chain equilibration deteriorates [48, 52, 66].

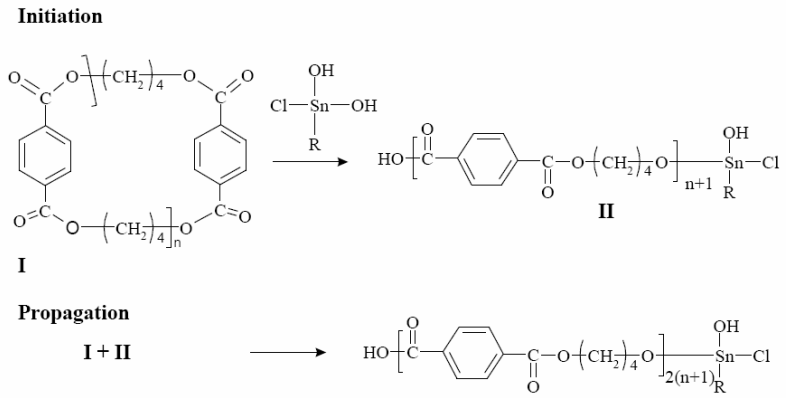

Figure 9. Polymerization and propagation of cyclic butylene terephthalate oligomers [49, 52]

2.4.1. Properties of cyclic butylene terephthalate

Cyclic butylene terephthalate is available in powder and pellet forms with (CBT160) and without (CBT100) catalyst [67]. CBT without catalyst is mainly used as viscosity reducing agent for other polymers or as an additive for rubbers and epoxies [68, 69]. This CBT without catalyst is out of scope of this thesis so will not be discussed further here. In this thesis CBT refers to CBT160, the catalyzed version of this matrix material in the followings.

CBT oligomers contain 2-7 monomers (for atomic structures of a tetramer see Figure 10) and polymerizes via a ring-opening way which is entropically driven, athermic and no by-product is formed. This latter property is important in industrial applications because no or much less ventilation is necessary contrary to crosslinking resins.

This ROP reaction can be frozen by decreasing the temperature and the oligomer conversion-time-temperature function can be examined for example by gel permeation chromatography (GPC). This work was done by Steeg in his PhD thesis (Figure 11) [46].

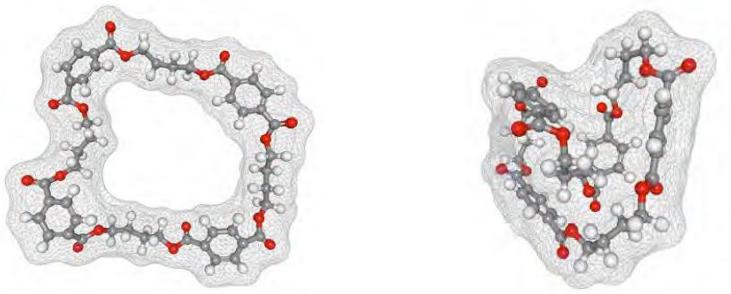

a) *b)*

Figure 10. CBT tetramer in two different conformations at different energy levels: 998 kJ/mol (a), 950 kJ/mol (b) [46, 70]

To achieve a conversion of 95% at least 15 minutes are required at 190°C (see Figure 11/a). For continuous processing methods this is intolerable, for cyclic processes like thermoplastic RTM it is also long. So the above 200°C temperature range should be chosen where at 250°C a conversion of at least 98% is reached in 2 minutes (Figure 11/b). These results are reported by Steeg and based on kinetic studies and modeling [46].

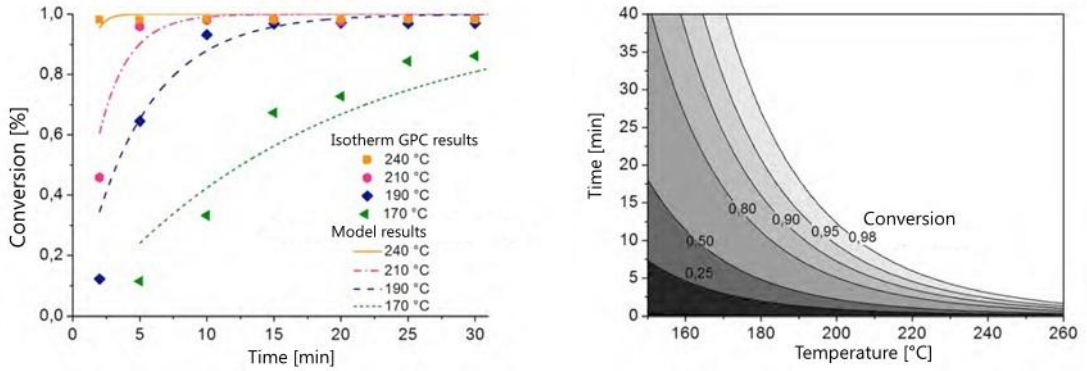

a) *b)*

Figure 11. Polymerization of CBT160 in function of time and temperature (a); Time-Temperature-Conversion diagram for isothermal conditions (b, modeled values) [46]

Polymerization and crystallization of CBT

Polymerization of CBT was investigated by some researchers. Hakmé and coworkers [71] followed polymerization by dielectric sensing and found that below 200°C polymerization and crystallization of CBT occurs parallel. Between 200 and 220°C the material first polymerizes and then crystallizes and above the melting point (220°C according to the article) no crystallization occurs.

Tripathy *et al*. [72] investigated the effects of different catalysts and polymerization temperatures on CBT. This research team worked together with Cyclics Corp. and used experimental batches of CBT designated as XB2 (catalyzed with stannoxane) and XB3 (catalyzed with butyltin chloride dihidroxide) and OGTR (catalyzed with tetrakis-(2-

ethylhexyl)titanate. According to their results XB2 completes the *in-situ* polymerization within 2-3 min, necessary for reaction injection molding (RIM), at polymerization temperatures of 165°C and higher. If XB3 or OGTR are used 15 minutes of induction time was obtained which is ideal for the resin transfer molding (RTM) technique. Their further results showed that OGTR initiator results in the highest-molecular-weight polymers ($5.47x10^4$ g/mol at 200°C) among all initiators used, and the molecular weight remains the same irrespective of polymerization temperature. However, the molecular weight using XB3 initiators is about 90% ($4.62x10^4$ g/mol at 200°C) of that of the OGTR system when the polymerization temperature is higher than 200°C. Stannoxane catalyzed systems give the same molecular weight at all polymerization temperatures (eg. $4.1x10^4$ g/mol at 185°C) and are around 75% of that of the OGTR-catalyzed polymer. According to WAXS results, crystallinity increases with increasing polymerization temperature in the XB3 system (64% at 185°C, while 68% at 205°C) due to kinetic control in the examined temperature range, but a reverse trend was noticed both in XB2- and OGTR-catalyzed systems (66 and 60% was found, respectively). The XB3-catalyzed pCBT crystallizes faster than the OGTR.

Tripathy *et al*. besides his above mentioned work carried out fire-resistance tests [73] with several additives for CBT like BPADGE; TBBPA and Carbinol PDMS. They utilized *in-situ* polymerization and stated that pCBT with these additives are applicable as high performance thermoplastic matrix materials for composites. These materials may even be used by the army and the navy. Some copolymers (eg. (50/50, w/w) pCBT/BPADGE) produced by this research group showed not only better flame retardancy properties than that of Kevlar, PEEK (commercial products from DuPont) and Ultem (product of GE) but also showed enhanced processing properties.

Harsch and his colleagues [74] followed the polymerization and crystallization of CBT by Fiber Bragg Grading (FBG) and normal force measurements at isothermal conditions. Two temperatures were chosen: 170 and 190°C. According to their results crystallization of CBT occurs in two steps: In the first stage shrinkage of several hundred ppm/min was observed while in the second stage this value was several tens according to FBG results. A difference in crystallinity and crystallization parameters was also found: at 190°C slightly more perfect crystals grew and crystallinity was also slightly higher than at 170°C.

Mohd Ishak, Karger-Kocsis and their research team published a series of articles regarding polymerization and composites of CBT [75-78]. In one of these articles [78], related to a modulated differential scanning calorimetry (MDSC) study on CBT polymerization, it was

found that polymerization of CBT may not be athermic, if the exothermic peak found on the non-reversing belongs to the polymerization. This shows a heat release of 22 J/g. The authors draw a consequence on the basis of additional rheological measurements that this peak belongs to the initiation of the reaction. So the athermic reaction is a sum of an exothermic initiation/polymerization and a subsequent melting of the resulting pCBT, which is endothermic. An also interesting result is the 'double melting characteristics' which appears during the polymerization above the melting point (T_m) of (the resulting) PBT. This phenomenon is assigned to the remelting/recrystallization process, which is already known among PBTs.

Another article by Karger-Kocsis *et al.* [77] is also based on modulated DSC, and was published about organoclay-modified pCBT. Samples were produced in two ways, dry and melt blending, and then polymerization was studied. Results showed that sample preparation affects crystallization and melting behavior, and the presence of organoclay induces more perfect crystals to grow.

Lehmann and Karger-Kocsis [79] studied the isothermal and nonisothermal crystallization kinetics of CBT and compared it to classic PBT. For this study CBT XB3, CBT160, PBT B4520 and B6550 (the latter is the raw material of CBT) was used. In case of isothermal experiments at 250°C morphology of the growing crystals do not change with crystallization temperature except for PBT B6550 where geometry of growing crystal phase depends on the crystallization temperature. For the different kinds of CBT athermal nucleation was assumed due to the presence of the catalyst. In case of CBT160, the Avrami exponent is n~3, showing a spherical crystal growth, while n~2 for CBT XB3 indicating a plate-like two dimensional crystal growth. These results were compared to commercial PBTs: in case of B4520, the Avrami exponent was found to be n~4 showing thermal nucleation with spherical crystal growth and for PBT B6550 n~3 was found and in this case n~3 means athermal nucleation with three-dimensional crystal growth or thermal nucleation plate-like crystal growth. Additionally their results showed that crystallization of pCBTs occurs in a temperature range where a change in activation energy takes place.

Drying of CBT

CBT as a polyester is very sensitive to air humidity before processing. It takes the humidity up from the air which hinders polymerization through deactivating the catalyst so conversion will not be completed. According to [46] the aim is to reach a moisture content below 200 ppm. The necessary times for drying regarding the forms (eg. pellet or powder)

of CBT and the drying methods are depicted in Figure 12. After drying CBT should be kept in a desiccator or stored under nitrogen atmosphere [46]. For industrial use an on-line drying system may be useful. After polymerization pCBT has the same moisture uptake and excellent outdoor resistivity properties as conventional PBT.

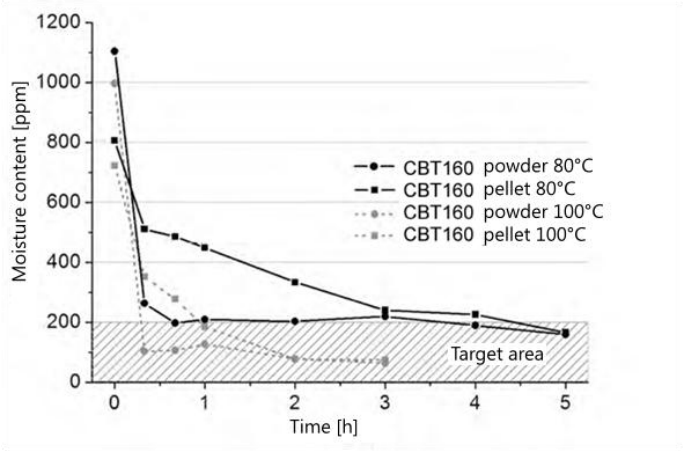

Figure 12. Necessary drying times for different forms of CBT with different methods [46]

Rheological properties

Dynamic viscosity of CBT changes in time and temperature during its processing (see Figure 13) [76]. This property is very important in case of processing CBT, so researchers have studied it in detail, as presented in the followings. Rheological properties were examined by Mohd Ishak *et al.* [76]. They stated that viscosity curves below 210°C have a constant initial stage where viscosity is below 1 Pas which is ideal for impregnation [80, 81]. After this constant stage viscosity starts to increase. The speed of this increase and the slope of the curve is related to polymerization speed [76].

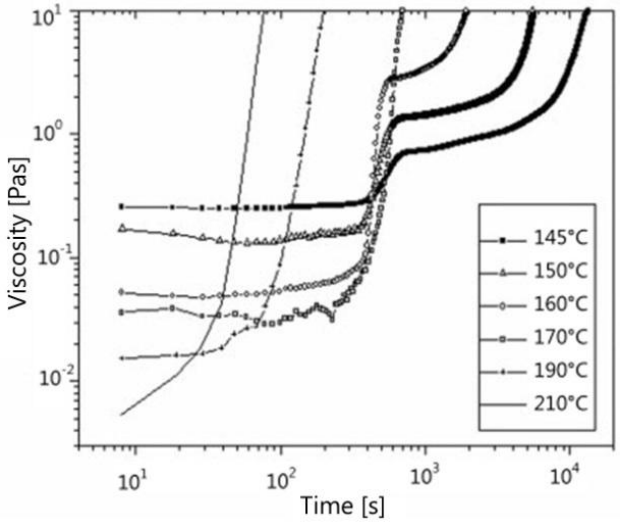

Figure 13. Dynamical viscosity of CBT in function of time and temperature [76]

2.4.2. Properties of polymerized cyclic butylene terephthalate

CBT can be polymerized into pCBT by different methods, as it is presented here by summing up the results of some research teams. For the detailed values see Table 3. Parton *et al*. [64] used resin transfer molding (RTM) with a subsequent *in-situ* polymerization step at different temperatures, 190 and 230°C respectively. According to their results, higher polymerization temperature resulted led to higher tensile strength, elongation at break and molecular weight (MW). Crystallinity of this higher temperature sample was lower, which explains the better mechanical performance.

Abt *et al*. [82] used *in-situ* polymerization method in a hot press at 250°C. This resulted in high elongation at break and low crystallinity, but low MW and moderate tensile strength and Young's modulus.

Baets *et. al.* [83-85] used similar RTM method like Parton at 190°C and achieved good results: a Young's modulus above 3 GPa, and tensile strength above 60 MPa. Crystallinity of the samples were different, and the highest value resulted in rigid material with only 1.9% elongation at break.

Mohd Ishak *et al*. [75] used *in-situ* polymerization method in a hot press, like Abt, but at 190°C. Their results show high crystallinity, and as a consequence, low elongation at break and moderate Young's modulus and tensile strength.

From the above one can conclude that some kind of toughening is necessary for CBT to reduce its brittle nature. The known solutions for this problem are discussed in the next chapter.

Processing temperature [°C]	E [MPa]	σ_{break} [MPa]	ε_{break} [%]	χ_c [%] (DSC)	MW [kg/mol]	Reference
190	3.2±0.1	54±5	1.6±0.2	47±2	61.4±0.5	Paron *et al*. [64]
230	3.1±0.2	73±14	2.3±0.7	42±2	73.3±0.6	
250	2.7±0.3	56±8	6.7±2.9	29.6	22.6	Abt *et al*. [82]
190	3.2±0.1	74±4	3.8±0.7	43	104	Baets *et al*. [83]
190	3.1±0.1	74±4	3.9±0.7	42.5	-	Baets *et al*. [84]
190	3.5±0.1	61±3	1.9±0.1	44±1	78	Baets *et al.* [85]
190	2.3±0.1	58±2	2.3±1.6	48.6	-	Mohd Ishak *et al*. [75]

Table 3. Properties of in-situ polymerized cyclic butylene terephthalate samples

2.4.3. Chemical modification and other toughening methods of pCBT

Chemical modification or other kind of toughening of pCBT may be necessary due to its rigid nature caused by the crystalline structure, and the high crystalline fraction (Table 3). Increasing toughness is possible through making crystals less perfect or using chain extenders and nonisothermal processing methods [53, 86]. Most of these methods are patented without industrial realization only studied by researchers [87-89].

Polycaprolactone (PCL) is a polyester, that polymerizes via ring-opening polymerization from ε-caprolactone monomers and is used as an additive to modify the end use properties of polymer products. As a catalyst for ROP TiN-based materials are used like in the case of CBT. So either the monomer or the polymer may be used as a toughening agent for pCBT because during the ROP, CBT can either copolymerize with ε-caprolactone monomer or PCL [90]. Based on the above these materials were examined by several research groups [85, 91, 92]. These works are reviewed in the followings.

Tripathy *et al*. [91] used CBT and ε-caprolactone to produce copolymers. A CBT without catalyst was used. First, liquid CBT was mixed with ε-caprolactone then stannoxane catalyst was added. Polymerization temperature was 180-185°C. The obtained material was investigated by the following methods: GPC, NMR Spectra, FTIR, DSC, DMA, WAXS. Dielectric and mechanical properties were also determined. Results showed that conversion was around 95% with a number-average molecular weight varying between 30-40.000 g/mol and a polydispersity index of 2. The reaction between CBT and ε-caprolactone with stannoxane catalyst is a transesterification reaction. According to their DSC results the onset of PBT melting point decreases with the increasing caprolactone content – this is common for such random copolymers where only one component has segments long enough to allow crystallization to take place. DSC and WAXS results showed a decreasing crystallinity with increasing caprolactone content. X-ray scattering showed also that PCL sequences were not long enough to form crystalline domains if the polymer contains more than 50% pCBT. Concerning mechanical properties, increasing caprolactone content decreased tensile strength but increased the strain at break.

Baets and his coworkers [85] used polycaprolactone to form a copolymer and through this they reduced crystallinity and made pCBT tougher in this way. The structure of the formed copolymer is depicted in Figure 14.

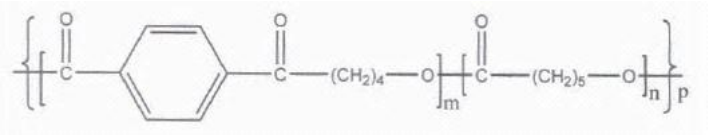

Figure 14. Structure of the pCBT-PCL copolymer [93]

CBT-XB0-C (an unanalyzed experimental batch), as catalyst Fascat 4101 and polycaprolactone from Sigma Aldrich with an average molecular weight of 10.000 g/mol was used. Composites were also produced with an uniaxial and a biaxial E-glass fabric from Ahlstrom and Saertex Wagener, respectively. Processing method was an RTM-like vacuum-assisted process at 190°C. These composites were compared to unreinforced ones and to injection molded PBT samples. All of these samples were subjected to mechanical, viscosity, DSC and GPC tests. According to the results, initial viscosities (Figure 15/a) do not change significantly with the addition of polycaprolactone. A shifting of the melting point indicated that a copolymer was formed (Figure 15/b). GPC measurements showed that the presence of polycaprolactone hinders polymerization (Figure 15/c) but a final conversion of 99% was reached. Tensile testing of the matrix showed an increase in failure strain from ~2% to 4% with a decrease in Young's modulus and tensile strength. In case of composites, PCL causes an increase in strain-at-break and impact resistance is more than doubled.

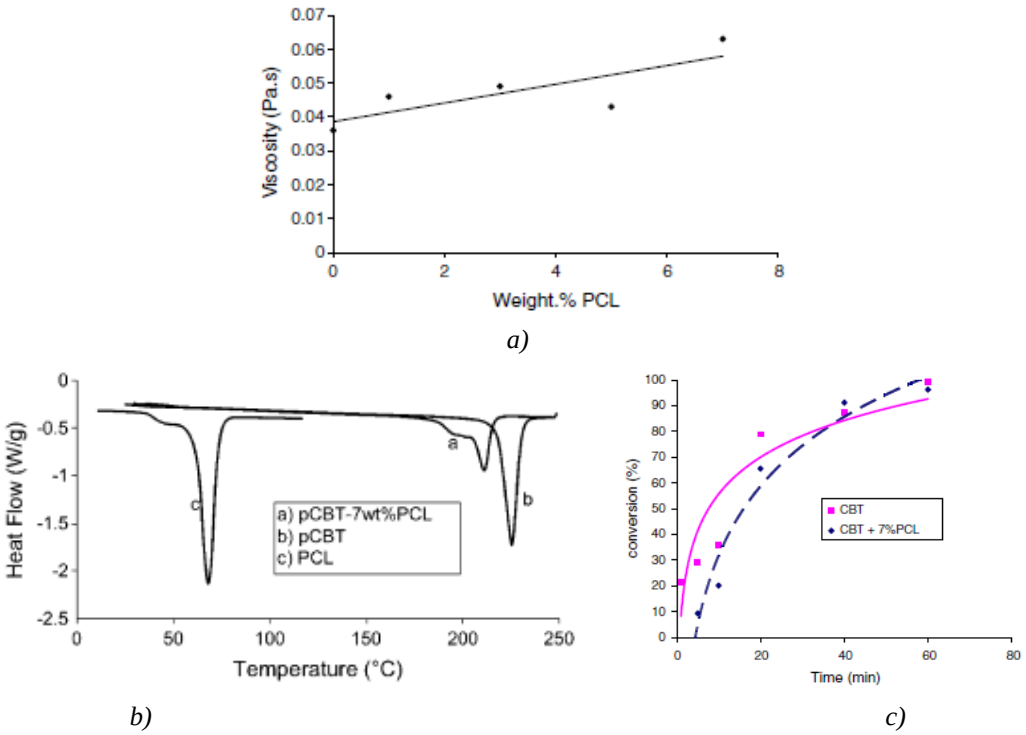

Figure 15. Initial viscosity at 190°C (a), differential scanning calorimetry traces (b) and conversion curves (c) of neat and 7 wt% PCL containing pCBT samples [85]

Effect of polycaprolactone on the crystallization and melting behavior of CBT was also studied by Wu and Huang [92]. Applied materials were CBT160 and Capa 6500 from Solvay Chemicals with an average molecular weight of 50.000 g/mol, and 7 wt% of PCL was added to CBT. Crystallization kinetics were studied by DSC in the following method: samples were heated up to 230°C, held there for 30 minutes to ensure polymerization then cooled down with different cooling speeds. Finally specimens were heated up to 265°C at a heating speed of 20°C/min to study melting properties. According to FTIR results copolymerization between CBT and PCL was a transesterification reaction. DSC results also prove copolymerization with no clear glass transition and a shifted melting point of the copolyester. An interesting phenomenon is the change of melting peaks and enthalpies caused by different heating rates. If cooling speed is below 5°C/min, only one melting peak is seen, but if cooling speed exceeds 5°C/min, two peaks can be observed due to the instable crystalline structure (two peaks: recrystallization and a subsequent melting). The slower the cooling, the higher is the melting enthalpy due to the higher crystallinity. According to DSC results, authors stated that crystallization occurs in the cooling phase, not simultaneously with polymerization as it was reported by Baets [85]. There is a possibility for this at a temperature range between 190-202°C but supercooling is very limited so the latter process is not favorable for processing. So according to Wu's results faster cooling results in lower crystallinity which means from a producer's point of view that a faster cooling is necessary. This also corresponds with Steeg's results regarding the cooling speed [46]. Note, that from one side fast cooling reduces crystallinity and results in a tougher material, from the other side this instable crystalline structure may lead to changes in the mechanical properties in longer periods of time.

Baets *et al.* [94] used quenching which was designated as a 'nonisothermal method' to toughen pCBT. The aim of this was to reduce crystallinity by fast cooling. For this work CBT100 and CBT160 and basalt fibers (ROV 1600 roving and BSL 200 weave) from Basaltex were used. Specimens were produced in a special prepreg method with a drumwinder followed by compression molding. Film-stacking was also utilized (these methods are discussed later in Chapter 2.4.5.). Two cooling speeds were applied, 8 and 100°C/min, respectively. The effect of cooling speed is clearly seen in the results of three point bending: quenched samples showed much higher flexural strength and failure strain than the slow-cooled ones. Quenching seemed to be better also in case of mode II interlaminar fracture toughness tests. Crack propagation fracture toughness was doubled by

fast cooling. This phenomenon was explained by reduced crystal perfection caused by quenching. Degree of crystallinity was the same but quenching caused defects in the crystalline structure. Changes in the crystalline structure was not studied above the glass transition range, however, it could show some recrystallization phenomenon and changes in mechanical properties.

Abt and coworkers [82] used tetrahydrofuran (THF) to toughen CBT. They found that 1.5 wt% of THF increased the molecular weight and caused a narrower molecular weight distribution. According to their DSC scans THF hindered crystallization which has effect on the mechanical properties. Their most important result is that THF increased toughness and resulted in a strain at break well above 100% in a tensile test. Other mechanical properties, such as tensile strength, tensile modulus and glass transition temperature were not significantly affected.

2.4.4. Composites made with pCBT matrix

CBT with its low melt viscosity is an ideal matrix material for both nano and macro-scale reinforcements as mentioned above. This was studied by several research groups.

Lanciano *et al.* [95] prepared nanocomposites of CBT and montmorillonite (MMT) and followed polymerization by DSC then crystalline structure was studied by WAXS. It was found that CBT polymerizes and crystallizes below its equilibrium melting point, but if CBT and MMT are premixed, polymerization takes place above the melting point and the material crystallizes during the cooling stage. Further results showed that if CBT polymerizes and crystallizes below its melting point then the resulting crystals have higher lamellar thickness.

Berti and coworkers [96] polymerized CBT at 205°C and used MMT to prepare nanocomposites. Results were promising since the low viscosity of molten CBT ensures good nanoclay dispersion. Beside this, better thermomechanical properties and high molecular weight were achieved.

The only work regarding the fiber-matrix adhesion is Mäder and her colleagues' article [97]. According to their results obtained by single fiber pull-out tests and atomic force microscopy (AFM) surface topography showed sizings containing aminosilane and epoxy film former improved interfacial adhesion strength and critical energy release rate for CBT glass fiber composites. In this article it was also stated that increasing the polymerization temperature increases chain mobility which will increase interfacial properties.

Composite sheets were produced by Mohd Ishak and his colleagues [75] with woven glass fabric reinforcement by compression molding with both pressure and displacement control. These sheets were compared to unreinforced pCBT sheets and commercial injection molded PBT sheets. Their results are shown in Table 4 and Table 5.

	Density [g/cm^3]	Tensile strength [MPa]	Tensile modulus [GPa]	Tensile strain at break [%]	Flexural strength [MPa]	Flexural Modulus [GPa]
IM-PBT	1.3	55.9±3.5	2.4±0.2	8.0±1.4	112.4±4.2	2.3±0.1
ISP-PBT	1.32	58.6±2.5	2.3±0.1	2.3±1.6	104.2±9.2	2.4±0.7

Table 4. Density, tensile and flexural data of injection molded (IM) and unreinforced *in-situ* polymerized (ISP) PBT [75]

	Tensile modulus [GPa]	Tensile strength [MPa]	Tensile strain at break [%]	Flexural strength [MPa]	Flexural Modulus [GPa]	Inter-laminar shear [MPa]
WGF-PBT (DC)	18.8±0.8	302±5	1.8±0.03	482±13	22.3±0.1	28.2±1.5
WGF-PBT (PC)	20.6±0.3	356±9	1.5±0.04	578±8	24.5±0.3	34.3±1.1

Table 5. Tensile, flexural and interlaminar shear strength (ILS) of woven glass fabric reinforced (WGF) pCBT prepared by displacement control (DC) or pressure control (PC) [75]

According to these results applying pressure during composite processing resulted in higher strength and modulus both in flexion and tension. Fiber wetting was studied by scanning electron microscopy and found to be appropriate [75].

Baets, Parton and their colleagues published a series of articles about processing CBT into a proper matrix material with different methods [64, 98], and also toughening CBT with isothermal [83] and nonisothermal [94] methods. They tested some additives like polycaprolactone [85] and used basalt fibers [94] and carbon nanotubes [84]. Both Baets [93] and Parton [99] wrote a PhD about processing CBT. Their results are discussed in the following pages.

Parton and Verpoest [98] prepared composites with CBT matrix and investigated its properties compared to unreinforced ones. According to their GPC results, presence of fibers resulted in a lower conversion (92% compared to the 98% of the unreinforced ones) owing to an interference of the fiber sizing in the measurements. In spite of this low conversion and molecular weight values, the molecular weight of this pCBT is comparable to commercially available PBTs.

Also the application of a thermoplastic RTM process was examined by Parton [64]. CBT100 was used and catalyst was added prior to injection. Two polymerization temperatures were examined: 190 and 230°C, respectively. Lower processing temperature resulted in higher strength but these materials were brittle owing to the high degree of crystallinity. Even though, these composites were brittle, these experiments showed the applicability of a thermoplastic RTM process with CBT resin.

Nanocomposites were also prepared with pCBT matrix by Tripathy *et al.* [100]. They used Cloisite 20A montmorillonite (MMT) produced by Southern Clay Products and uncatalyzed CBT. Production method was the following: catalyst (cyclic stannoxane), and clay were dissolved in an antioxidant (Irganox 1010; Sigma-Aldrich), then the CBT powder was added and the solvent was evaporated. Then this mixture was polymerized at 190°C. According to WAXS measurements, most of the MMT was exfoliated but some agglomerates were still present in the polymerized CBT which was also supported by transmission electron microscopy (TEM). Thermogravimetrical analysis in nitrogen atmosphere showed an increased thermal stability, 8-10°C shift in the onset temperature, due to the presence of nanoclays. Mechanical properties were not studied; however their effect would be interesting for example on the tensile properties.

Hybrid composites with multiwalled carbon nanotubes (MWCNT) and E-glass UD fabric were produced by Baets [93]. He used CBT100 in a vacuum-assisted RTM (VARTM) process, amount of CNTs varied between $0 - 0.1$wt%. During production a faster polymerization reaction was experienced so a lower catalyst amount (0.2 wt%) was used than the conventional 0.45 wt% (equal to 3 mol‰). The lower catalyst amount did not affect final conversion but led to a slightly tougher material. Mixing was 'rotational mixing' of the molten CBT for 5 minutes which resulted in a good dispersion according to TEM pictures. For unreinforced samples, 0.05 wt% of CNTs caused an increase in stiffness and strength, but their presence decrease failure strain and had no effect on crystallinity. In case of hybrid systems glass fibers acted as filters so dispersion of CNTs was not satisfactory.

2.4.5. Reactive processing techniques for CBT

CBT needs a processing technique which allows the ROP reaction to be completed at temperatures around or above 200°C. So conventional composite processing methods are not applicable here. Hot consolidation, thermoplastic prepreg methods and pultrusion may be suitable for CBT. Hot consolidation is a simple method where CBT powder and reinforcing agents are layered upon each other and then heated up. After ROP the composite is cooled down and the part is ready [101]. The existing processing methods for CBT are discussed here – cable core manufacturing technique development is based on these methods.

Prepregs were produced by Baets [93, 94] via a special drumwinder. CBT was molten in a resin bath at 180°C and a basalt roving was pulled through it. This resin bath was small in

order to reduce residence time of molten CBT. This impregnated roving was wound onto a drum to form a quasi-unidirectional (UD) prepreg. Finally, this prepreg was hot-pressed into a composite sheet. Beside this prepreg method a VARTM process was also developed [84] where uncatalyzed CBT was used. First, the resin is heated up to 190°C and as the whole amount melts, catalyst is added, stirred for 20 sec and then vacuum infused into a closed mold. Vacuum pressure is important, because too high vacuum would lead to too fast mold filling that would result in a porous structure. Too low vacuum would lead to slow mold filling and the increasing viscosity hinders proper mold filling and impregnation.

Steeg built a so-called interval hot press (IHP) [46] to produce composite sheets with pCBT matrix (Figure 16). For this device first a 'powder-prepreg' was made in a tunnel-oven at 140°C. In this process molten CBT flows among the reinforcement and so a prepreg is formed. During the melting process the conversion of CBT runs only up to 5-10% so complete polymerization takes place inside the press. The press-tool was 1000 mm long with a 700 mm long heating and a 300 mm long cooling zone. Temperatures were the following in the heating zone: 140, 200, 260, 260, 230°C and 50 and 20°C in the cooling side for 10 m/h process speed. With this press a production speed up to 62 m/h was realized. Composites were tested for interlaminar shear strength (ILS) and was found that these values were between 30 – 40 MPa in Short Beam Shear (SBS) arrangement [46]. This is a pultrusion-like process capable to produce post-formable sheets.

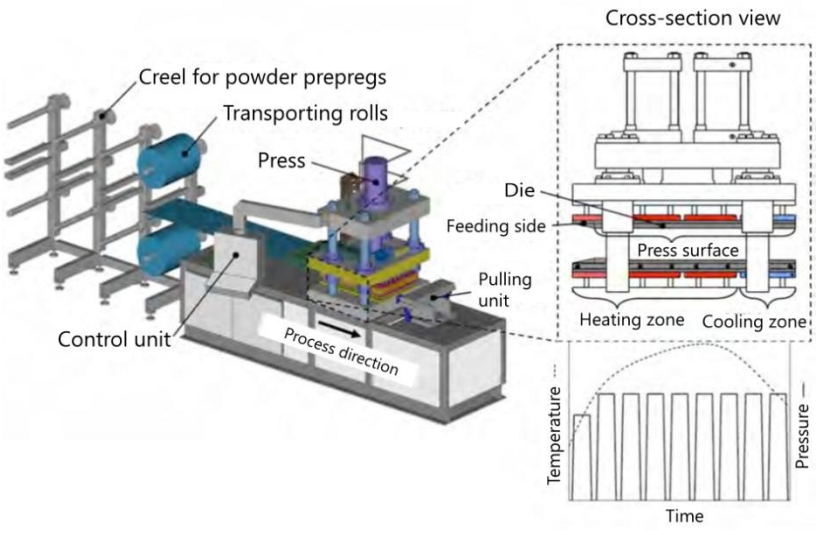

Figure 16. Intervall hot press to produce composite sheets with pCBT matrix [46]

Besides IHP, a special hot press system called 'Cage System' (see Figure 17) was also tested by Steeg. Its advantage is the rapid heating by magnetic induction (up to 700°C/min

heating speed) and its capability to cool down the samples rapidly (up to 300°C/min cooling speed). Via this 'Cage System' method can the lowest viscosity and perfect impregnation be reached. Drawbacks of this machine are the price and its enormous energy consumption. However, high quality composites were produced with it [46].

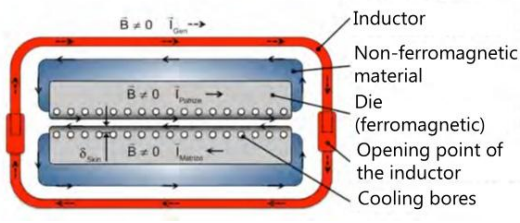

Figure 17. Sketch of the Cage System™ [46]

2.5. Pultrusion

Pultrusion is a method for manufacturing composite profiles with continuous cross-sections, high fiber volume fraction and high strength. Usually these products are unidirectionally reinforced but multiaxial or mat reinforcements are also applicable. With this method fiber volume fractions up to 70-80% can be achieved. So pultrusion seems to be adequate for producing HVTL cable cores [102].

Pultrusion may be classified on the basis of the applied resin or the mode of matrix impregnation. A classification is presented in Table 6 and Figure 18 on the basis of Luisier's work [103]. In this work thermosetting pultrusion will be introduced first as pultrusion was developed on the basis of this kind of resin.

	Pultrusion of Thermoset Materials	**Pultrusion of Thermoplastic Preforms**	**Reactive Pultrusion of Thermoplastics**
Reinforcement Type	Wide variety available	Limited to preimpregnated preforms	Types available like thermoset pultrusion Reaction-compatible resin
Reinforcement structure	Wide variety available, various structures	Limited by preform	Same as in thermoset pultrusion
Fibre content	Variable wihtin limits, up to 80 m%	Fixed by prefrom	Same as in thermoset pultrusion
Resin	Medium viscosity (~1Pas) Adequate fiber wetting	High viscosity (1-10 Pas) Poor wetting	Low viscosity (0,01-0,1 Pas) Perfect wetting
Die Temperature	Critical for proper cure inside the die	Less critical Preheating is necessary for proper consolidation	Critical for proper polymerisation Preheat for fiber drying
Die Design	Straight die front Inlet with radius Long enough for curing Specified to profile geometry	Tapered die front Cooling zone Same die for different profiles with on-line thermoforming	Injection port Long enough for polymerisation Cooling zone Same die for different profiles with on-line thermoforming
Pulling (process) Speed	Critical Has to be optimised	Critical Has to be optimised	Critical Has to be optimised

Table 6. Grouping of different pultrusion methods [103]

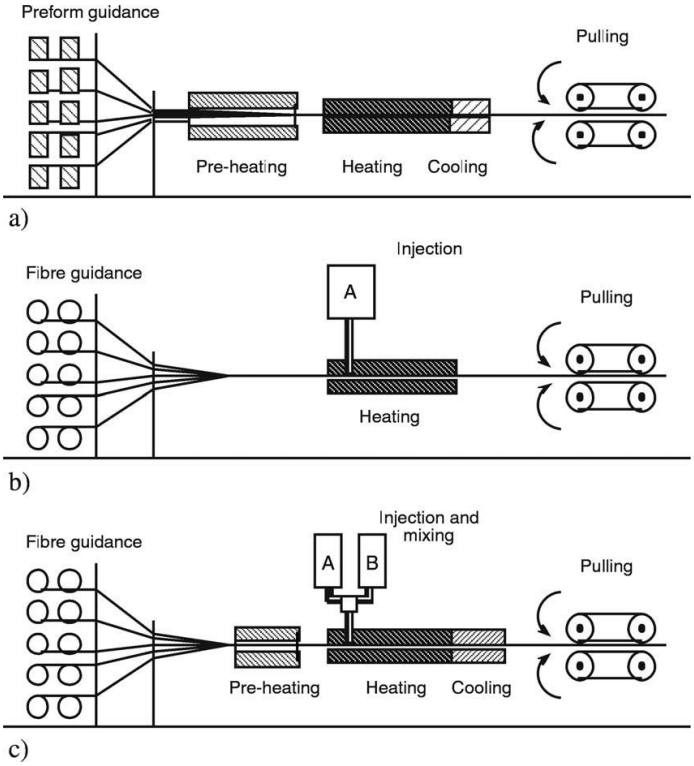

Figure 18. Sketches of different pultrusion processes: (a) non-reactive pultrusion of thermoplastic performs; (b) reactive pultrusion for thermoset composites; (c) reactive pultrusion for thermoplastic composites [104]

According to Table 6 [103] application of thermosetting resins are the simplest from process control point of view compared to the other methods. Die temperature profile is to be kept constant beside the constant process speed. This ensures proper crosslinking and constant product quality. During thermosetting pultrusion (Figure 19) fibers (a) are led through guides into a resin bath (c) to impregnate with a thermoreactive resin, usually unsaturated polyester. The impregnated fiber structure is led into a heated die (d) which forms the composite and where the crosslinking reaction starts. Then comes the post curing (e) unit which is preheated and crosslinking is completed there. Thereafter the puller (f) is found which sets up process speed and is usually a reciprocating caterpillar device. After this the profile is cut by a pneumatically moved cutoff saw [102].

Thermoset pultrusion is widely used all over the world owing to its high productivity and constant good quality of these products. Construction profiles, antenna radomes, cable ducts, linings and any other constant cross section profiles are produced by this method [105].

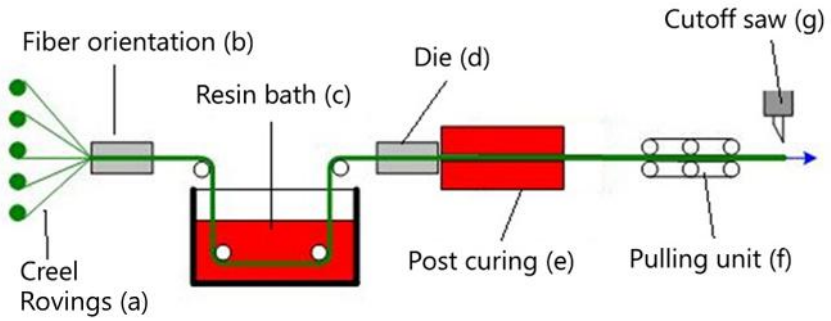

Figure 19. Thermosetting pultrusion process [106]

Pultrusion of non-reactive preforms (Figure 18/a) needs similar process management as thermosetting pultrusion (constant die temperature profile and process speed), but requires higher pulling forces owing to the high viscosity of the applied thermoplastics.

Reactive pultrusion of thermosetting resins (Figure 18/b) is an existing, but not widely applied method since better impregnation can be achieved with the classic 'resin bath' method. In this case moderate impregnation pressure is necessary parallel to precise temperature control.

By using low viscosity reactive thermoplastics (Figure 18/c) better impregnation and faster processing speed may be achieved since the reaction is much faster, but process control is more complicated. Injection ratio and temperature profile of the two or more resin components have to be controlled during injection and the temperature profile also has to be kept constant along the die. In case of choosing a pultrusion technology these properties also have to be taken into account beside the parameters of the final product.

2.5.1. Thermoplastic pultrusion of preimpregnated reinforcements

The main difference between thermosetting and thermoplastic pultrusion is the crosslinking reaction. In thermoplastic case there is none, or just a fast polymerization reaction takes place. Another difference is the cooling zone of the die and the process temperature. There are several methods for wetting fibers – commingled yarns, powder beds, electrostatic spray systems and melt impregnation/injection. The latter is also called reactive injection pultrusion while the others are 'pultrusion of preforms' (see Figure 18/a) usually without any chemical reaction.

In case of commingled yarns [107, 108] fibers or yarns are mixed: reinforcing and thermoplastic fibers are placed beside each other (see Figure 20). Thermoplastic fibers melt inside the die and due to compression this high viscosity liquid impregnates glass, carbon or other kind of fibers.

Bechtold, Wiedmer and Friedrich [107] used glass fiber/polypropylene fiber commingled yarns to produce specimens with rectangular cross sections and unidirectional reinforcement. Reinforced pipes were also produced starting from a braided preform. All of these composites possessed appropriate mechanical properties showing the applicability of this commingled yarn method.

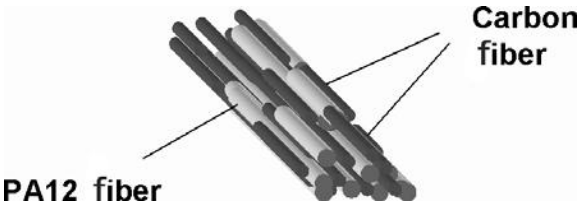

Figure 20. Scheme of a commingled yarn [108]

In case of powder impregnation (Figure 21) the fibers are pulled through a powder bed where the polymer powder sticks to the reinforcing fibers. This polymer powder will be the matrix through the above described process. Several researchers have dealt with this topic with slightly different methods [109-112], some of them made numerical models to simulate the pultrusion process [113]. Miller *et al.* [109] used fiberglass by Owens-Corning Fiberglas with amino-silane sizing and Phillips Ryton PPS powder at a line speed of 1 m/min. Impregnating temperature was 310°C and applied pressure was 0.8 and 1.2 MPa as process progressed. In spite of high viscosity of PPS a satisfactory wet-out was achieved. A small decrease in the ILS was observed as fiber volume fraction and void content increased. The flexural strength values varied between 1100 and 1300 MPa, depending on the fiber and void content, and void content decreased flexural strength.

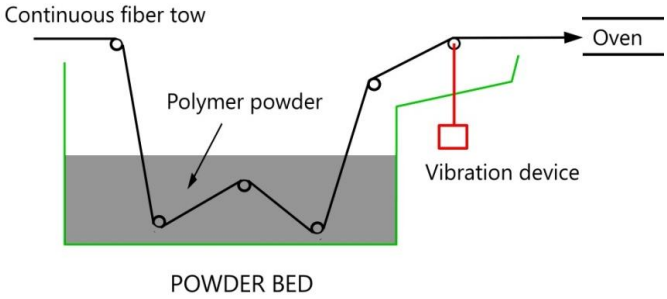

Figure 21. Scheme of powder impregnation [109]

Electrostatic powder spray coating means that electrostatically filled fiber bundles are covered by thermoplastic powder using an electrostatic spray gun (Figure 22). This prepreg-like material is lead into an oven or some kind of heating device to form a prepreg. Some researchers have already studied this topic [114, 115]. Ramani *et al.* used polyether keton keton (PEKK) with Owens Corning glass fibers in a powder spray impregnation

process at different process speeds. Through this experiment the applicability of this process was demonstrated along with the finite element model which predicts pulling forces [114]. This process was also examined by a finite element analysis method and a 'wrap-around' electric effect was shown and powder deposition along the length of the fiber bundle follows the electric field distribution [116].

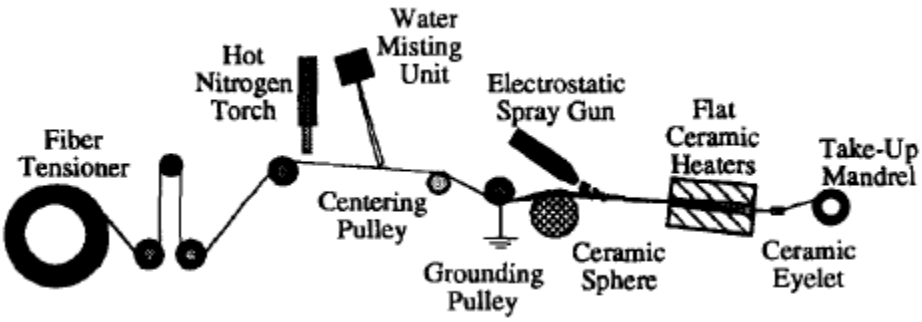

Figure 22. Schematic of electrostatic impregnation process. Water misting is necessary to make glass fibers conductive [116]

2.5.2. Injection pultrusion of thermoplastics

In case of injection pultrusion the matrix is in liquid state and is injected into the die where the resin impregnates the reinforcement. This method is applicable for both thermoplastic and thermosetting resins, but in this work only the thermoplastic version is discussed.

For injection and mainly for proper impregnation low matrix viscosity is necessary so mostly monomer or oligomer systems can be injected since polymer melts have too high viscosity. According to Luisier's work [103] polyamide 12 (lauryllactam) is adequate for this method with its low melt viscosity (around 10^{-2} Pas depending on the temperature in the range of 180-250°C). Reactive materials like this usually have two or more components so mixing is necessary. This may be a powder or liquid premix if the reaction does not start at room temperature - like in case of CBT160 powder. If premixes are not applicable special mixers with metering pumps have to be utilized. These machines can be precision gear pumps, extruders, and such devices which are capable to meter and keep warm liquid material. In case of Luisier it was a self-cleaning mixer head capable to operate up to 250°C.

Pressure is necessary for impregnating fibers, but it has to be controlled precisely. Pressure is needed to inject the matrix, but if pressure is too high, the liquid material may flow back. Backflow causes problems like mixed polymerization and viscosity profile along the die causing improper impregnation, so this is not acceptable. According to this a pressure

control and special die geometry is necessary. This problem was studied by Luisier who tested several geometries for the low viscosity lactam 12 monomer system (see Figure 23) [103].

a) *b)* *c)*

Figure 23. Special back flow and impregnation zones: a – straight; b – conical; c - siphon [103]

To avoid backflow, a conical (Figure 23/b) or siphon (Figure 23/c) die geometry seems to be useful. But examining these geometries revealed that manufacturing of a proper conical geometry is complicated and circular matrix flow may occur with the same effects of backflow. A siphon stops any backflow, but its fabrication is expensive. Wearing effects caused by the friction between the moving reinforcing fibers and the die cannot be neglected either as during production the geometry would change which affects product quality. Another problem is the higher pulling force required by the complex geometry. Taking this into consideration, Luisier [103] used a straight geometry with different inlet positions to study backflow to find out which leads to the best composite. The die is divided into three sections from a polymerization point of view (see Figure 24). First section is for impregnation where polymerization already starts but viscosity does not increase too much. The second one is for polymerization at elevated temperature. Finally comes the cooling zone where the profile is cooled down below its glass transition temperature to avoid further significant geometrical change.

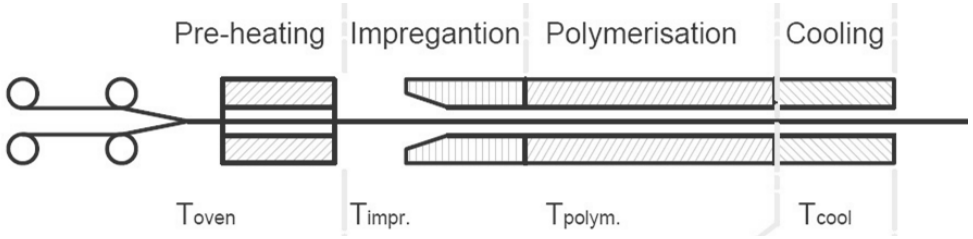

Figure 24. Scheme of Luisier's pultrusion die [103]

Composites with carbon and glass fibers were produced by Luisier [103, 104, 117] with appropriate mechanical properties. The reason why this method did not become widespread in the industry is the extreme sensitivity (the whole process has to be under nitrogen atmosphere) and high price of the polyamide 12 resin system.

2.6. Critical review of literature, aims of the thesis

From the overview of the literature it is clearly seen that high voltage industry needs new materials for cable cores. These materials have to have low CTE and be capable of operating up to 160°C and have to be crimpable since it has to be fixed somehow. After reviewing composite materials it is obvious that carbon fiber reinforced ones are ideal for this purpose with the almost negligible CTE of the fiber and its electrical conductivity. Choosing the appropriate matrix material is more complicated since thermosetting materials are widespread and a lot of experiences are known with regard to their processing. But these materials tend to micro-crack under long-term cycling load to which they are very much subjected between the utility poles their 30-year-long lifespan. Surprisingly, bending was found to be a more crucial load than tension in case of composite cable cores due to the special loads during mounting and application. Tough thermoplastic materials were overviewed and found to be proper for this application with its special loads. Thermoplastics usually have high melt viscosities originated from their long molecular chains. This problem can be overcome by the *in-situ* polymerization of a reactive thermoplastic resin. Finally a reactive polyester was chosen (Cyclic Butylene Terephthalate, abbreviated as CBT by Cyclics Corp.) with a low melt viscosity of 0.02 Pas at 190-200°C and good outdoor resistivity of the resulting pCBT, which is chemically identical to PBT. The low viscosity makes impregnation fast and easy but CBT is rather sensitive to process conditions. More than 40 scientific papers were studied to understand its polymerization kinetics and crystallization properties. According to the literature CBT can be polymerized into a proper matrix material with appropriate adhesive connection to the reinforcement. Some of the processing parameters are described, but for example a function between degree of crystallinity and cooling speed or one between viscosity and time in the whole processing temperature range have not been set up. Composites were also produced by different methods like hot consolidation, resin transfer molding and a kind of prepreg method. All of them are complicated and no continuous production method was realized. The IHP process developed by Steeg [46] is a quasi-continuous method, but capable of producing literally endless sheets and is rather complicated. These composites were mostly reinforced with glass fibers, carbon fiber reinforced ones were hardly studied.
Toughening agents may be useful for CBT to overcome special processing conditions, like quenching. For this purpose the tough polyester, polycaprolactone was chosen on the basis

of the literature. The application of this additive has been partially studied by Baets, but some questions are still unanswered especially in the field of CBT/PCL matrix composites. Some nano-scale modifiers were also examined and found to be useful with CBT, but these nano-materials were not successfully applied in fiber-reinforced composites. Graphene was also not tested but this material is believed to be a suitable agent to increase electrical and heat conductivity. Graphene and carbon fiber reinforced hybrid systems are also to-be-developed.

Production of profiles with continuous cross section geometries is the simplest by pultrusion. This process was reviewed and found to be applicable for low viscosity reactive thermoplastics seen in the example of Luisier's work [103]. According to this the pultrusion technology can be adapted to CBT which has not been done so far.

According to the above the aims of this PhD thesis are the followings:

1. Development of a pultrusion method, design of a device and description of the process parameters for CBT.
2. Development of a manufacturing method for carbon fiber reinforced composite sheets with CBT matrix that may serve as semi-finished products for the composite industry and investigates the properties of the resulting composites.
3. Increase toughness with polycaprolactone and find an optimal proportion of it for HVTL-like applications.
4. Increase of the heat and electrical conductivity of CBT with graphene nanoplatelets.
5. Increase of the interlaminar shear properties of the composites through adding polycaprolactone or graphene to the matrix.

3. Materials and methods

In this section the applied materials and processing methods will be introduced.

3.1. Applied materials

Matrix material

As matrix material CBT160 powder was used. For all experiments material from the same lot (#000071-25S-01) was used and it was supplied by Cyclics Europe GmbH. (Schwarzheide, Germany). This CBT160 contains 3 mol‰ catalyst [67] - Fascat 4101 (butylchlorotin dihydroxide) by Arkema Inc. (PA, USA) [118]. Before usage the CBT160 powder was dried in an air-circulating oven at 80°C for 8 h in order to remove residual moisture [46].

Matrix modifiers

As toughening agent, polycaprolactone (CAPA 6505) with an average molecular weight of 50kDa was supplied by Perstorp Ho9lding AB. (SE) and used as received.

Graphene was used to increase electrical and heat conductivity and to improve interlaminar shear properties of the composites. This material was purchased from XG Sciences Inc. (Lansing, MI., USA). Grade H graphene was used with an approximate layer thickness of 15 nm and a typical surface area of 50-80 m^2/g and an electrical conductivity of 10^7 Siemens/m. The nanoplatelets have functional groups, eg. hydroxyls, which were placed there during the production of these materials (these data were provided by the supplier). These nanoplatelets were used as received [119].

Reinforcing materials

Two different kinds of carbon fibers were used throughout this study. *Unidirectional* carbon fiber fabric was supplied by ZOLTEK Zrt (Nyergesújfalu, Hungary) with a product designation of Zoltek PX35 FBUD0300. This fabric is built up by 50k rovings which are held together with glass yarns. PX35 has sizing for epoxy which is compatible with CBT160 and contains a binder for epoxy resins which does not affect the cooperation with CBT [97]. *Woven* carbon fiber structure was produced by the SGL Group under the trade name of Sigratex KDL 8003 with a surface weight of 200 g/m^2. This fiber structure has sizing for epoxy which is compatible with CBT [97].

3.2. Applied experimental methods

Two types of experimental methods were used: *characterizations* to examine processing properties and *'classical' mechanical tests* to analyze the quality of the produced composites. All mechanical tests were performed at room temperature (25°C) and at a relative humidity of 40±5%.

3.2.1. Characterization methods

Several characterization methods were used, such as thermal analyses and rheology to study processing parameters and understand how the modifiers alter them.

Rheology

Rheological tests were performed on a plate-plate rheometer (Ares, Rheometric Scientific, NJ, USA), with a plate diameter of 25 mm. The testing procedure was the following: the chamber was preheated to the desired temperature, and then the dried CBT was introduced to the platen. The complex viscosity and its changes with time were measured at constant temperatures. ω had a constant value of 40 rad/sec, the frequency was 20 Hz and the gap size was set to 1 mm.

Differential Scanning Calorimetry

Calorimetry tests were performed using a Mettler Toledo DSC821 device. For the differential scanning calorimetry (DSC) tests 6-8 mg samples were used and subjected to a heating-cooling-heating cycle between 20-270°C with a heating/cooling rate of 10°C/min, if other is not indicated.

To investigate crystallization-cooling speed function, the following set-up was used: heating rate was set for 10°C/min, whereas the cooling rate was varied (20, 40, 60, 80 and 100°C/min) to study the effect of cooling speed on the degree of crystallinity of the pCBT. The crystallization enthalpy ($\Delta H_{c,sample}$) was determined via integrating the area under the melting peak of the second heating cycle. The degree of crystallinity (χ_c) was calculated by assuming 142 J/g ($\Delta H_{c,total}$) for the heat of fusion of the 100% crystalline PBT according to equation (1) [77, 120].

$$\chi_c = \frac{\Delta H_{c,sample}}{\Delta H_{c,total}} \cdot 100 \quad (1)$$

where χ_c is the crystalline fraction [%]; $\Delta H_{c,sample}$ is the crystallization enthalpy of the sample [J/g]; $\Delta H_{c,total}$ is the crystallization enthalpy of the 100% crystalline PBT [J/g].

Modulated DSC (MDSC) analyses were performed with an amplitude of 0.5°C and a frequency of 40 sec with a heating rate of 5°C/min.

Gel permeation chromatography

Gel permeation chromatography (GPC) was performed in the GPC Laboratory of Cyclics Europe GmbH with the kind help of Dr. Thorsten Hartmann.

GPC conditions were the following: A 95%/5% mixture of chloroform and HFIP (1,1,1,3,3,3-hexafluoro-2-propanol) was used as eluent. Different polystyrene standards between 2970 and 2061000 g/mol are suited for calibration. The GPC operated at 1 ml/min at 40°C column temperature, the injection volume was 1 µl, all peaks are detected at 254 nm and the runtime is 27 min. All data were generated using the Phenogel^{TM} columns.

Determination of molecular weights was the following: After polymerization of CBT160 to pCBT a small crushed sample of ~30-70 mg was dissolved in a 1 ml mixture of CH_2Cl_2/HFIP (75%/25%) at 70°C. After complete dissolving 3 ml of chloroform and a few microliters of oDCB as internal standard were added to the solution followed by filtration into a HPLC vial through a 0.45 µm filter. The measurements were performed with a mixture of chloroform/hexafluoro-2-propanol (HFIP) as solvent (98/2 $CHCl_3$/HFIP). The flow rate was 0.8 ml/ min at a constant temperature of 20°C.

Dynamic Mechanical Analysis

Dynamical mechanical analysis (DMA) was performed on a TA Instruments Q800 device. The applied temperature range was -120 to 150°C with a heating range of 2°C/min. The applied experimental method was tensile mode with a fixed strain of 5 µm at a frequency of 10 Hz. The tensile arrangement was chosen due to the sample thickness (~1 mm).

Thermogravimetry

Thermogravimetrical (TGA) analysis was performed on a Shimadzu DTG60 device in a temperature range of room temperature to 600°C in order to examine decomposition. Oxygen atmosphere was chosen because the materials developed throughout this study will be used outdoors and an inert atmosphere would lead to different decomposing mechanism. For these measurements aluminum pans were used with an approximate sample weight of 20 mg.

Thermal conductivity

The applied thermal conductivity test method was the following (Figure 25): A sheet specimen is introduced between two known-temperature reference. Thermal power is

calculated on the basis of the input electrical heating power at the higher temperature side (T_1). Based on this heat flow and thermal gradient can be calculated and finally their quotient is the coefficient of thermal conductivity (α_{heat}).

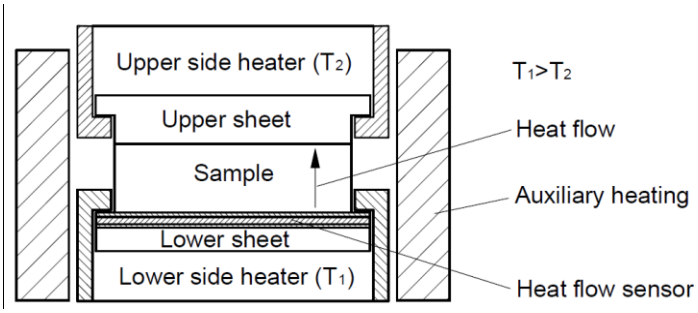

Figure 25. Schematics of heat conductivity test

Electrical conductivity

Electrical conductivity was determined via the 4-point resistivity test. Sensors were placed at 20 mm intervals. Since the tested sheets were thicker than the distance between the sensors, specific resistivity was obtained as follows (2):

$$\rho_s = \frac{\pi \cdot b}{ln2} \cdot \left(\frac{U}{I}\right) \tag{2}$$

where ρ_s is the specific resistivity [Ohm/cm]; b is the specimen thickness; U is the applied voltage [V], I is the current [A].

Conductivity was calculated knowing that resistivity and conductivity are in reciprocal relation (3):

$$\sigma_c = \frac{1}{\rho_s} \tag{3}$$

where σ_c is the conductivity [S/m].

X-ray diffraction

Both small and wide angle X-ray diffraction was performed on pCBT and graphene-modified pCBT sheets. Radiation was CuK alpha in reflexion mode.

Crystalline layer distance was calculated according to Bragg's law [121] (4):

$$2 \cdot d \cdot sin\theta = n \cdot \lambda \tag{4}$$

where d is the crystalline layer distance [m]; Θ is the Bragg angle [°]; n is the reflexion order (in this case 1) [-]; λ is the wavelength – for CuK alpha: 1.54×10^{-10} m.

Microscopy

Three different microscopy methods were applied during my work: optical, scanning and transmission electron microscopy.

Optical microscopy

Pictures were taken of the cross-sections of the composites by an Olympus BX51M optical microscope equipped with Canon Camedia C5060 digital camera with AnalySIS software.

Scanning electron microscopy (SEM)

The broken surfaces of the specimen were first gold plated by a JEOL FC1200 fine coater device in argon atmosphere then pictures were taken of the surface by a JEOL 6380LVa scanning electron microscope. Note, that specimens were broken in room temperature.

Transmission electron microscopy (TEM)

Dispersion of the graphene nanoplatelets in the pCBT matrix was studied by TEM. The TEM device (Zeiss LEO 912 Omega) was working at an acceleration voltage of 120 kV. Thin specimens (50 nm) were prepared by ultramicrotome (Leica EM UC6, Wetzlar, Germany) cut with a diamond knife (Diatome, Biel, Switzerland), and were subjected to TEM investigations without any staining.

3.2.2. Mechanical tests

Mechanical tests were performed to analyze the properties of the composites produced and to study the effect of the modifying agents.

Tensile test

Tensile tests were carried out by a Zwick Z005 universal tensile tester (Zwick/Roell GmbH, Ulm, Germany) according to EN-ISO 527 standard with a crosshead speed of 20 mm/min in case of the unreinforced specimen.

Interlaminar shear test (ILS)

Static ILS

Static interlaminar shear tests were performed on a Zwick Z020 (Zwick/Roell GmbH, Ulm, Germany) universal tensile tester according to ASTM-D 3846-94 standard with a test speed of 1.3 mm/min.

Dynamic ILS

Dynamic interlaminar shear tests were performed on a Ceast Resil Impactor Junior instrumented pendulum equipped with a DAS 8000 data collector according to EN-ISO 8256 standard with specimen according to ASTM-D3846-94 standard. The impact energy was 15 J, and pendulum speed was 3.7 m/s. This test set-up was first introduced by Szebényi *et al.* [122] and is depicted in Figure 26.

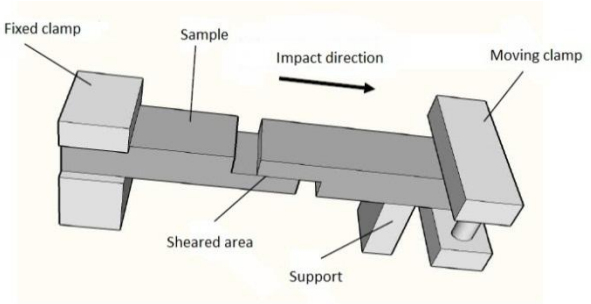

Figure 26. Sketch of the dynamic interlaminar shear stress test setup [122]

Dynamic interlaminar shear strength is given according to formula (5).

$$\tau_{din} = \frac{E}{t_n \cdot b} \tag{5}$$

where τ_{din} is the dynamic interlaminar shear strength [kJ/m^2]; E is the absorbed energy [kJ]; b is the width of the specimen (12.5 mm) [mm]; t_n is the distance between the notches (6 mm) [mm].

Flexural test

Flexural tests were performed by a Zwick Z020 (Zwick/Roell GmbH, Ulm, Germany) universal tensile tester according to the standard EN-ISO 14125 at a deformation speed of 5 mm/min. The span length applied was depending on specimen thickness and the type of the reinforcement. The width of the specimen was 15 mm in every case.

Charpy dynamic impact test

Instrumented Charpy dynamic impact tests were performed on a Ceast Resil Impactor Junior with a DAS 8000 data collector device according to EN-ISO 179 standard. The applied energy was 15 J and span length was 62 mm for the unnotched type I samples.

Ash (fiber) content determination

Fiber content (weight percentage) was determined by ashing the matrix in a Nabertherm furnace heated to 600°C for 30 minutes according to the standard EN-ISO 3451.

3.3. Sample preparation

3.3.1. Samples for characterizations

Samples for characterization experiments were produced in a hot press (Collin P200E) at 240°C. Polymerization time was 15 min under 2 MPa pressure and 1 mm thick sheets were obtained by this method.

Additives (polycaprolactone and graphene) and CBT was melt-mixed in a Brabender PlastiCorder PL 2000 type mixer at a temperature of 200°C, and at a revolution speed of

180 min^{-1} for 2 minutes. Then this mix was fine-grinded in a blender. The mix was hot-pressed according to the above written parameters. This method resulted in satisfactory nanoplatelet dispersion, which was examined by TEM (Figure 53.)

3.3.2. Composite samples

On the basis of the results achieved in 'Characterizations' chapter, composite manufacturing methods were developed. This chapter describes the one-by-one composite sample processing method in detail. These composite sheets represent a necessary product category for the automotive industry as semi-finished products.

In-situ melting and polymerization method

First composite samples were produced via an *in-situ* melting and polymerizing method described as follows: an alumina mold was covered by a PTFE foil and first a CBT powder layer was placed into the mold, which was topped by one UD carbon fiber layer. This was repeated until 4 layers of CF were placed in the mold. Finally, CBT powder was placed on the top of this "package" (for mold scheme see Figure 27). The filled mold was put into an oven, heated to 250°C, and held for 10 min. During this time all the CBT powder became molten and polymerization started. Then the mold was closed and a pressure of 2 MPa was applied for 5 min. in order to remove voids and improve fiber wetting. Finally the mold was cooled to 20°C using tap water for direct cooling. This method resulted in an average fiber mass fraction of ~20wt% (obtained according to EN-ISO 3451 standard). Unreinforced samples were produced in the same way for reference purpose [123].

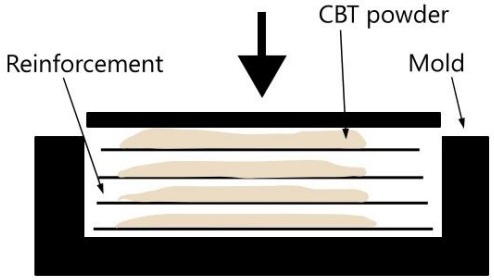

Figure 27. Composite sample production via *in-situ* melting and polymerizing method

Prepreg method

For hot consolidation a two-step method was developed based on the findings described in 'Characterizations' and in the literature. Steeg developed a single-step method for producing large parts [46]; Baets utilized a special prepregger drum-winder for unidirectional layers [93]. Both of these methods require special devices. The aim was to

develop a simple method which does not require any special device and can be easily scaled up for industrial usage.

First step - prepregging

CBT powder was dispersed onto the carbon weave (Figure 28/a). Then this structure was put into a preheated (195°C) oven for 1 min to melt the CBT powder. Due to its low viscosity and capillary action the molten CBT flowed among the fibers [123]. After 1 min the prepreg was taken out of the oven and cooled down to ambient temperature (Figure 28/b). This caused the ROP to stop and the prepreg to be ready. Due to frozen ROP, this prepreg has theoretically unlimited shelf life with a non-sticky surface which makes storage easy [46, 124].

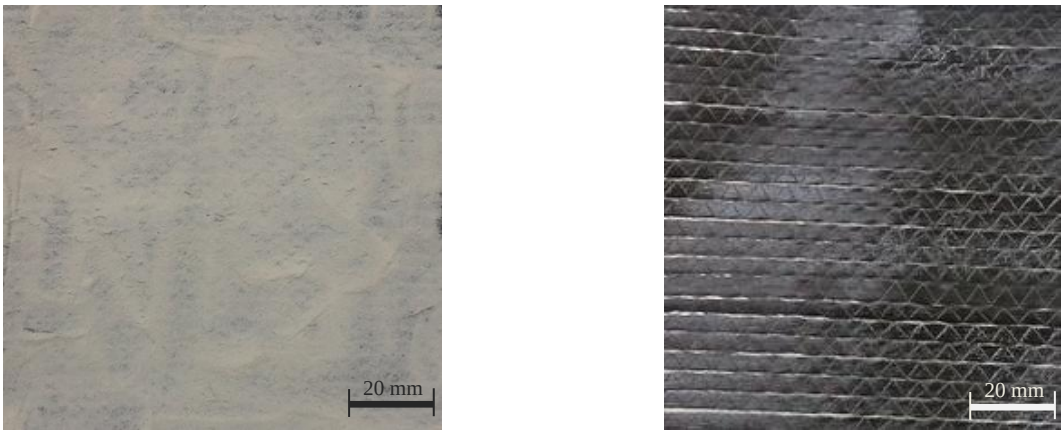

a) *b)*

Figure 28. Production of prepregs: CBT powder dispersed on UD carbon fiber weave (a), prepreg sheet (b)

Second step – hot consolidation

Composites were produced from the above described prepregs via the hot consolidation method. A composite structure was built up by 8 layers of prepregs with the orientation of (0/90°) in case of fabric, while an UD orientation was built up by the UD weave. This structure was put into a hot press (Collin P200E) preheated to 240°C. Pressing time was set to 15 min. Then it was cooled down to ambient temperature at 50°C/min. Composite sheets were obtained by this method with a thickness of ~1.5 mm and a fiber mass fraction of ~60wt% (result obtained according to EN-ISO 3451 standard) [124].

Modifying agent (polycaprolactone) was added to the pCBT after drying and a powder mixture was made in a blender. Since initial viscosity was not increased by PCL, appropriate impregnation was achieved and PCL modified matrix composites were produced via the above described method.

Premix method

Graphene and CBT were melt-mixed in a Brabender PlastiCorder PL 2000 type mixer at 200°C, 180 min^{-1} for 2 minutes which do not affect polymerization – see 'Torque curves' chapter. Then this mix was fine-grinded in a blender. The fine powder was dispersed onto the reinforcement then a new layer is placed onto the first layer and powder mix is also dispersed onto it. In this way 8 layers are built up and placed into the preheated hot press and pressed for 15 min at 240°C and 2 MPa pressure. This method resulted in ~2 mm thick composite sheets with an average fiber mass fraction of ~60wt% (result obtained according to EN-ISO 3451 standard).

3.3.3. Torque curves

During premix preparation the time-torque curves were recorded from the Brabender mixing device. In case of the polymerizing CBT torque increases after 3 min, this show a delay if compared to the polymerization kinetics examined by rheometry – see Figure 36 (the reason of this is the filling of the mixing chamber). So the two-minute premix preparation ends before polymerization could start.

If the mixing torque exceeds the value of unmodified CBT, then it decreases, than the formed peak indirectly indicates a reaction between CBT and the additive.

Polycaprolactone and CBT powder mix was tested and a massive torque increase was seen after 2 minutes (Figure 29). Based on this a reaction between PCL and CBT is assumed which is supported by a single T_g peak appearing in a DMA curve (Figure 41).

A copolymerization between CBT and PCL was also reported by Baets [93], Wu and Huang [92] and Tripathy [91], but a torque-time curve was not published by any of them.

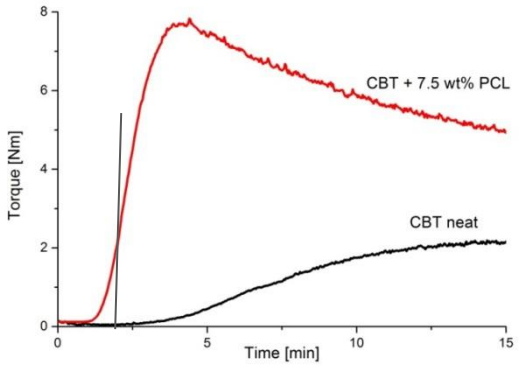

Figure 29. Torque-time curves of polycaprolactone-modified CBT samples

Graphene and CBT were also tested with different amounts of graphene. Here 0.5 and 1 wt% cases are introduced and an increase is seen in both cases (Figure 30). So the hydroxyl groups on the graphene reacted with the functional groups of CBT during ROP.

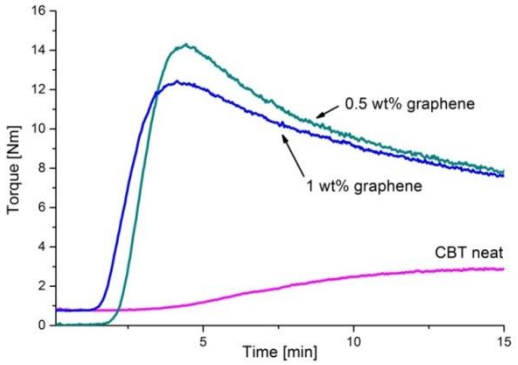

Figure 30. Torque-time curves of graphene-modified CBT samples

4. Results and discussion

Achieved results are discussed in detail in the following chapter.

4.1. Characterizations of CBT

In this chapter processing properties of CBT and effects of additives are investigated and discussed. Based on the findings of this chapter processing technologies are developed for producing composites.

4.1.1. Properties of neat CBT

Thermal, rheological and crystallization properties of CBT were examined. Based on the obtained results composite processing methods were designed, which are discussed in Chapters 3.3.2. and 4.2.

Differential Scanning Calorimetry

Calorimetrical analyses were performed in order to determine melting range, crystallization and melting temperatures. In the DSC trace (Figure 31) it is seen that melting (black line) starts at 112°C where dimers melt – first melting peak on the trace. Endothermic peaks between 112°C and 185°C are associated to the melting of different oligomers. The oligomer rings open through a nucleophilic attack of the ester groups by the Lewis acid.

During cooling one sharp peak is seen which belongs to crystallization with a peak value of 186°C.

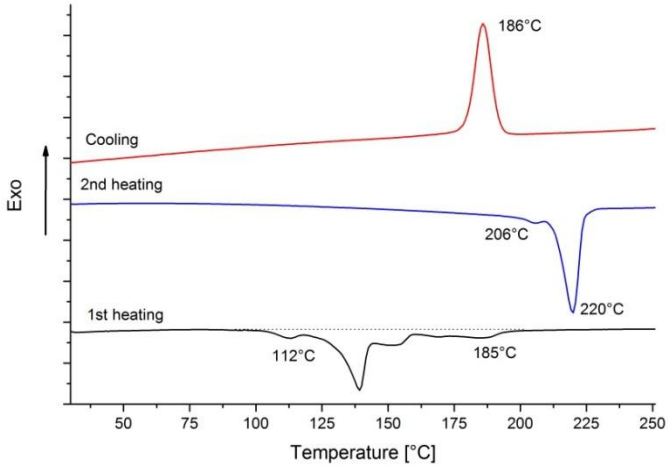

Figure 31. Heating-cooling-heating DSC trace of neat CBT160

During the second heating (blue line) two melting peaks can be observed, which have the following explanation:

Simultaneous melting and recrystallization occurs in the material: Crystals with low perfection partially melt and recrystallize at lower temperatures, in this case at 206°C. These crystals were formed during the dynamic circumstances of the relatively fast cooling (10°C/min). Similar effects were observed and studied in by CBT by Mohd Ishak *et al.* [78]. This statement was also proved by modulated DSC (Figure 32). The reversible (red) curve indicates the melting of the lower melting point instable phase (3) and the stable phase (4). Both of these phases were formed during cooling. 10°C/min cooling speed means that crystallization took place under dynamic circumstances. However, stable phase could be formed at the early, high temperature stage. The first peak (1) on the non-reversible (blue) curve indicates the recrystallization at 213°C with a released energy of 16 J/g. The second peak (2) indicates the melting of both the recrystallized and the stable phases at 225°C with a melting enthalpy of 29.4 J/g.

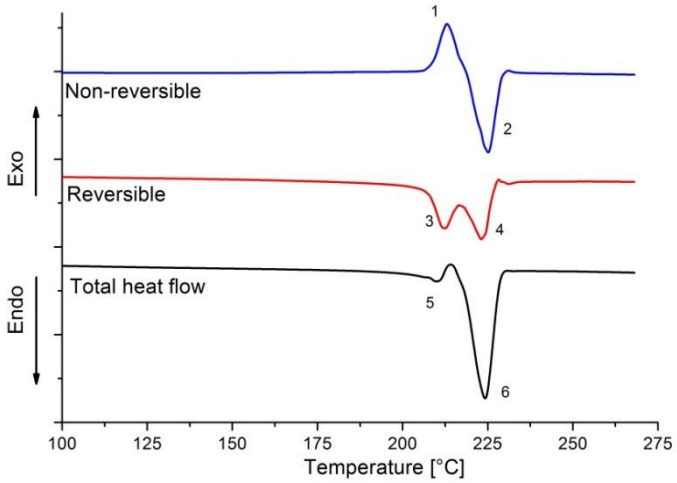

Figure 32. MDSC heating trace of pCBT

Looking at this crystallization process from the manufacturer's point of view, one can note that if pCBT is slowly cooled, the molecules have time to form perfect crystals. These crystals result in a rigid material, which is not suitable for application (see also literature data in Chapter 2.4.2). In order to have a ductile matrix material, low crystallinity is necessary. The simplest way to control the latter is the cooling speed, since fast cooling results in low crystalline fraction.

Effect of cooling speed was examined in the range of 20-100°C/min. Results are depicted in Figure 33 and show a decrease in χ_c with the increasing cooling speed.

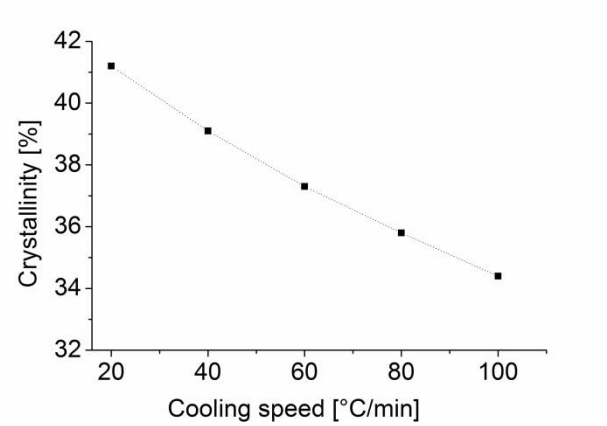

Figure 33. Crystallinity values of pCBT samples in function of cooling speed

Dynamic Mechanical Analysis

DMA was performed study glass transition and the change of storage modulus in function of temperature. Looking at Figure 34 a clear glass transition peak (α_r relaxation) at 60°C and also a β_r relaxation around -75°C is seen on the tangent delta curve (solid line). Storage modulus is decreasing with temperature as it was expected, however this decrease is less pronounced between -10 – +35°C.

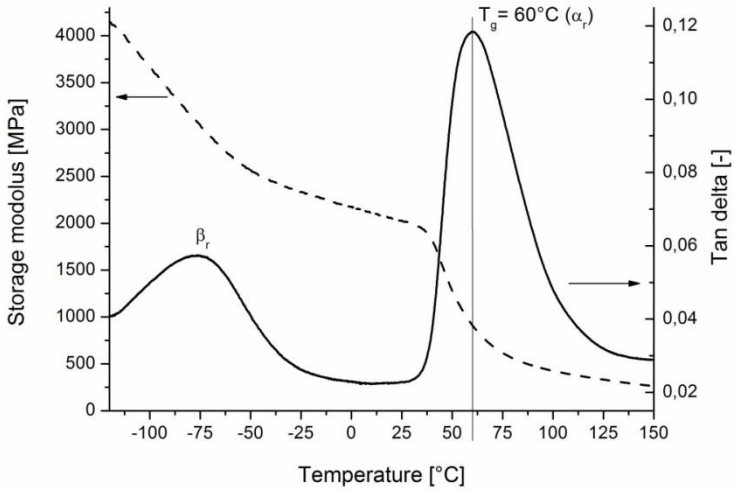

Figure 34. DMA results of a neat pCBT sample

The changes in tensile parameters are also to be taken into consideration [124]. However, the unreinforced pCBT shows a drop in storage modulus, according to the literature, fiber-reinforced PBTs may be used up to 210°C according to heat distortion temperature (HDT/A) tests (POCAN, 30wt% glass fiber filled) [125]. This suggests that carbon fiber reinforced pCBT is also applicable at least 160°C as a cable core.

Thermogravimetry

Thermal decomposition of pCBT is similar to PBT as their chemical structure is the same.

The thermal decomposition is a complex mechanism, but can be divided into two main stages: the first stage is an ionic decomposition process that leads to the evolution of tetrahydrofuran. The next stage is ester pyrolysis that results in butadiene. Parallel to both stages decarboxylation reaction takes place [126, 127].

In case of pCBT decomposition starts at 392°C – indicated by 5% weight loss (Figure 35) with the evolution of tetrahydrofuran. Weight loss is the most pronounced at 420°C, which is also shown by the derivative curve (dotted line) and after decomposition 1.2% of the original weight remains as residual ash.

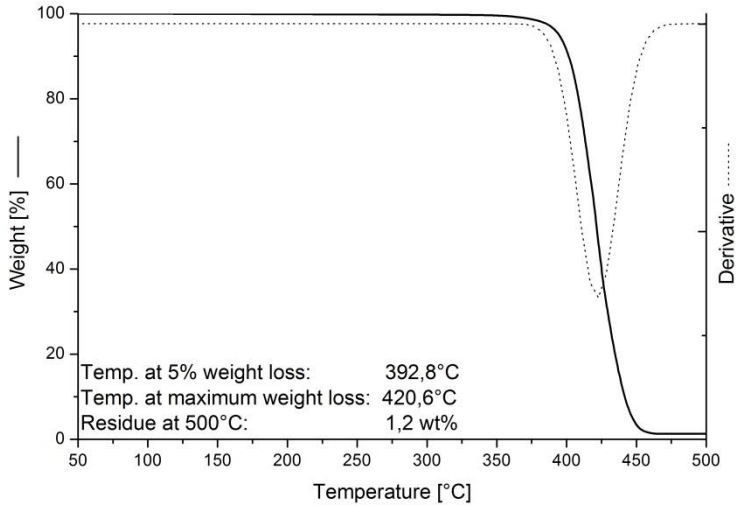

Figure 35. Thermal decomposition of pCBT

Rheology

For direct matrix impregnation a dynamic viscosity below 1 Pas of the applied resin is necessary [100]. From rheology results (Figure 36) it is clearly seen, that molten CBT has a significantly lower viscosity than this 1 Pas treshold. But the viscosity changes in function of time and temperature. This was already examined in [76], but until 210°C, and for this work experimental data is necessary until at least 240°C. At 180°C, the minimum viscosity of 0.02 Pas is not reached, while at 195°C it is. A strong viscosity increase starts after 80 seconds at the latter temperature. This increase is not that pronounced at 180°C, and it is related to polymerization. This mostly depends on the temperature and the catalyst amount (in this case it is 3 mol‰). So the higher the temperature applied, the faster the reaction is. (As a consequence, time for impregnation will be shorter at higher temperatures.) Both the 180°C and the 195°C curves end at a final viscosity of 10^5 Pas, at which point the material can be considered a solid. (Note that CBT crystallizes from the molten state rapidly below its melting point as it is a superchilled liquid [123].)

All other viscosity curves, except for the one at 255°C, go through a minimum viscosity. The viscosity increase occurs in a shorter time at higher temperatures. For example at T=210°C there are 60 seconds to impregnate the reinforcing structure before the viscosity reaches the 1 Pas threshold. The polymerization reaction, and related to this, the viscosity increase determines the time range during which molten CBT is able to wet out the reinforcement in a suitable process technology [123].

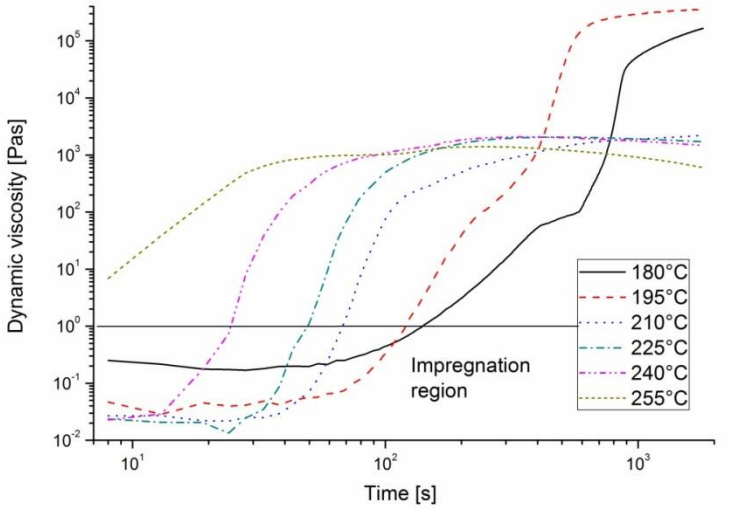

Figure 36. Dynamic viscosity change of CBT160 in function of time at various temperatures

All the viscosity curves at 210°C and above end at a final viscosity of 10^3 Pas, i.e. at the melt viscosity of PBT. Note that at the highest temperature examined (T=255°C) no viscosity minimum below 1 Pas could be detected. The reason for this is the fast polymerization reaction where CBT is converted into molten pCBT. Summing up, for impregnating reinforcement, temperatures above 185°C is ideal – all the oligomer rings are opened so minimum viscosity is reached and several tens of seconds are given for impregnation. For fast composite processing 225-240°C should be chosen [123].

X-ray diffraction

Both small and wide angle X-ray diffractions were utilized to study the crystalline structure and layer distance (d-spacing) of pCBT. The resulted scatters are depicted in Figure 37. Based on short angle scatter (Figure 37/a), crystalline d-spacing was calculated according to the Bragg equation (4) and was found to be 0.93 nm. This d-spacing belongs to the <001> crystalline plane in case of α PBT crystals.

Wide angle scatters also show that pCBT is in its alpha crystalline form with a triclinic unit cell. Characteristic peaks of this cell are theoretically the following: 16.1; 17.22; 20.506;

23.19; 25.371; 27.442; 30.72; 39.344° (2 theta) [125, 128]. All of these peaks are well resolved in the scatter (Figure 37/b).

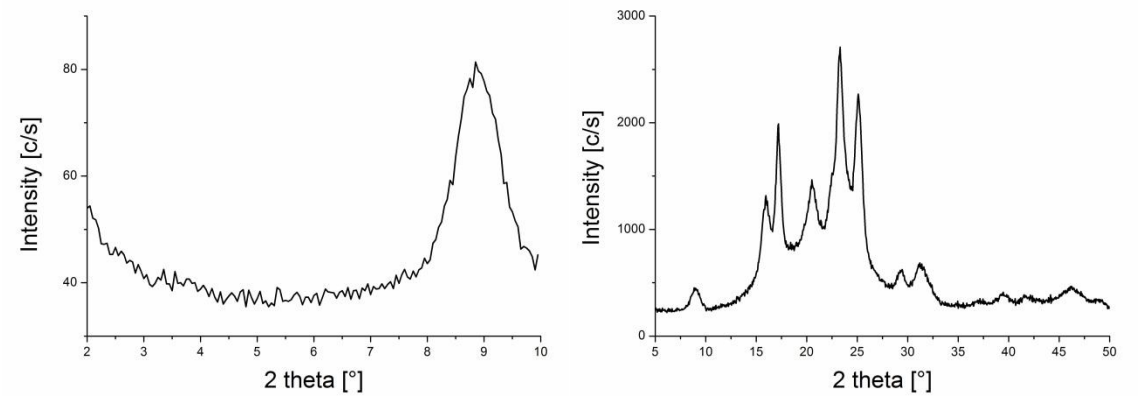

a) *b)*

Figure 37. Small (a) and wide (b) angle X-ray scattering graph of pCBT

4.1.2. Effect of polycaprolactone

Effect of polycaprolactone on the thermal and the rheological properties was investigated in order to see how these properties are influenced. Copolymerization between CBT and PCL was also studied.

Determining the optimal polycaprolactone content

Polycaprolactone was utilized to increase toughness. The main goal was to achieve appropriate properties for a matrix material for high voltage composite applications, as follows: elongation-at-break above 5% while having a minimal tensile strength of 25 MPa and a Young's modulus of 1.25 GPa in tensile test at a test speed of 20 mm/min which simulates dynamic loads [7, 27].

PCL amount was tested in the range of 0-10 wt%; with steps of 2.5 wt% and the results obtained are shown in Figure 38. Optimal value was determined by using the above criteria. According to these 7.5 wt% of PCL was chosen for further experiments [124].

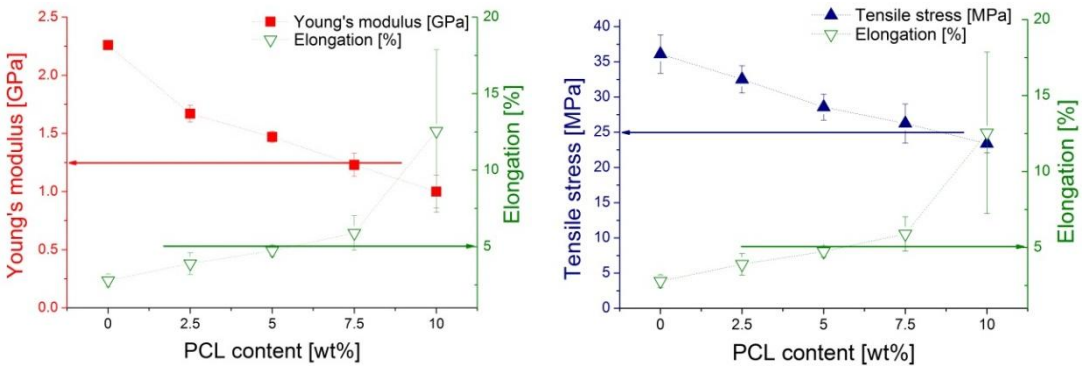

Figure 38. Tensile results to determine additive amount: Young's modulus (a); strength and elongation (b)

Differential Scanning Calorimetry

According to calorimetry tests a decrease in melting temperature and in crystallization enthalpy can be observed (Table 7). Change in enthalpy is believed to be caused by PCL which copolymerizes with CBT. Copolymerization resulted in lower crystallinity which toughens the material (as will be discussed later). Copolymerization between pCBT and PCL was also studied by DMA.

	Crystallization enthalpy [J/g]	Melting temperature [°C]
pCBT neat	47.3±0.8	224±2
pCBT + 7,5w% PCL	31.5±1.2	218±3

Table 7. Calorimetry results of neat and 7.5wt% PCL modified pCBT

DSC heating scans also show a difference in the crystalline melting properties (Figure 39). In case of unmodified pCBT two melting peaks are seen (1) indicating the melting-recrystallization-melting process as it was discussed earlier. Adding PCL to the system decreased the onset temperature of melting and a broader peak appeared (2). Melting peak temperature has moved from 224 to 218°C. This finding suggests that crystals with different perfection grow in presence of PCL and this caused the broadening of the melting peak [124].

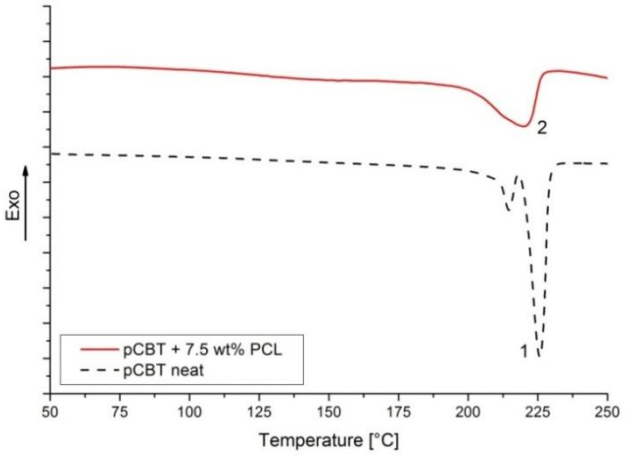

Figure 39. Heating DSC traces of 7.5 wt% PCL modified and unmodified pCBT

Taking a look at Figure 40 cooling properties of PCL modified pCBT is seen in comparison with neat pCBT. In case of pCBT (dashed line) a narrow crystallization peak (1) is seen at 187°C. After adding polycaprolacrone to the system crystallization range moved down and two peaks appeared (2) at 182 and 175°C. This finding suggests that PCL reduces the supercooling effect and due to this crystallization peak shifts towards to lower temperatures [124].

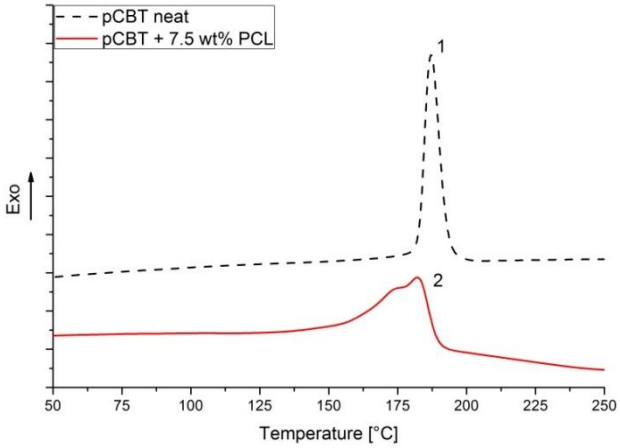

Figure 40. Cooling DSC traces of 7.5 wt% PCL modified and unmodified pCBT

Dynamic Mechanical Analysis

In case of using PCL as a toughening agent a decrease in both glass transition and β relaxation is seen in Figure 41. T_g is decreased from 60 to ~50°C (see peaks 5 and 6 in Figure 41), which means that CBT and PCL are copolymerized. The measured T_g is close to the theoretical T_g according to the Fox equation (6). This equation can be used here since the CBT-PCL copolymer can be considered as a random copolymer [93, 129].

$$\frac{1}{T_g} = \frac{W_1}{T_{g1}} + \frac{W_2}{T_{g2}} \tag{6}$$

where T_g is the glass transition of the copolymer [K]; T_{g1}, T_{g2} are the glass transition temperatures of the base materials [K] (pCBT: 335 K, PCL: 213 K); W_1, W_2 are the mass fractions [wt%]. According to (6) the T_g of the copolymer is 46.5°C, while the experimental value is 50°C. These values are close enough to each other to prove copolymerization (transesterification) indirectly between pCBT and PCL [124].

The single T_g peak in Figure 41 (point 5) suggests that copolymerization occurred, since no T_g peak of PCL is seen around -60°C, whereas a decrease in β relaxation peak (point 1). The onset temperature of the glass transition also decreased about ~40°C (see points 3 and 4). An additional peak shoulder is appeared (point 3*) which is caused by structural changes in the molecules owing to the presence of PCL.

In Figure 42 the plateau on the storage moduli curves before glass transition onset is narrower than in case of the reference material (points 1 and 2). An additional shoulder is also appeared here (1*), same as the other one (3* on Figure 41) owing to the structural changes caused by the addition of polycaprolactone. These findings indicate higher sensitivity to temperature rise for polycaprolactone-modified pCBT, even though it is

tougher. This reduction has to be taken into account in application design, but does not reduce applicability [124].

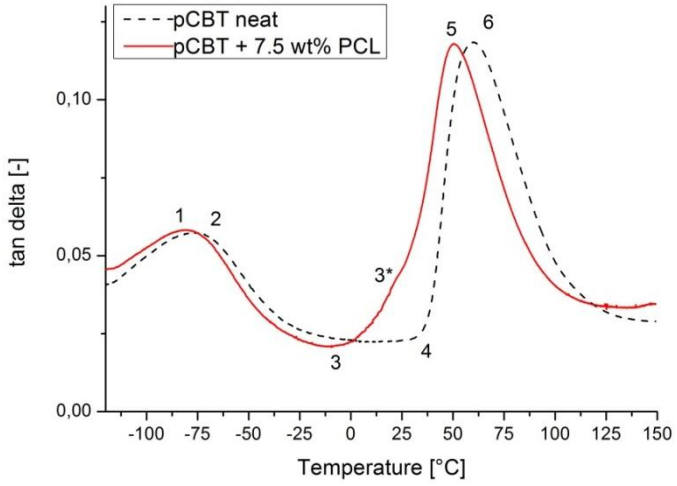

Figure 41. Tangent delta values of neat pCBT and pCBT+PCL samples

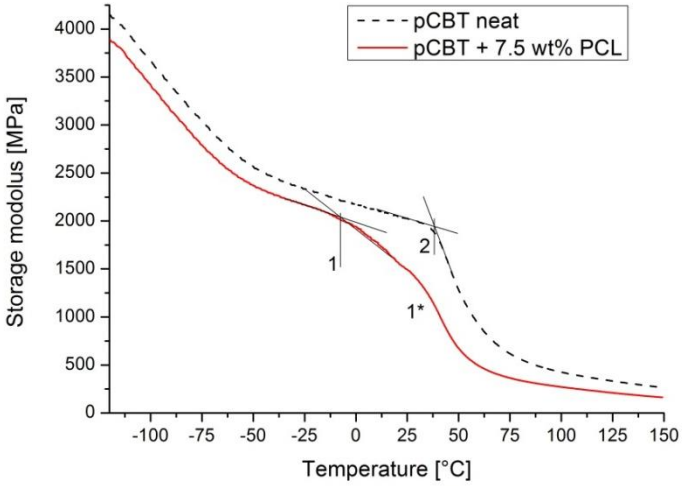

Figure 42. Storage moduli values of neat pCBT and pCBT+PCL samples

Thermogravimetry

Decomposing properties of pCBT and PCL-modified samples are depicted in Figure 43 and data are shown in Table 8. According to these data it is clearly seen that addition of PCL decreased the onset of thermal decomposition indicated by the temperature belonging to 5% weight loss. Temperature belonging to maximum weight loss rate has also decreased with more than 20°C. This phenomenon is explained by the less thermally stable molecular structure of the copolymer. It is also observable, that at 500°C much more char is produced during the decomposition of PCL than in case of pCBT.

Decomposition of neat PCL is a two-step method, starting with a statistical rupture of the polymer chain via ester pyrolysis which results in water, carbon dioxide and 5-hexanoic

acid. The second step is unzipping depolymerization resulting in ε-caprolactone cyclic monomer [130, 131]

Decomposition of the copolyester is suggested to be the following: Due to the small amount of PCL in the system and because both material decomposes via ester pyrolysis the process is mainly governed by the decomposition of pCBT. However, the thermal stability of the copolymer is lower than neat pCBT (note, that decomposition of PCL start at 360°C as reported by Persenaire [130]). Reason of the significantly more char is unzipping depolymerization of PCL resulting in cyclic monomers which are considered to be thermally stable.

	Temperature at 5% weight loss [°C]	Temperature at maximum weight loss [°C]	Residue at 500°C [wt%]
pCBT	392.8	420.6	1.2
pCBT + 7.5 wt% PCL	373.7	393.2	5.6

Table 8. Thermal decomposing properties of pCBT and PCL modified pCBT samples

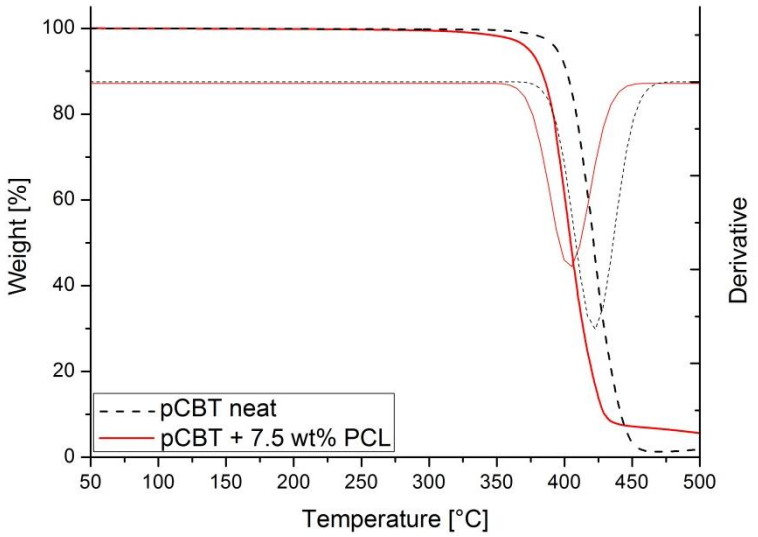

Figure 43. Thermogravimetrical curves of pCBT and PCL modified pCBT samples

Rheology

Initial viscosity of polycaprolactone-modified CBT was examined in order to determine the processing window with regard to impregnation. According to Figure 44 both modified and unmodified CBT have the same initial viscosity ~0.04 Pas at 240°C. (240°C was selected for rheology because this temperature seems to be the best for composite processing.) This water like viscosity starts increasing after 30 seconds. This time is enough for impregnation of literally any reinforcement due to the low viscosity of the material especially in case of pultrusion. One can note that polycaprolactone does not

hinder the ROP process, but even increases it slightly. Viscosity starts increasing more than 10 seconds earlier than in case of neat CBT. This suggests that PCL incorporates in the polymerization process and this supports the previous statement about copolymerization.

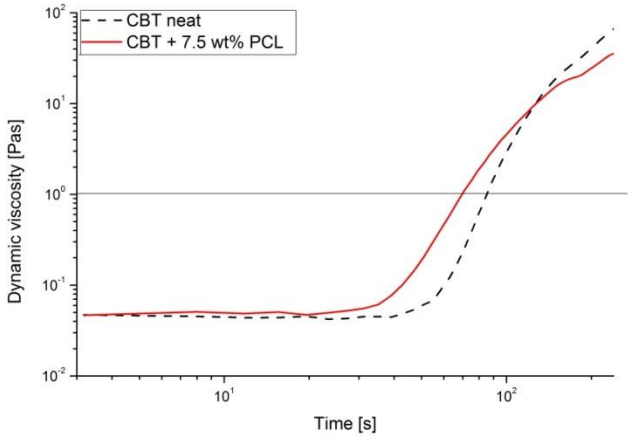

Figure 44. Effect of 7.5 wt% PCL on the initial viscosity of CBT at 240°

4.1.3. Effect of graphene

Graphene was utilized to increase the heat and electrical conductivity of pCBT. So thermal, crystallization, rheological, heat and electrical conductivity properties were determined.

Differential Scanning Calorimetry

DSC was carried out to study the effect of graphene on the melting and crystallization properties of the nanocomposites. An initial assumption was made regarding the effect of graphene: these nanoplatelets may act as crystallization nucleation agents. This would mean that crystallization starts at higher temperatures during cooling.

Results obtained from graphene modified pCBT samples clearly verify this assumption. Figure 45 shows the change of the crystallization peaks and Figure 46 indicates the change of the peak values. During cooling graphene nanoplatelets serve as nucleation points from where crystallization can start so graphene-filled CBT can be less supercooled. This type of nucleation is called heterogeneous nucleation since there are foreign solid particles from where crystal growth can start [129]. Due to the hydroxyl groups on the nanoplatelets chemical bonds are formed between graphene and pCBT. (These functional groups were placed during the manufacturing of the nanoplatelets.)

The more graphene is in the system the easier the start of the crystallization – the higher the peak temperature will be. In case of 3 and 5 wt% graphene crystallization starts above

210°C (see the onset temperatures in Figure 45). According to this the more nucleation agents are in the crystallizing system the higher the onset temperature will be.

In case of melting an interesting phenomenon was explored. Unmodified pCBT has double melting peak (206 and 220°C respectively; see Figure 31). Possible explanations for this were discussed in the Section 'Properties of neat CBT'. What is surprising after adding different amounts of graphene is that the smaller peak starts growing (Figure 47). This occurs due to the nucleating effect of graphene – the more graphene is in the system, the more perfect structure is formed. So recrystallization starts at higher temperatures.

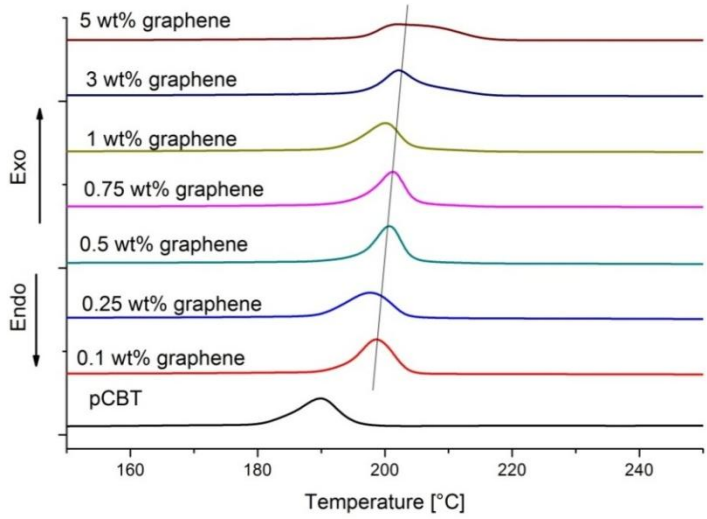

Figure 45. Cooling DSC scans of graphene modified pCBT samples

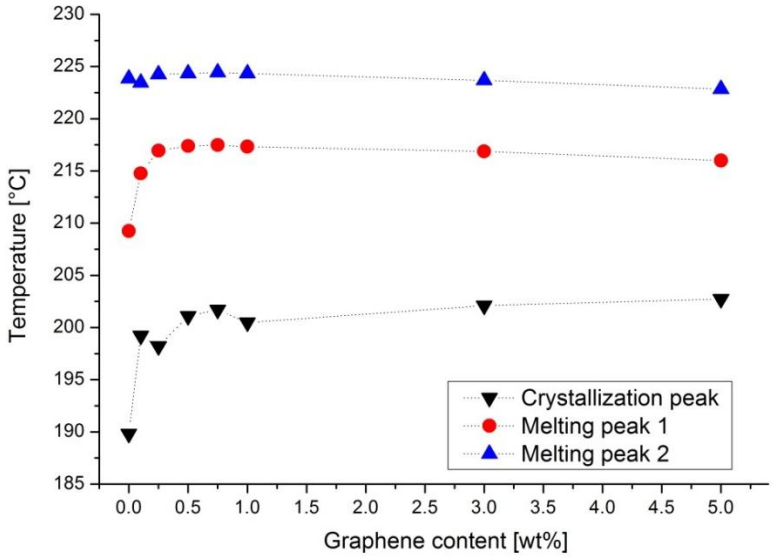

Figure 46. Change of melting and cooling peak temperatures in function of graphene content

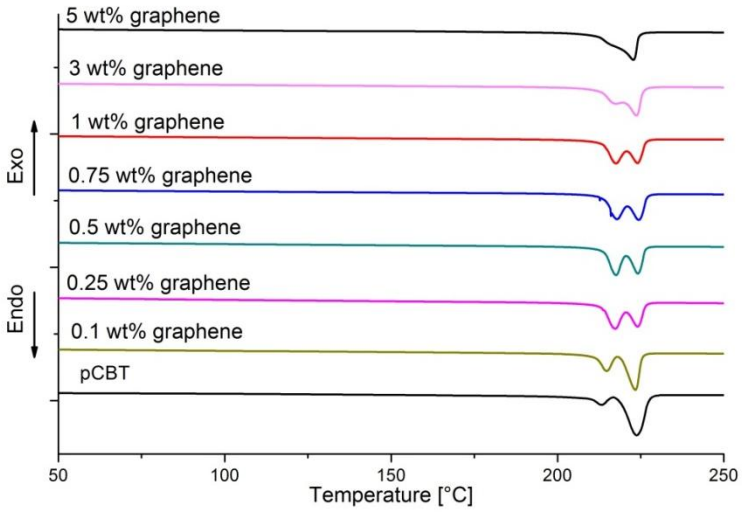

Figure 47. Melting DSC scans of graphene containing pCBT samples

Based on both melting and crystallization enthalpies, crystalline fraction was determined according to (1). Results are depicted in Figure 48. One can note that crystallinity based on the cooling data show a slight increase in function of graphene content. On the other hand, data obtained from the melting enthalpies show also a slight change, and these χ_c values are higher than the cooling-based one. This likely indicates the extra energy necessary for the partial recrystallization. The reason of the maximum at 3 wt% graphene content of χ_c curves (dotted lines in Figure 48) is the too much graphene which demobilize the polymer. Through this, the amount of crystalline fraction is limited.

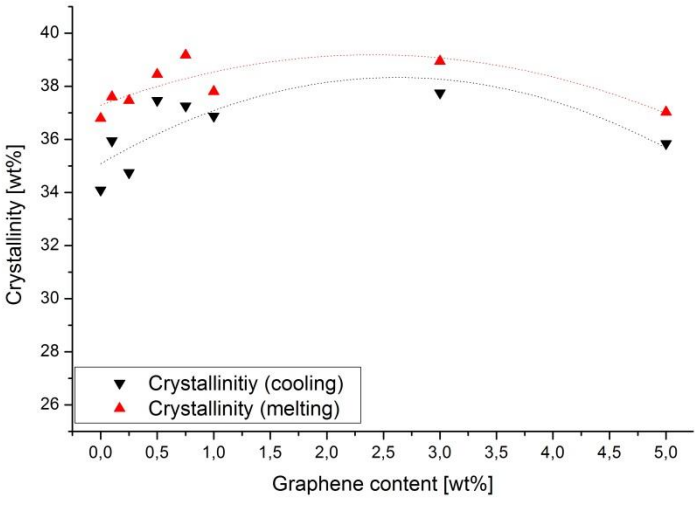

Figure 48. Crystallinity in function of graphene content

Dynamic Mechanical Analysis

DMA was utilized to examine the effect of graphene content on glass transition temperature and other temperature-dependent mechanical properties. For this purpose

measurements were performed between 0 and 150°C. According to Figure 49 there is no significant change in the peak of the tangent delta curves – as it was expected. T_g remains in the range of 60±5°C range so graphene has no significant effect on the glass transition. However, it has to be noted, that a slight decrease in T_g occurred through the presence of graphene.

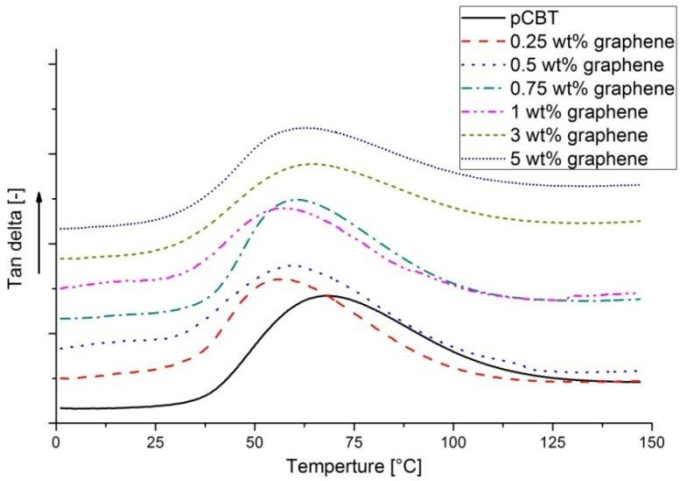

Figure 49. Tangent delta curves of pCBT samples containing different graphene amount (curves shifted along the y axis for better visibility)

Figure 50 shows the change of storage moduli in function of graphene content. According to these data a significant reinforcing effect is seen, graphene clearly increased the storage modulus. Around the T_g range a pronounced decrease is seen, but above glass transition the nanoplatelets still show some reinforcing effect, especially in case of 5 wt% graphene. Interestingly 0.75 wt% graphene also has a significant reinforcing effect, probably because of the better-than-the-average dispersion.

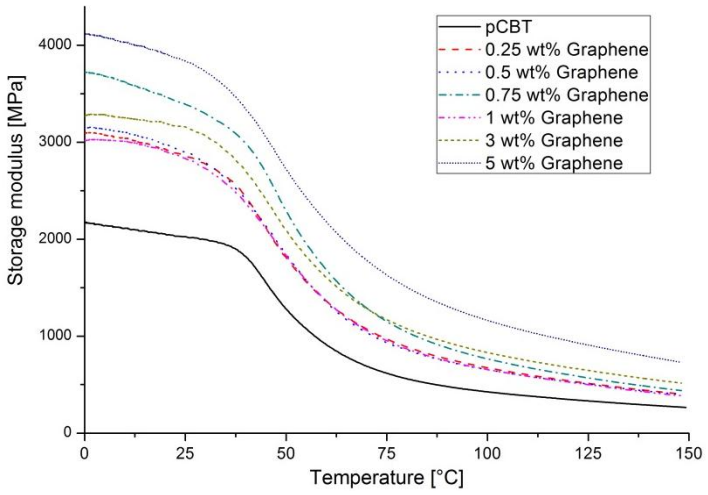

Figure 50. Storage modulus curves of pCBT samples containing different graphene amount

Thermogravimetry

Thermogravimetrical curves (Figure 51) allow us to study the thermal decomposing properties of graphene-modified pCBT. Temperatures indicating the maximum weight loss and residual char are depicted in Figure 52. These results suggest a slight thermal stability-increase induced by the presence of graphene. This does not correspond to the literature, where increased thermal stability was found among polyesters filled with graphene owing to the enhanced barrier properties [44, 132], however, pCBT/graphene nanocomposites have not been studied yet. Similar, moderate increase in thermal stability was reported about PBT-CNT nanocomposites [133, 134] so this result is not surprising

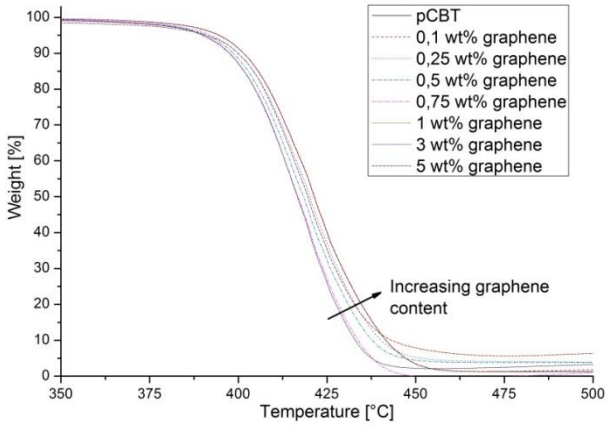

Figure 51. Thermogravimetrcical curves of graphene-modified pCBT samples

In the current case the possible reason may be the improper exfoliation of graphene nanoplatelets which is also confirmed by the TEM pictures (Figure 53) but the enhanced thermal conductivity and the interlaminar properties of the carbon fiber reinforced composites are against it (Figure 55). The resulted increase in the amount of ash is due to the presence of graphene – these nanoplatelets are thermally stable and do not decompose in the examined temperature range.

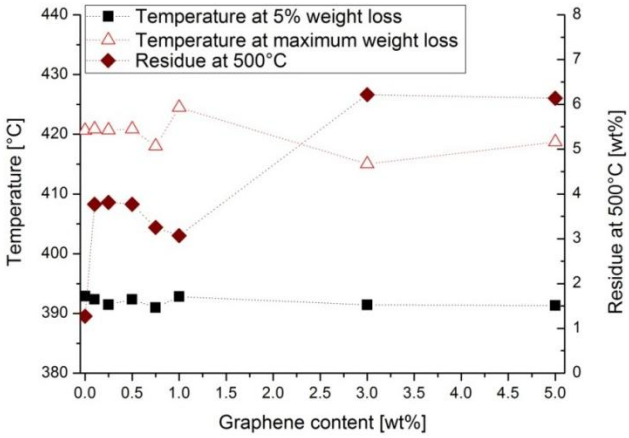

Figure 52. Thermal decomposing properties of graphene-modified pCBT samples

Transmission electron microscopy

Dispersion of graphene nanoplatelets were studied by transmission electron microscopy. The TEM images (Figure 53) show some nanoplatelets (a) as reference and pCBT – Graphene nanocomposites with 1 wt% filler content. According to this small agglomerates remained in the composite which suggests that exfoliation was not complete. This finding helps explaining the modest results of the electrical conductivity test.

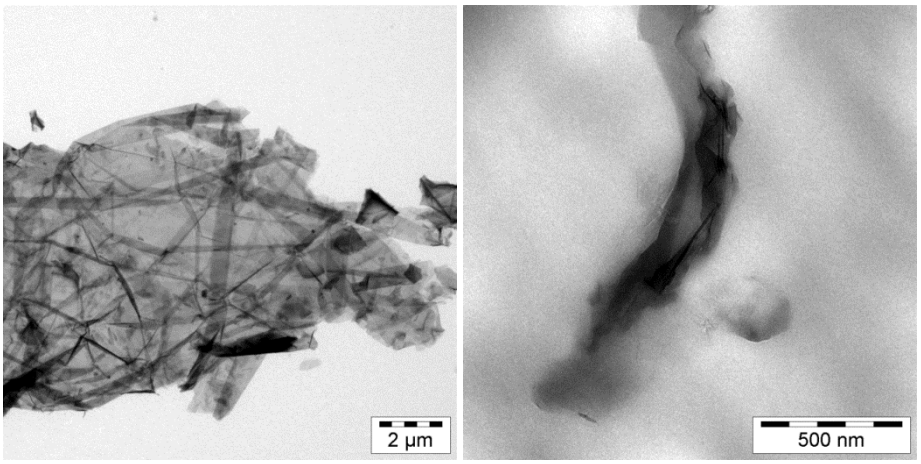

a) *b)*

Figure 53. TEM images of graphene nanoplatelets (a) and graphene-pCBT nanocomposite

Rheology

Effect of graphene on the initial viscosity of CBT-graphene mixtures was examined by plate-plate rheometry. Question was if initial viscosity remains under the 1 Pas threshold at a processing temperature of 240°C. According to the results (Figure 54) no significant change is seen up to 1 wt% graphene content and initial viscosity remains below 0.06 Pas. 3 and 5 wt% increases initial viscosity, but with 3 wt% graphene reinforcement may still be impregnated. At 5 wt% viscosity does not move below 1 Pas so impregnation is not recommended, while at 3 wt% difficulties may arise due to relatively high viscosity. Reason of the viscosity increase is the formation of a network structure by the graphene nanoplatelets which governs the electrical and heat conductivity (see below). This finding corresponds to the results of Kim and Macosko who used poly(ethylene-naphthalate) and flake graphite [135]. Note, that the here studied samples were made of premix powder. So the mixing in the Brabender device does not result in observable increase in the initial viscosity. This proves that composites can be produced via this way.

Taking into consideration the shape of the curves a sharp increase is to be observed in case of neat CBT while viscosity of graphene-modified ones has a moderate increasing period.

This finding suggests that graphene slightly hinders viscosity increase through hindering polymerization, allowing more time for the producer to impregnate the reinforcement.

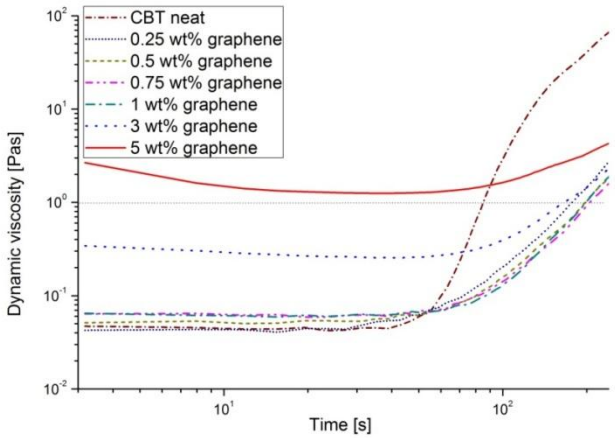

Figure 54. Effect of graphene content on the initial viscosity of CBT at 240°C

Electrical conductivity

Electrical conductivity of polymers containing conductive particles is usually governed by the theory of percolation. According to this electrical charge jumps from one conductive filler to another if these fillers are close enough to each other. If not enough conductive filler is present in the matrix no conductivity can be measured. In the present case one can note that the percolation threshold is between 3 and 5 wt% (Figure 55/a). This data does not correspond to the literature since lower percolation thresholds were achieved with graphene and other polyester matrices [44]. Reason of this is believed to be the improper exfoliation or the agglomerates were evenly dispersed. This finding was confirmed by transmission electron microscopy pictures showing small agglomerates in the matrix (Figure 53/b), however other results (heat conductivity and ILS of composites) indirectly show satisfactory exfoliation. These moderate electrical conductivity values are appropriate for cable cores, but may be increased through better exfoliation of the graphene particles for example by high energy ball milling.

Heat conductivity

Adding graphene to CBT increases its heat conductivity as it is seen in Figure 55/b. Heat is transferred by lattice vibration, in other words by phonons. To transfer heat proper coupling has to be present at the vibration nodes between the nanoparticle and the polymer. Usually this coupling is poor and so it is responsible for the low thermal conductivity of filled polymers. In the present case even 0.25 wt% graphene increases heat conductivity from 0.115 to 0.16 W/mK which means 40% increase. Higher amounts of graphene do not

result in such a pronounced increase. This finding suggests that between pCBT and graphene a covalent bond was formed due to the functional groups placed on the nanoplatelets and through this phonon scattering was successfully reduced.

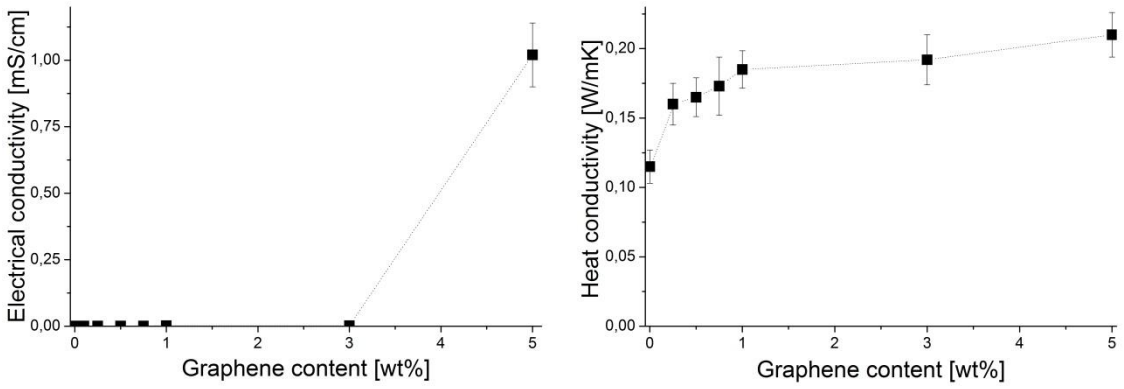

a) *b)*

Figure 55. Electrical conductivity of graphene reinforced nanocomposites (a), effect of graphene content on the heat conductivity of pCBT (b)

X-ray diffraction

Besides pCBT/graphene nanocomposites, graphene was also characterized by small and wide angle X-ray scattering. These scans are depicted in Figure 56. SAXS curve is as expected, no peaks are seen. In case of WAXS graphene has a massive peak at 26.45° (2 theta) indicating the <002> crystal plane which is also the same for carbon nanotubes [136]. A broad peak also appears at 12.2° (2 theta) belonging to the <001> plane.

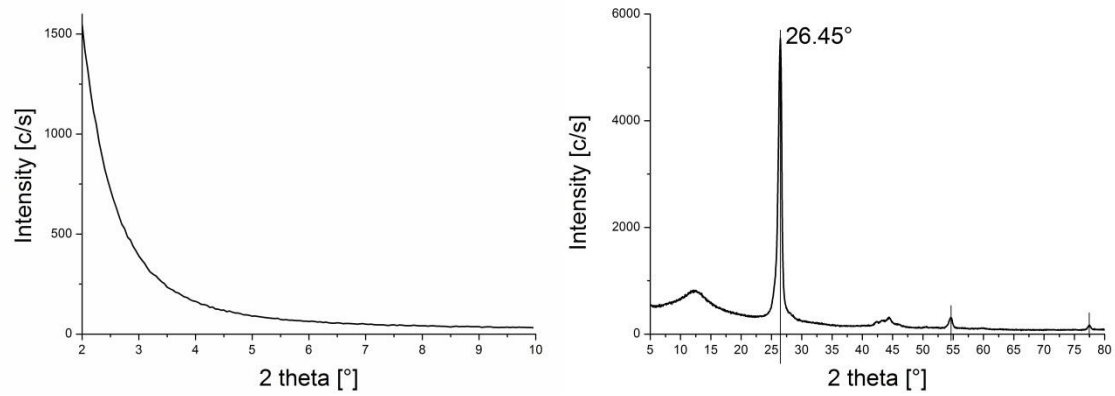

a) *b)*

Figure 56. Small (a) and wide (b) angle X-ray scattering graph of graphene

In case of nanocomposites no significant change is seen in the SAXS graph (Figure 57) compared to neat pCBT. This suggests good graphene nanoplatelet dispersion. The steeply increasing intensity of graphene toward 2° is probably due to the closeness of the primary X-ray beam (well pronounced in case of the red dashed line).

It can be observed on the WAXS graphs (Figure 58) a shoulder appears at 26.8° (2 theta). This is the <002> crystal plane of graphite – same as seen in Figure 56/b.

As it was mentioned in the 'Properties of neat CBT' Section pCBT is in its alpha crystalline form with its triclinic unit. Presence of graphene did not influence this structure as it is clearly seen in Figure 58 – all the above mentioned characteristic peaks are well resolved. Presence of graphene is proved by the peak appears at 26.8° (2 theta) (indicated by an arrow in Figure 58).

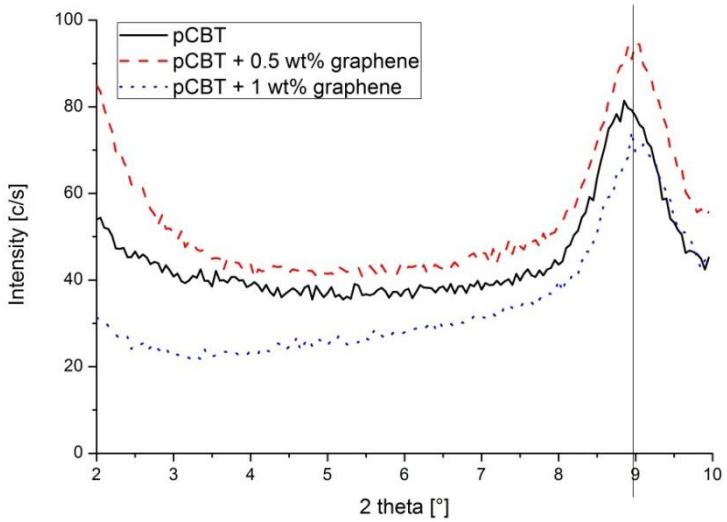

Figure 57. Small angle X-ray scattering graphs of graphene-containing samples

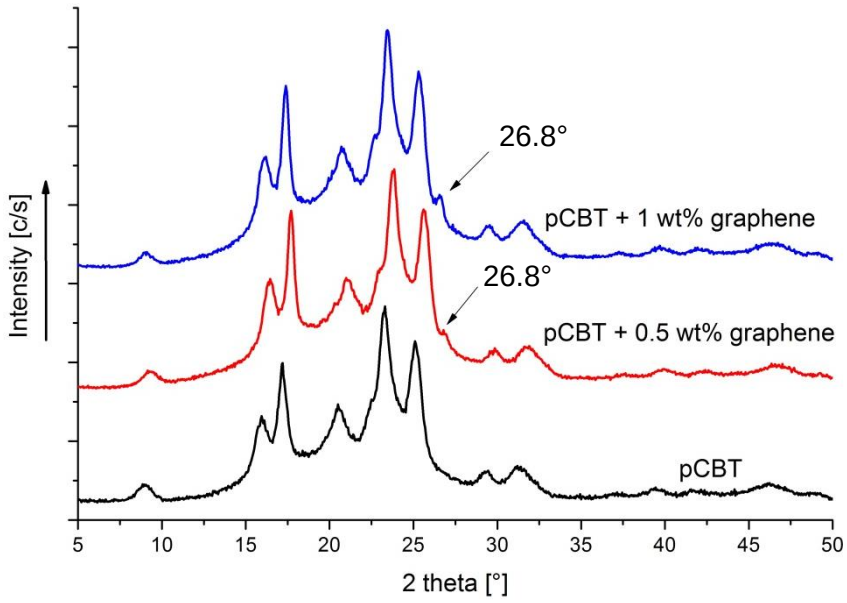

Figure 58. Wide angle X-ray scattering graphs of graphene containing pCBT samples

4.1.4. Short summary of characterizations

This chapter summarizes the results of the 'Characterizations' section from the point of view of a composite producer. According to the characterization results the CBT oligomer

could be polymerized into pCBT at 240°C. At 240°C temperature polymerization takes 120-150 seconds after melting if the material is completely dried. Once CBT is polymerized it should be cooled as fast as possible to obtain a low-crystalline (χ_c below 40%), ductile structure. Higher ductility may also be achieved by adding polycaprolactone to CBT prior to the ROP. During ROP a copolyester is formed which has significantly higher tensile strain than the unmodified pCBT. According to the rheological studies PCL modified CBT has appropriate viscosity for composite processing.

pCBT, as normally all the polymers, is a heat and electrical insulator. If it is necessary from the application side, with the addition of graphene these conductivity properties can be enhanced. Processing properties, such as initial viscosity was investigated and found to be appropriate up to 1 wt% graphene content. Moderate values of electrical and heat conductivity are acceptable for a matrix material, because these properties of the composites are mainly determined by the carbon fibers as it is studied and discussed later. Conductivity properties could be enhanced by using other graphene-dispersion methods like high energy ball milling. Since the resulting properties of the composites are appropriate for HVTL-like applications, this question is not discussed here, but the issue of dispersion is studied in more detail here: [38, 84, 136].

4.2. Pultrusion technology development

Two manufacturing technologies were developed on the basis of the 'Characterizations' chapter: reaction-injection pultrusion and hot consolidation. In this chapter the pultrusion will be described, while hot consolidation is introduced in the 'Sample preparation' section.

According to the classification in Luisier's thesis reaction injection pultrusion was used, because prior to ROP molten CBT flows like water and polymerizes inside the die [103].

This pultrusion method had to be optimized for CBT160. Development is based on the polymerization kinetics of CBT160: as it is heated the oligomer rings open and start to polymerize because catalyst is already present in the system. The higher the temperature the faster the polymerization will be and the shorter the time for impregnation. Three zones were formed within the pultruder die: a melting, an impregnating and a polymerizing zone. Temperatures were chosen as follows: 150°C for melting and injection, 190°C for impregnation, as lowest viscosity is reached at this temperature for the longest time (Figure 36). For polymerization 250°C was chosen as CBT polymerizes in the shortest time. No

thermal degradation occurs at that temperature within the processing timeframe according to the previously performed rheology analyses (see Chapter 4.1.1).

For pultrusion a time-estimation and a model-experiment was carried out based on a processing speed of 0.4-0.5 m/min. Both for injection and impregnation 40 seconds were planned in order to achieve a conversion less than 20%. This is because longer times would raise viscosity which may be too high for impregnation. For polymerization maximum 120 seconds were allowed to achieve an economically appropriate processing speed.

Pultrusion process was modeled via DSC then samples were analyzed by GPC in order to see how CBT polymerizes during this theoretical process. Conversion and molecular weight results are given in Figure 59 with the corresponding residence times and zone temperatures.

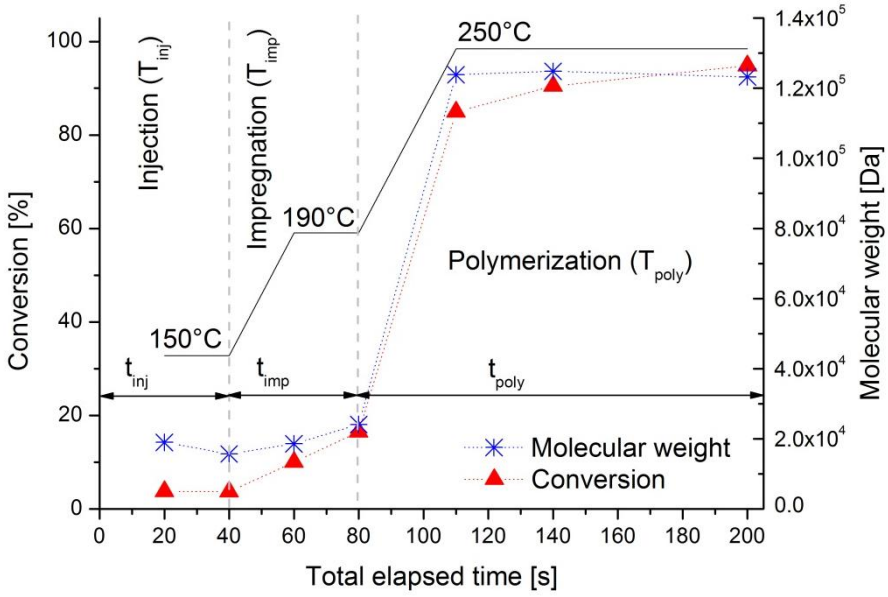

Figure 59. Conversion and molecular weight values obtained by a DSC heating followed up by GPC measurements

According to conversion values a pultrusion die was designed (Figure 66 and Figure 67 – for more drawings see CD Appendix). Results given in Figure 59 indicate that the parameters described above result in an almost completely polymerized composite structure.

Calculated process parameters

For raw material necessity calculations a rod with a diameter of Ø8 mm was chosen, since this is a common HVTL inner core diameter [7], with a fiber content between 50-80 vol%. Process speeds were examined between 0.25 – 2.5 m/min. Process speed is theoretically unlimited from one side because CBT has to be kept at a certain temperature (250°C) for at

least 120 sec excluding impregnation and according to Figure 59, 200 sec would be ideal for the whole reaction at different temperatures– so for further calculations 200 sec was used. The higher the process speed is the longer the die should be. But friction forces increase with die length and so too long dies cannot be applied – so it means a limitation from another side.

Since the injection system is given (Figure 66) and the injector length is L_{inj} = 280 mm, time spent inside the injector changes with processing speed. Figure 60 shows the time spent in the die at 250°C. These times are obtained from equation (7). This time has to be at least 120 sec and it means a lower limitation for processing speed [137]. For the sketch of the process, see Figure 61.

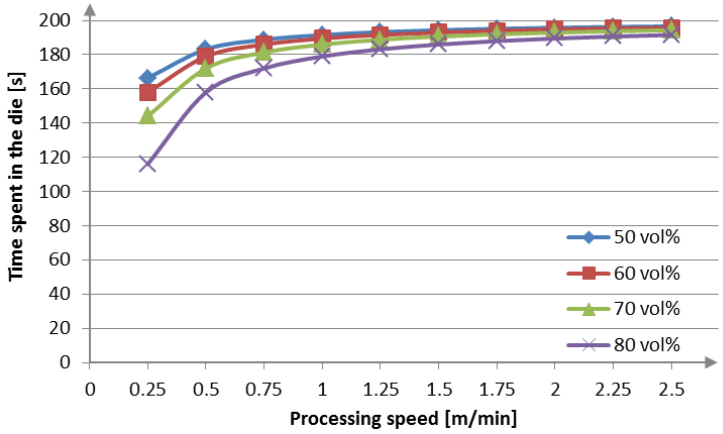

Figure 60. Time spent inside the die at 250°C in function of fiber content and process speed

$$t_{die} = t_{total} - \frac{L_{inj}}{v_{proc}} \cdot \frac{A_{comp,m}}{A_{inj}} \tag{7}$$

where t_{die} is the time spent inside the die at 250°C [sec]; t_{total} is the total time spent in molten state (180 sec) [sec]; L_{inj} is the length of the injector [m]; v_{proc} is the process (pulling) speed [m/min]; $A_{comp,m}$ is the matrix cross section area of the composite profile [mm^2]; A_{inj} is the cross section area of the injector [mm^2].

The injection is realized through a special melting and injection system mainly driven by a gear pump.

The melting system is a conical bore in a chrome plated heatable steel plate (Figure 66/1). After this the molten CBT flows down into a gear pump which was specified for this purpose. Boundary conditions for the pump were the following: capable to handle a minimum dynamic viscosity of $5x10^{-3}$ Pas and a maximum of 10^6 Pas. Besides this a minimal material transport should be 0.5 cm^3/min (≈0.65g/min) (Figure 63). According to this a VPC 1,28 gear pump from Variopumps was chosen (Figure 62) [137].

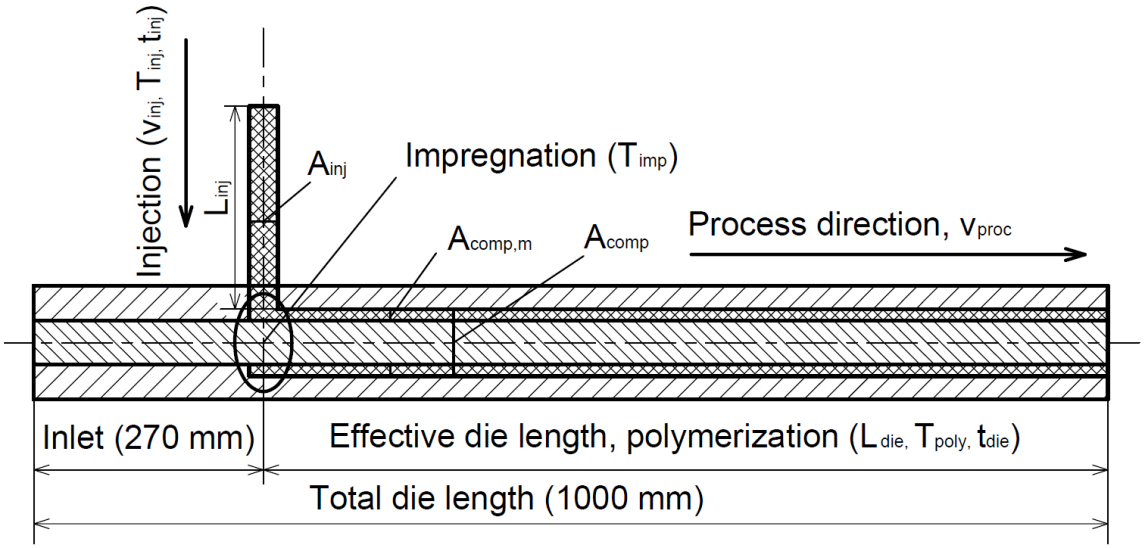

Figure 61. Sketch of the designed pultrusion process with the process parameters

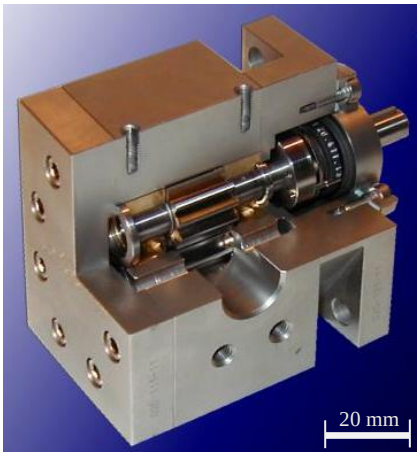

Figure 62. Variopumps VPC 1,28 gear pump [138]

The gear pump is followed by an injector pipe and an injector bore in the die (Figure 66/3). The melting sheet, the pump and the die are heatable, while the other parts are in direct contact with the others and are thermally insulated. Necessary flow rates for different process speeds were determined according to equation (8) (Figure 63)

$$\dot{Q} = \frac{V_{total} \cdot v_f \cdot \rho_f + V_{total} \cdot v_m \cdot \rho_m}{l} \cdot v_{proc} \qquad (8)$$

where $\dot{Q}$ is the required mass flow [g/min]; V_{total} is the total volume of 1 m profile [cm^3]; V_f is the fiber volume fraction [-]; ρ_f is the fiber density [g/cm^3]; V_m is the matrix volume fraction [-]; ρ_m is the matrix density [g/cm^3]; v_{proc} is the process speed [m/min]; l is the length of 1 m profile [m].

From equation (8) and Figure 63 is seen that not more than 20 g/min resin is necessary.

The overall length of the die is 1 meter with a 270 mm long conical inlet with an angle of 1°. Three injection bores are formed along the die to be able to test different compression ratios and backflow properties. For the placement of these bores see Figure 64. At the middle bore an impregnation zone is formed to enable resin flow around the fibers.

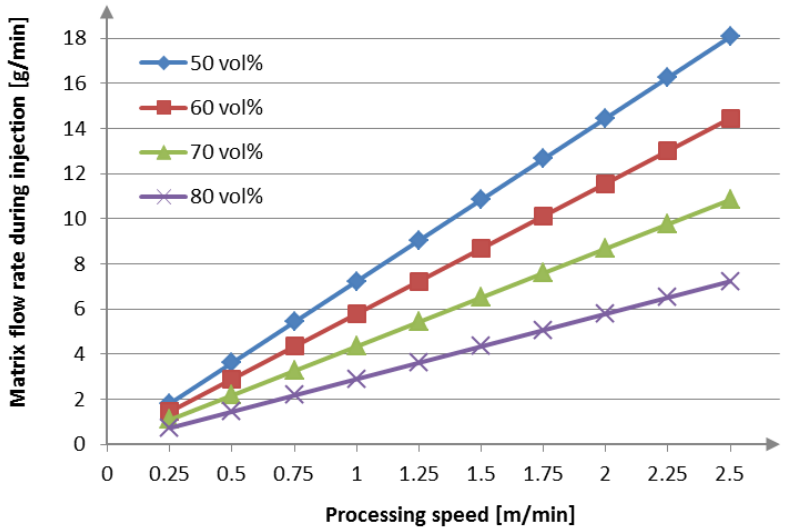

Figure 63. Necessary matrix flow rate in function of process speed and fiber volume fraction

Required die lengths for different process speeds were calculated using equation (9) taking into consideration that CBT has to spend 180 sec inside the injector and the die.

$$L_{die} = \left(t_{total} - \frac{L_{inj}}{v_{inj}} \right) \cdot v_{proc} \tag{9}$$

where L_{die} is the desired die length [m]; t_{total} is the total time spent in molten state (in this case 180 sec) [s]; L_{inj} is the length of the injector system [m]; v_{inj} is the matrix flow speed in the injector [m/min]; v_{proc} is the processing speed [m/min]. The results are depicted in Figure 65 and show inapplicably long dies above 0.75 m/min process speed.

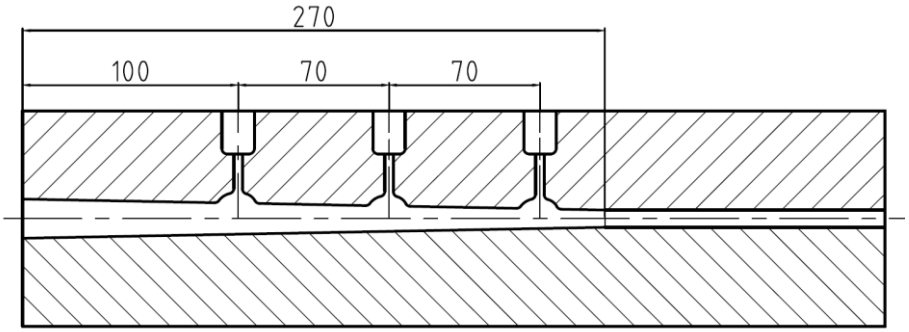

Figure 64. Sketch of the die showing the placement of the injection bores

Summing up the limitations (minimum residence time has to exceed 120 sec; die has to be shorter than 2 m; matrix flow rate has to exceed 1 g/min) it was shown that a suitable processing speed for all fiber contents is between 0.5-0.75 m/min.

In case of the designed pultruder, the efficient length of the die is 830 mm. To this length belongs a maximum speed of 0.415 m/min which assumes 120 sec residence time inside the die. This speed is satisfactory for research purposes.

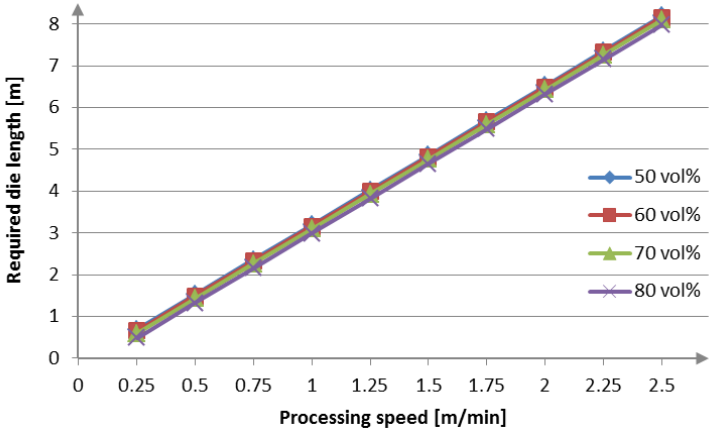

Figure 65. Required pultruder die length in function of process speed and fiber volume fraction

Auxiliary and here not detailed equipment for this pultruder could be ordered from the following sources:

- Creel and fiber guidance system: Texkimp Ltd, Norwich, UK. This creel is capable to give the necessary pretension to the fibers.
- Heating cartridges and the whole controlling system (tailor made): Ernő Őry, Budapest, Hungary. The heating system is capable to heat the die up to 400°C with an accuracy of ±1°C.
- Reciprocal caterpillar pulling unit (tailor made on the basis of a Px1000-12T type puller): Pultrex Ltd, Lawford, UK. The speed of the pulling unit is infinitely adjustable between 0.04-2.5 m/min with a pulling force of 12 kN
- Take-up reel (tailor made): András Koltai, Budapest, Hungary. The speed of the reel is infinitely adjustable within the limits of the pulling unit.

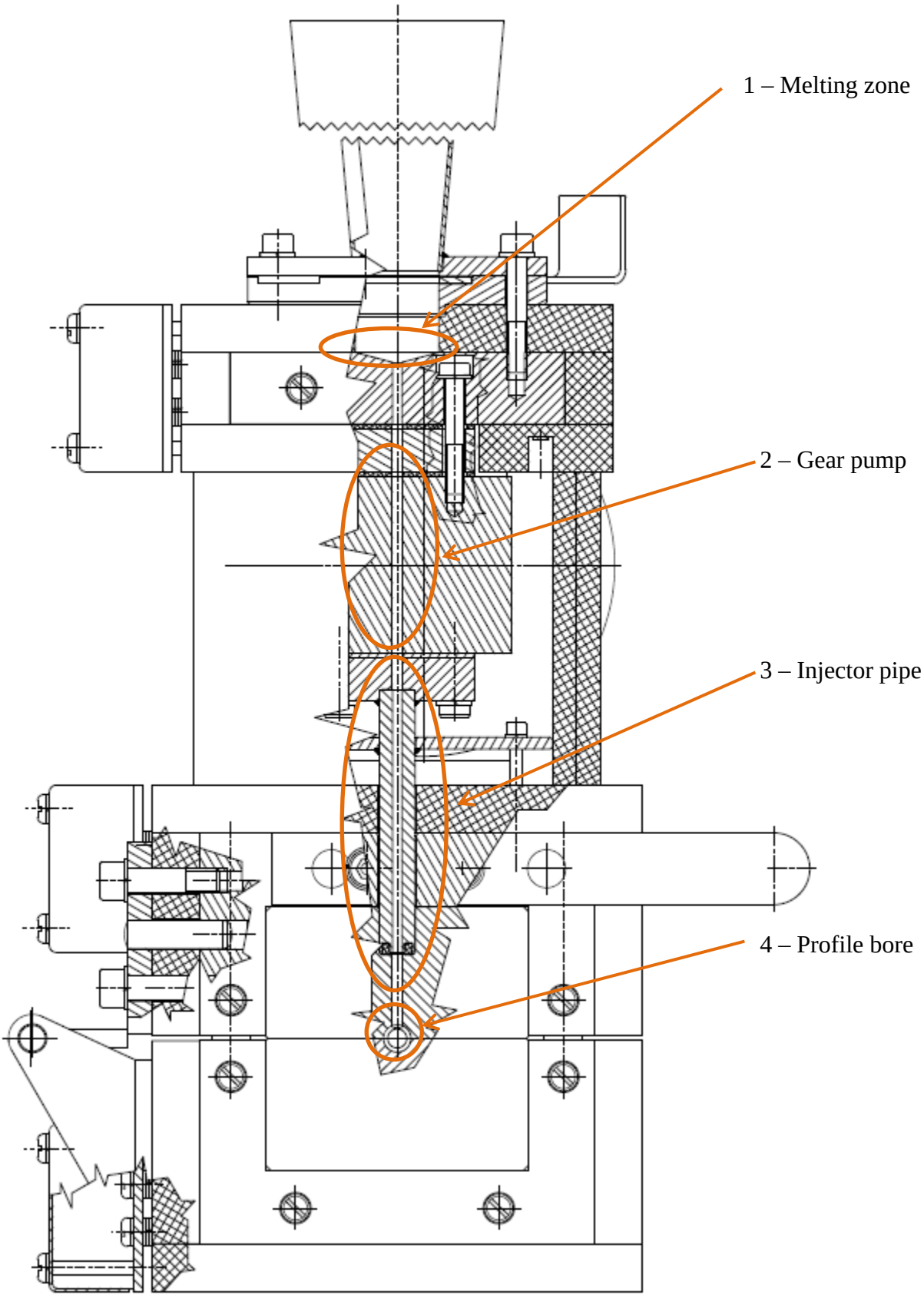

Figure 66. Section view of the pultruder die focusing on the injection system. For the whole drawing, see CD Appendix

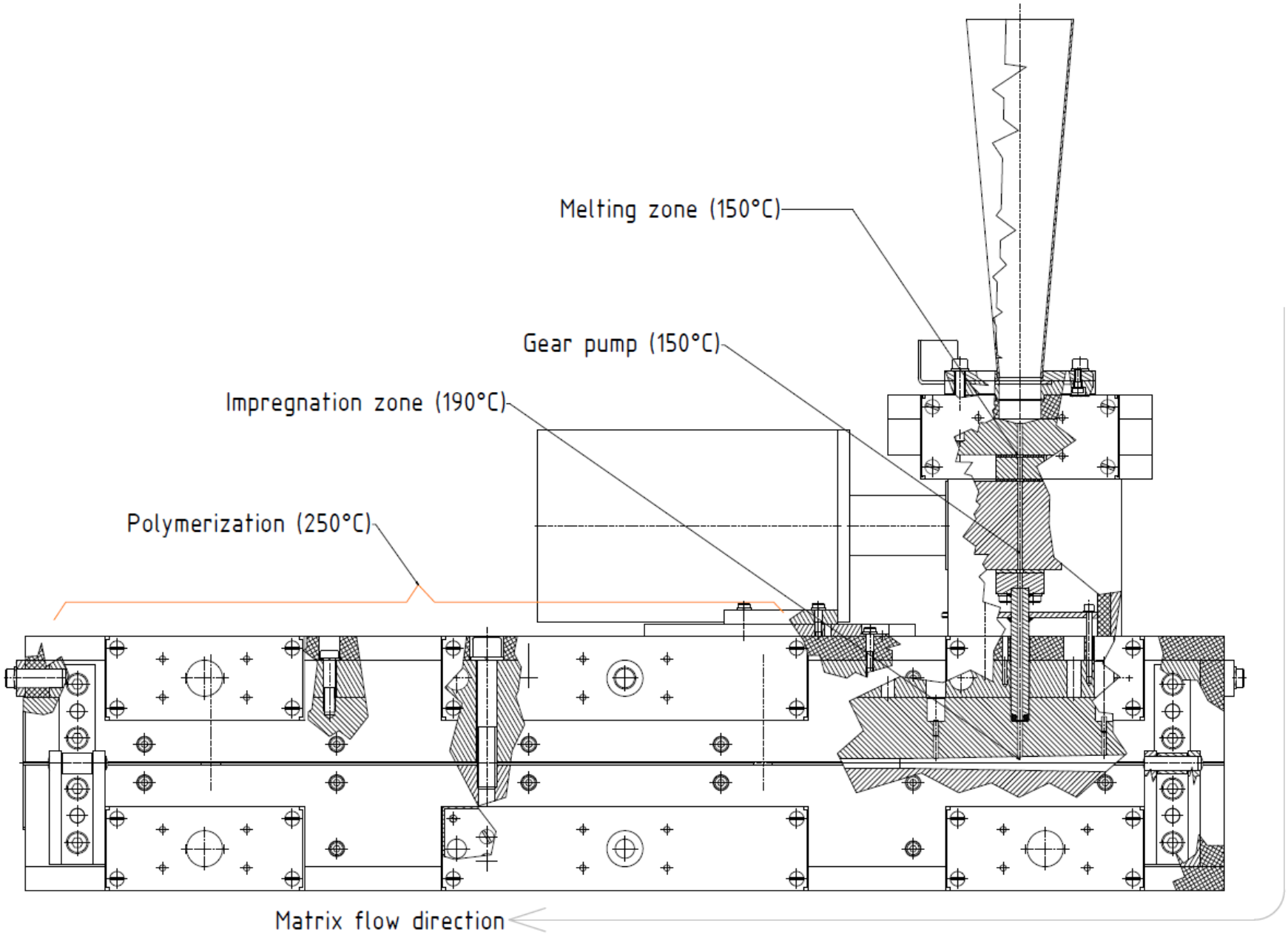

Figure 67. Special pultrusion die for low viscosity CBT resin

4.3. Mechanical testing

In the following chapter results of the mechanical analyses are introduced and discussed extensively.

4.3.1. Samples made by the in-situ melting and polymerizing method

Via this method UD carbon fiber reinforced composites were produced without any modifications of the matrix.

Before mechanical testing, these samples were subjected to gel permeation chromatography test to study oligomer conversion and molecular weight. The conversion results (Table 9) show a very good rate of conversion, over 98% for both the neat pCBT and the composite pCBT-CF composites. This is due to the appropriate processing temperature and providing enough time for CBT to polymerize. Note, that complete conversion cannot be achieved within polyesters, since they undergo ring-chain equilibrium reactions in molten state, and oligomers are present in 1~3% in the melt. However, the molecular weight (MW) values (mass average) are lower than those are given by Cyclics – over 10^5 Da [67]. The possible reason why this lower mean MW was achieved is possibly due to thermal degradation (remember, these samples spent more than 10 minutes in an oven heated to 250°C to melt all the CBT powder). According to rheological studies thermal degradation starts after 6-7 minutes at 255°C but the mold had to be kept in the oven to melt all the CBT powder. So this could cause degradation in the outer layers of the composite [123]. According to the above this method is only suitable for research purposes.

	MW	MP	Conversion [%]
pCBT	67634	61573	98.53
pCBT-CF	89977	75977	98.35

Table 9. Conversion results of the neat pCBT and pCBT-CF composite samples

Flexural properties

Flexural properties of the *in-situ* molten and polymerized samples are presented in Table 10. The neat samples showed great ductility, did not break until conventional deflection (10% of span length) – so flexural strength values are calculated at ε=10% deflection. This is because of the low degree of crystallinity of pCBT and good conversion from CBT to pCBT and high molecular weight – see GPC results in Table 9. The obtained flexural strength is 56.7 MPa with a Young's modulus of 2.1 GPa. The low amount of the applied UD carbon fiber reinforcement increased these values by ca. 6 times (Table 10). The modulus of the composite samples is raised to 13.3 GPa with the flexural strength of 242.9 MPa, respectively. This

result shows good fiber-matrix cooperation but less than the values achieved by other methods due to the low reinforcement content (Figure 78) [123].

Flexural	Modulus [GPa]	Strength [MPa]	Strain at break [%]
pCBT	2.1±0.3	56.7±12.7	3.2±1.1
pCBT-CF	13.3±1.5	242.9±1.3	2.1±0.2

Table 10. Flexural properties of the neat pCBT and pCBT-CF composite samples

Charpy dynamic impact test

The Charpy impact strength results (Table 11) show an average energy absorption capability of the unreinforced samples (7.9 kJ/m^2). CF reinforcement raised this value to ~53 kJ/m^2. The failure of the composites was fiber break instead of pull-out or any other failure mode. This means that fiber-matrix adhesion was good – the quality of fiber-matrix adhesion is also well reflected by in the SEM pictures (see Figure 68) [123].

	Charpy impact strength [kJ/m^2]
pCBT	7.9±0.8
pCBT-CF	53.1±2.1

Table 11. Charpy impact strength values of *in-situ* molten and polymerized samples

Scanning electron microscopy

Figure 68 shows a broken composite surface with both broken pCBT matrix and carbon fibers. A good wet-out is clearly seen beside the ductilely broken pCBT. No fiber pull-outs are seen which suggests good fiber-matrix adhesion. In Figure 68/b a covered fiber can be observed with a crack going through it and stop after passing the fiber. These pictures support the previous statement about the good fiber-matrix adhesion in the 'Flexural properties' section [123].

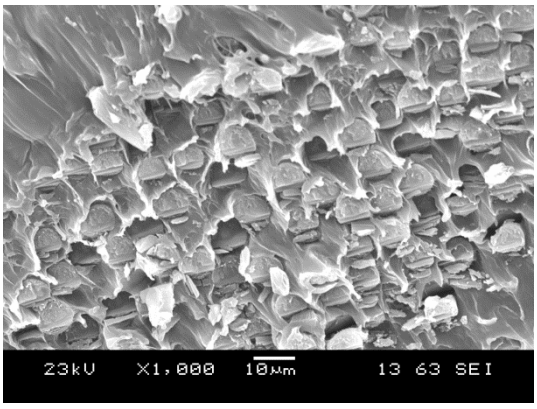

a)

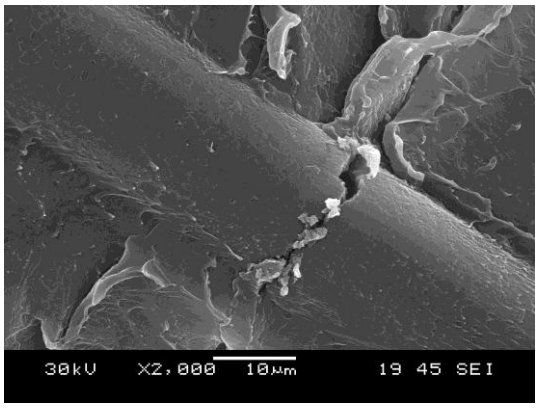

b)

Figure 68. SEM picture of the broken pCBT-CF composite surface (a) covered single carbon fiber embedded into the pCBT matrix (b)

4.3.2. Prepreg method – effect of polycaprolactone

Composite samples for testing the effect of polycaprolactone were produced via the prepreg method. For the experiments two different reinforcements were used: UD carbon fabric by ZOLTEK and a plain carbon weave by Sigratex designated as UD and fabric, respectively. In this case neat pCBT and polycaprolactone-modified pCBT matrix was used. Effect of PCL on the mechanical properties of the composites was studied and compared to neat pCBT. Based on the results obtained in the 'Characterizations' chapter, toughening effect was expected due to the presence of the PCL.

Interlaminar properties

During the installation of the HVTL cables they undergo a lot of dynamical load. For example they are pulled through and reeled onto mandrels where the composite cores are bent and in this point both static and dynamic interlaminar shear properties are important.

On the basis of the above interlaminar properties were examined by both static and dynamic methods because these properties are important and clearly indicates fiber-matrix cooperation. ILS results show a clear increase owing to the addition of polycaprolactone in both static and dynamic cases. *Static case* (Figure 69/a)*:* A slight increase is to be observed when UD-reinforced composites were applied and a more pronounced increase is seen in case of fabric reinforcement. So PCL has positive effect on the static interlaminar properties through enhancing fiber-matrix adhesion. A probable mechanism of this is the following: a bridge is formed of PCL between the carbon fibers and pCBT. Since the different reinforcements have different sizings, the fiber-matrix adhesion is different. According to the results PCL-modified pCBT cooperated better with the fabric than the UD reinforcement, so a more pronounced increase is not surprising. Better static ILS cannot be explained by the toughening effect since PCL decreases strength and would only increase strain-at-break which is almost negligible in this case. *Dynamic case* (Figure 69/b)*:* Polycaprolactone enhanced dynamic ILS. In this case no differences were observed between the fabric and the UD reinforcements. ILS change in this case may also be explained by the toughness-increasing effect of PCL-modification. Besides fiber-matrix adhesion dynamic ILS indicates indirectly the toughness of the matrix film between the reinforcing layers. After adding polycaprolactone to pCBT its toughness is increased which results in a more crack-resistant material. This is likely another reason for the growth of ILS mainly in dynamic, but also in static case – crack propagation is hindered in a tougher material [124].

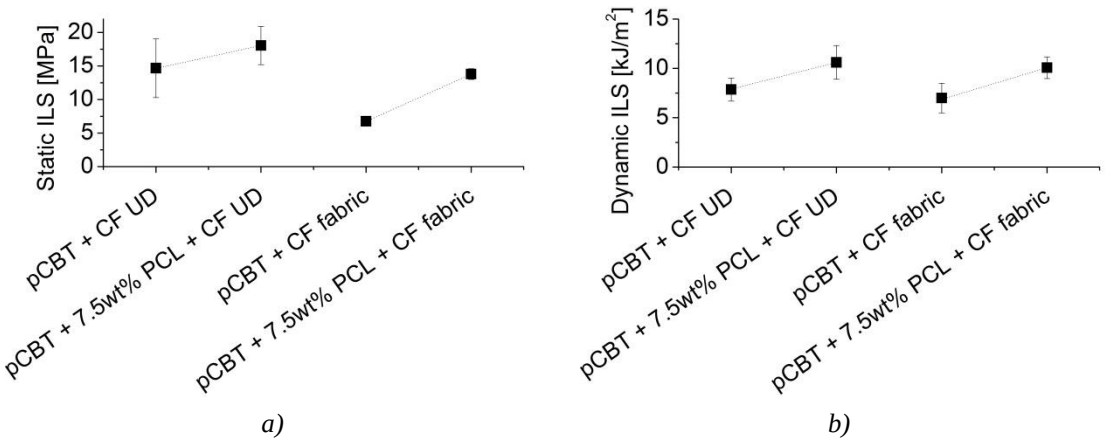

a) *b)*

Figure 69. Interlaminar properties obtained by *static* (a) and *dynamic* (b) methods in cases of modified and unmodified matrices and reinforcements

Flexural properties

According to the flexural results (Figure 70 and Figure 71) both strength and modulus have decreased due the addition of PCL. In case of *fabric reinforcement* strain at break has increased slightly. Decrease in modulus was smaller than as of tensile results of the unreinforced material – the main reason of this is the presence of the fibers and the different load mode. In case of flexural strength the phenomenon was reversed: a more strong decrease is to be observed. This is because the specimen broke on the compressed side and the PCL-modified pCBT has lower compressive strength than the unmodified one. These results with the slightly increasing flexural strain show the toughening effect of PCL. Applying *UD carbon fibers* led to a different result: strain at break also decreased by the addition of PCL. Comparing these to ILS and unreinforced tensile results, a dissimilarity is seen: PCL has positive effect in tension and in interlaminar shear but in flexion it depends on the applied reinforcement which is not surprising in case of composites [124].

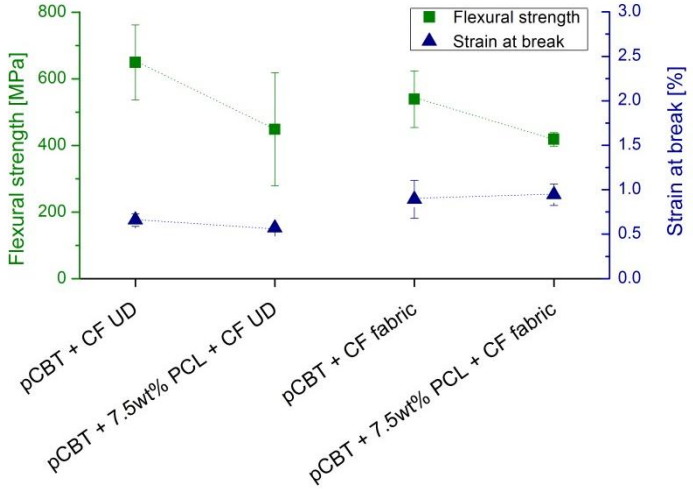

Figure 70. Flexural strength and strain in cases of PCL-modified and unmodified matrices

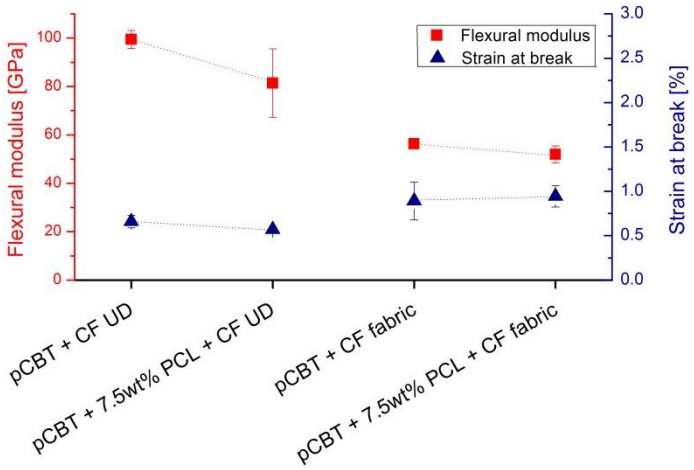

Figure 71. Flexural modulus and strain in cases of PCL-modified and unmodified matrices

Optical microscopy

From the optical microscopy pictures it is clearly seen that both neat and PCL-modified CBT matrices have impregnated the carbon fibers well (Figure 72). There are no voids in the cross sections so the above described manufacturing method results in a good quality composite [124].

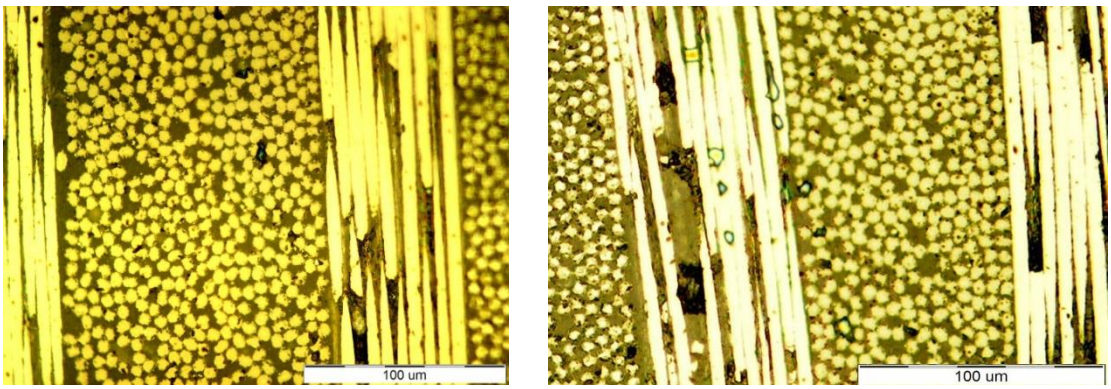

a) *b)*

Figure 72. Cross section of a CBT (a) and a CBT+PCL (b) matrix composite with fabric reinforcement

Scanning electron microscopy

Broken surfaces of the ILS samples were analyzed by SEM. After taking a look at Figure 73 one can note that unmodified pCBT impregnated the carbon fibers well. The images show a few signs of ductile failure – see the white edges in Figure 73/b.

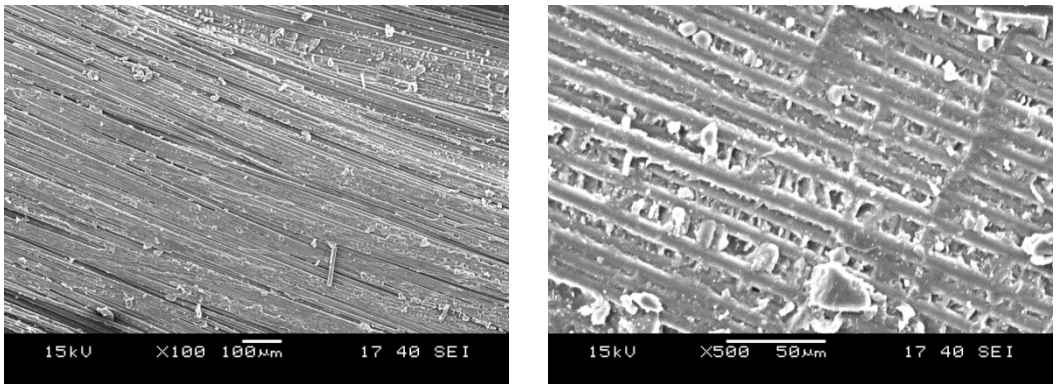

a) *b)*

Figure 73. SEM pictures of the *static* ILS samples with a magnification of 100x (a) and 500x (b) in case of neat pCBT matrix and CF UD reinforcement

Adding polycaprolactone to the pCBT matrix increases its interlaminar shear strength as it was discussed above. Signs of improved fiber-matrix bond are seen in both images (Figure 74 and Figure 75): matrix covered the carbon fibers. In *dynamic* case (Figure 74) sharp edges indicate a rigid break, but in *static* case (Figure 75) a more ductile failure was seen. One characteristic sign of it is indicated by an arrow and a circle in Figure 75/b.

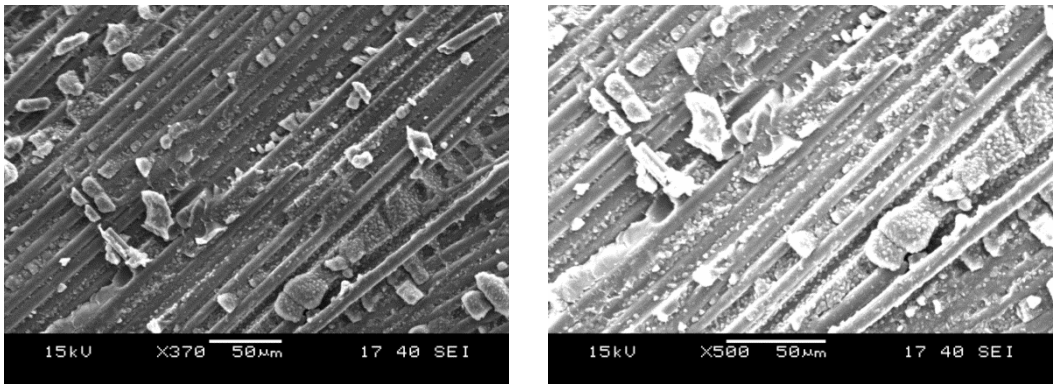

a) *b)*

Figure 74. SEM pictures of the *dynamic* ILS samples with a magnification of 370x (a) and 500x (b) in case of PCL-modified pCBT matrix and CF UD reinforcement

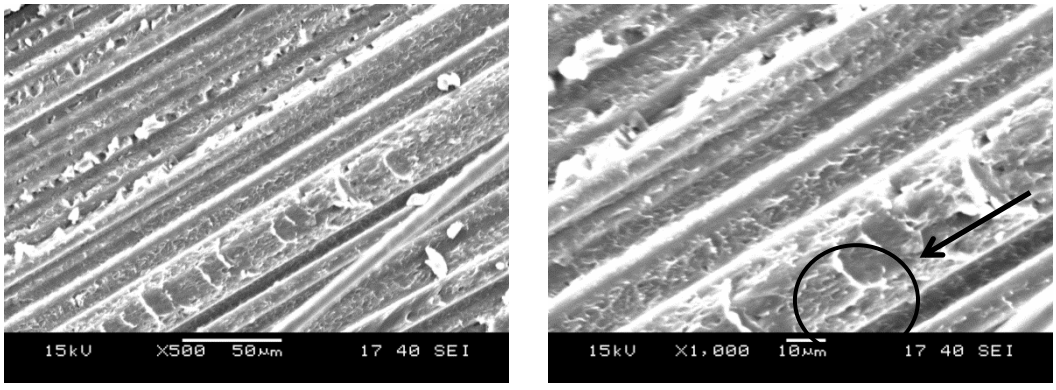

a) *b)*

Figure 75. SEM pictures of the *static* ILS samples with a magnification of 500x (a) and 1000x (b) in case of PLC-modified pCBT matrix and CF UD reinforcement

4.3.3. Premix method – effect of graphene

Graphene-modified composites were produced by the premix method. Effect of graphene was examined on the interlaminar, flexural, heat and electrical conductivity properties of the pCBT-CF composites. For these experiments unidirectional carbon fabric by ZOLTEK was utilized.

Interlaminar properties

Interlaminar properties are important mainly because of the loads during the installation of the HVTL cables. So interlaminar shear properties were studied by two different methods: a *static* and a *dynamic* method. Results obtained by the *static method* are depicted in Figure 76. According to these results a clear positive effect of graphene is to be observed. A variance analysis was performed on the results, which supported that the effect of graphene on the static interlaminar properties is significant at $\alpha = 0.05$ confidence level. (For the whole analysis data, see Appendix) This positive effect may have several reasons. One of it assumes graphene bonds both to the carbon fibers and to pCBT [139]. Another explanation suggests that graphene particles in the pCBT matrix hinder crack propagation and forces cracks to constantly change its propagation direction. Similar effects were found by Szebényi [122] for carbon nanotubes. Nanoparticles also have a general reinforcing effect on the pCBT matrix which also explains better interlaminar properties. Looking at the curve (Figure 76) one can note that results obtained by *static* method go through a maximum value at 0.5 wt% graphene content. So nanoplatelets can enhance interlaminar properties the best at this weight proportion. Results suggest that above 0.5 wt% graphene content big agglomerates remain in the matrix and act as weak points. These weak-point agglomerates may be origins of cracks; this is why 0.75 and 1 wt% graphene containing composites have lower ILS values.

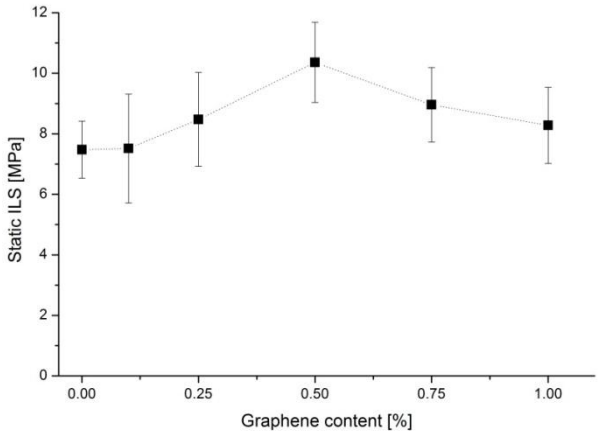

Figure 76. Effect of graphene on the interlaminar properties of pCBT-CF composites– results obtained by the *static* method

Looking at the *dynamic results* (Figure 77) a peak on the ILS curve is seen at 0.25 wt% graphene content. This indicates that graphene increases *dynamic* interlaminar properties besides the *static* one. Reinforcing effect is much slighter compared to static case because the presence of graphene makes the matrix film between the reinforcing layers less resistant to dynamic load. Critical size of 'weak-point-agglomerates' are also smaller – this is also explained by the dynamic load. Above 0.25 wt% graphene content the dynamic ILS value decreases below the initial value – this finding suggests not proper exfoliation for dynamical applications. A variance analysis was performed on the results, which did not support that the effect of graphene on the static interlaminar properties is significant at $\alpha = 0.05$ confidence level. (For the whole analysis data, see Appendix). So the conclusions written above have to be dealt with care.

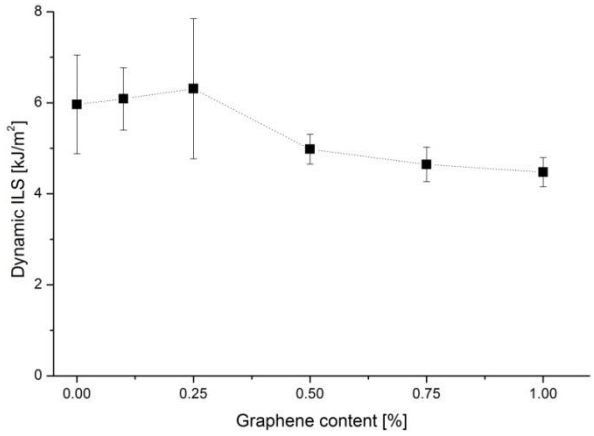

Figure 77. Effect of graphene on the interlaminar properties of pCBT-CF composites – results obtained by the *dynamic* method

Effect of graphene on the flexural properties

Carbon fiber reinforced pCBT composite samples with different graphene contents were examined by three point bending tests. Effect of graphene as an additive should be seen clearly since it is a matrix modifier and flexion is more matrix-dependent than for example tension. Flexural strength is decreasing with the increasing graphene content (Figure 78). This decrease is pronounced until 0.25 wt% thereafter the differences between these values are within deviation so considered to be insignificant. This phenomenon is likely explained by the dispersion of the nanoplatelets. Graphene agglomerates remained in the matrix and acted as weak points from where cracks started off. Above 0.5 wt% this played no important role. Interestingly flexural modulus was less affected than flexural strength; however increased modulus was expected by the addition of graphene. This could also be explained by the low

exfoliation level of the nanoplatelets. The agglomerates acted as ‘sliding agents’ resulted in a decrease in the modulus.

Taking flexural strain into consideration (Figure 79) a slight decrease is to be observed but only in the range of standard deviation. Summing up, graphene decreases flexural strength while does not significantly affect flexural strain and modulus.

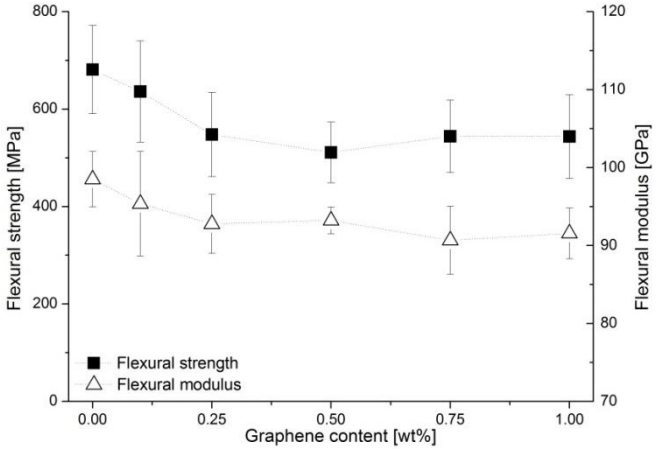

Figure 78. Flexural properties in function of graphene content

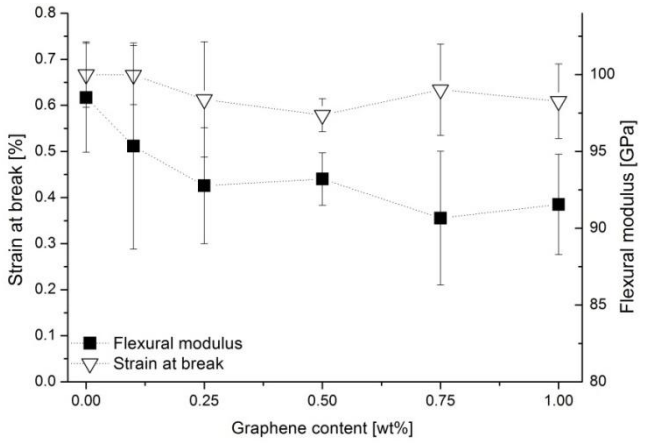

Figure 79. Effect of graphene content on flexural strain at break

Effect of graphene on the electrical conductivity properties

Electrical conductivity of carbon fiber and graphene reinforced composites were examined with an initial assumption that graphene increases electrical conductivity. Since the composites were unidirectionally reinforced conductivity in both parallel and perpendicular directions to the fibers were examined. Results are shown in Figure 80 with a not surprising phenomenon of the lower conductivity values perpendicular to the fibers. Parallel to the fibers electrical conductivity is slightly increased. Effect of graphene in this case is not so pronounced but sill observable since the composite contains much more carbon fibers which dominate electrical charge transfer. These relatively low electrical conductivity values are

appropriate for building a HVTL cable core, because the most of the electricity is transferred by the aluminum coating due to the skin effect.

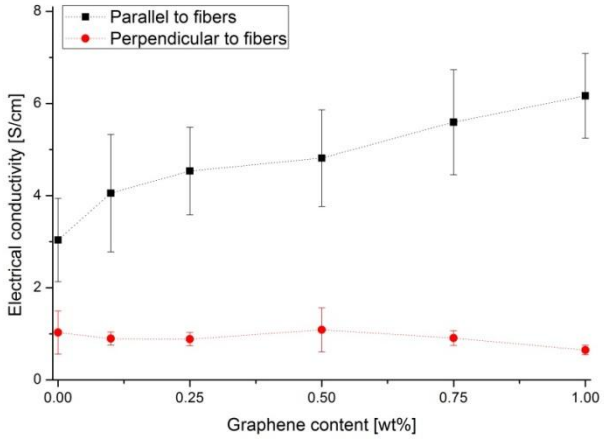

Figure 80. Electrical conductivity of the composites in function of graphene content

Effect of graphene on the heat conductivity properties

As the presence of graphene raises the thermal conductivity of pCBT the same effect was expected for carbon fiber reinforced composites. The results of thermal conductivity measurements are depicted in Figure 81. According to these no significant increase was indicated by the presence of graphene. If these results are compared to those obtained by graphene-filled pCBT (black points) a strong increase is to be observed due to the presence of carbon fibers – also indicated in Figure 81. This suggests that carbon fibers dominate heat conductivity and nanoparticles have only a little effect on it. Note that carbon fibers were perpendicular to the direction of the heat transfer. Higher values can be achieved if the fibers are parallel to the direction of heat transfer, but our device enabled only this perpendicular direction.

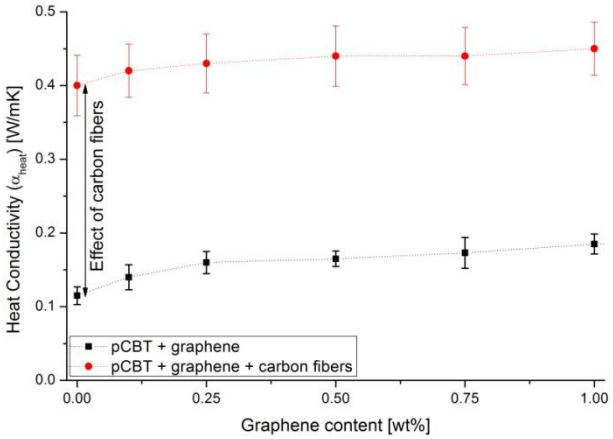

Figure 81. Heat conductivity of the pCBT-CF composites in function of graphene content

Scanning Electron Microscopy

Fracture surfaces of ILS samples were examined by SEM. Figure 82 shows fracture surfaces of static ILS samples with different magnifications. Appropriate fiber wetting is seen beside rigid failure which was caused by the crystallinity of the matrix. The little 'white' particles (indicated with a circle and an arrow in Figure 82/b) clearly show the rigid failure without any ductile deformation. However, failure in this case may show some ductile behavior because the deformation was quasi-static (1.3 mm/min) which enables plastic deformation of the matrix.

Figure 83 shows the surfaces of dynamic ILS samples. These pictures indicate different failure. The deformed matrix suggests a ductile behavior which was caused by the dynamic load. Reason of this is believed to be the yielded heat which enables at least ductile-like deformation of pCBT.

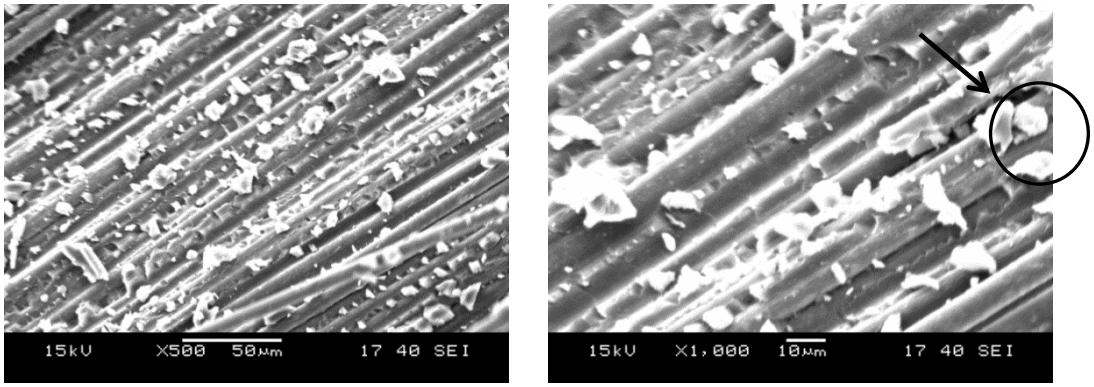

a) *b)*

Figure 82. SEM pictures of the *static* ILS samples (0.75wt% graphene) with a magnification of 500x (a) and 1000x (b)

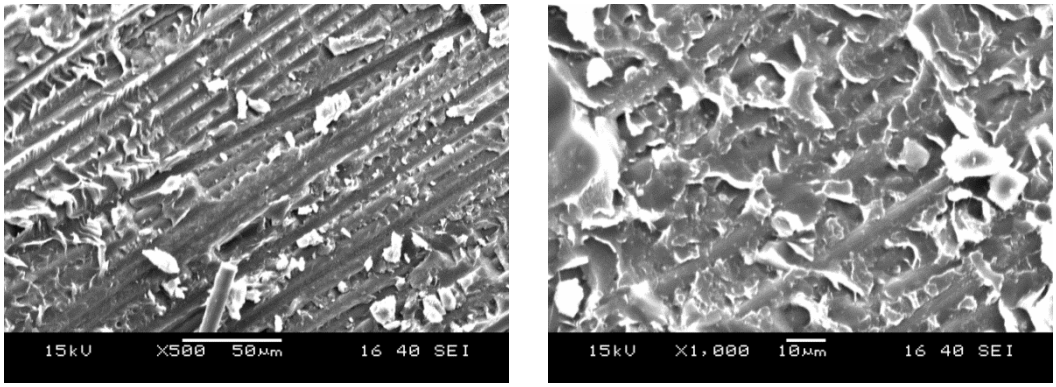

a) *b)*

Figure 83. SEM pictures of the *dynamic* ILS samples (0.75wt% graphene) with a magnification of 500x (a) and 1000x (b)

5. Summary

Our fast-developing world constantly requires new, high performance engineering materials. This statement is especially true for the energetic and energy transmission industry. The mankind needs more and more electricity which has to be transferred to long distances. Since the metal-based high voltage transmission line components have reached the frontiers of their performance, new composite based components are necessary. Such a change was already seen among the insulators, and now cable cores can be changed. Several attempts have already been taken into this direction (mainly in the USA and in the Benelux states) but production and performance of these parts are below market needs.

In this work an attempt was made to develop an efficient manufacturing technology and material composition for high voltage cable cores. As matrix material cyclic butylene terephthalate was chosen. This material is a perfect matrix for composites with its water-like (below 0.1 Pas) viscosity of the oligomer prior to polymerization with a subsequent fast *in-situ* polymerization. According to the results, the oligomer viscosity is strongly time and temperature dependent, but after choosing the appropriate parameters well impregnated and completely polymerized composites can be obtained. Further study revealed that pCBT is brittle if it is not cooled fast enough. This may require special and expensive devices so chemical toughening of pCBT was investigated.

According to the results polycaprolactone toughens pCBT and an optimum result was achieved with 7.5 wt% of this additive. The resulting copolymer was characterized and was found to be appropriate for composite production on the basis of the below-0.1 Pas initial viscosity. The presence of PCL lowers the melting point from 225 to 219°C. Composites were made with the PCL modified matrix and interlaminar shear properties were significantly enhanced due to the copolymerization of this additive. The enhanced interlaminar properties parallel to the low initial viscosity mean that the produced composites may theoretically be pultruded and applied as HVTL cable cores.

Since a carbon fiber reinforced composite for high voltage applications was developed, conductivity had to be taken into account. Not only electrical but heat conductivity had to be dealt with, since the new high voltage lines operate at high temperatures, up to 160°C. To improve these conductivity properties a newly discovered material, the graphene was utilized. Carbon nanotubes were proved to improve these properties but their price is too high for large-scale production, so the cheaper graphene was chosen. Taking nanocomposites into consideration, after adding 5 wt% graphene to CBT, heat conductivity was increased with

~90%, while electrical conductivity reached 1 mS/cm. These properties are acceptable for a matrix material since conductivity properties are mostly determined by the reinforcing carbon fibers.

Composites were produced with graphene-modified matrices and an increase in matrix-dominated properties was expected. One of these is the interlaminar shear stress which reached a peak value at 0.5 wt% graphene content. Above this amount agglomerates were not broken by the applied mixing method and these formulations acted as weak points in the matrix and cracks could easily start off from them. Otherwise propagating cracks had to go in a zigzag direction to get around the nanoplatelets. On the basis of the above, composites for HVTL cable cores should be produced with a maximum of 0.5 wt% graphene.

Graphene were melt-mixed into the CBT matrix which is a simple technique and may not lead to perfect exfoliation, but is easy to realize even in industrial scale. According to the increased mechanical and conductivity properties exfoliation was satisfactory and this method may be applied in the industry.

To manufacture composite cable cores the best technology is pultrusion. Since this method is mainly used for thermosetting materials it has to be adapted for thermoplastic matrices. Molten CBT has the necessary low viscosity for being injected among the reinforcing fibers. The additives studied within this work do not increase initial viscosity significantly so modified matrices may theoretically be pultruded. As a consequence, electrical conductivity of the cable core could be increased in this way conserving its ductility. However, the moderate conductivity properties (for example 4.8 S/cm at 0.5 wt% graphene) are satisfactory for a cable core. The charge distribution is not in linear proportion with cross section areas owing to the skin effect. So the majority of the electricity is transmitted by the outer aluminum coating.

Summing up, processing technologies were developed and a corresponding machine was designed for cyclic butylene terephthalate matrix composites within this thesis. These polymeric composites are potential replacements for metallic HVTL cable cores and beside this they may be act as thermoplastic preforms for the automotive, sports and construction industry.

5.1. Utilization of results

The results achieved in this work are summarized in the following theses:

- The pultrusion technology developed within this work may be utilized by the high voltage industry for producing cable cores. This would lead to increased electrical transmission capacities which are necessary for our developing world. Because of the applied thermoplastic matrix technology the cable cores would be potential raw materials for recycling and re-using. Grinding the cores and mixing them with fresh PBT carbon fiber reinforced parts can be recycled by injection molding.
- Thermoplastic prepregs are applicable for producing recyclable composite sheets as preforms or semi-finished parts for example for the automotive industry. Once large flat sheets are produced these can be hot pressed to their desired future shape due to thermoplasticity.
- Thermoplastic preforms are getting widespread in the composite industry (see the success of Bond laminates). Sheets built up by pCBT matrix thermoplastic prepregs could have lower price than these already available materials due to lower viscosity and simpler manufacturing process.
- A sort cable sample was prepared to represent that pCBT-CF composites are suitable to be a cable core (Figure 84).

Figure 84. Short Linnet cable sample with pCBT matrix and carbon fiber reinforcement

This cable sample was produced via hot compaction (240°C, 15 min, as described in 3.3.2) in a special die to represent that pCBT is a suitable matrix material for such purpose. Mechanical properties of the sample were examined, such as tensile strength to see whether this composite

is appropriate material for cable cores; flexural strength and flexion radius to prove that the composite core can be reeled up to a transporting reel. Electrical conductivity of the core was also measured. These data are summed up in Table 12. According to these results, the sample was found to be appropriate according to the valid Hungarian standards [3, 140].

Property	Standard value	Experimental value
Tensile stregth [MPa]	min. 1200 [140]	1320
Flexural stregth [MPa]	Not set in the standard	510
Flexion radius [m]	max. 2	1.39
Linear conductivity	0.1365 Ω/km (for the whole cable)	793 S/cm; 43 Ω/km

Table 12. Properties of the produced cable sample

According to the data in Table 12 it is clearly seen, that the sample has the appropriate tensile strength. Note, that the standard data refers to a single wire in the cable core ad these wires are twisted, so a complete conventional core has lower strength than a single wire [7].

Flexion properties are not set within the standard, but flexion radius of the sample is appropriate for wounding the cable onto a reel, since standard ones are available with Ø2 m.

Taking conductivity into consideration, 43 Ω/km is appropriate, since this property is mainly determined by the aluminum core which has the same structure as a standard Linnet cable.

5.2. Theses

The results achieved within this thesis are summed up in this section as short theses.

1st thesis

I proved by differential scanning calorimetry (DSC) studies, that at least 50°C/min cooling speed is necessary to obtain a tough, sub-40% crystalline polymerized cyclic butylene terephthalate (pCBT) matrix composite. Due to the fast cooling the molecules cannot be ordered into a perfect crystalline structure, so the polymer becomes less rigid [123, 124, 141, 142].

2nd thesis

I proved by rheology and gel permeation chromatography that cyclic butylene terephthalate (CBT) is suitable for a continuous composite processing technology. Since the ring-opening polymerization reaction takes place after impregnation, the viscosity of the matrix after ring opening until the start of the polymerization remains low (0.02-0.05 Pas) and it starts increasing only after the start of polymerization [123, 137, 141].

3rd thesis

I supported by dynamic mechanical analyses empirically and by the application of Fox equation theoretically the already known, but not necessarily proven fact, that CBT and polycaprolactone (PCL) copolymerize, which is shown by the shift in the glass transition peak. I proved by DSC studies, that due to the above copolymerization, crystalline fraction of the material decreases, which increases toughness. Toughening is also supported by tensile tests: adding 10 wt% PCL increases tensile strain by 600%. Parallel to this, PCL increased significantly the dynamic interlaminar shear strength of the carbon fiber reinforced composites by 25% since the matrix film between the reinforcing layers has been toughened [124].

4th thesis

I proved that the nucleation effect of graphene is prevailed in the ring-opening polymerizing CBT, since after adding 5 wt% graphene, crystallization peak rises from 189°C to 202°C at 10°C/min cooling speed due to heterogeneous nucleation, so supercoolability of CBT decreases if graphene is present in the melt. I also proved, that graphene increases initial viscosity parallel to heat- and electrical conductivity in the range of 0-5% weight proportion. The reason of the latter is a network structure of graphene in the pCBT matrix, which increases electrical conductivity by ten magnitudes to 1 mS/cm and heat conductivity with 80% to 0.21 W/mK [143].

5th thesis

I proved that the presence of 0.5 wt% graphene increases the static interlaminar shear strength of carbon fiber reinforced pCBT matrix composites, since the propagating cracks in the matrix have to get around the graphene particles in the matrix. Above 0.5 wt% a reverse phenomenon takes place: at higher nanoparticle contents agglomerates are present which may act as weak points and be origins of cracks [143].

5.3. Further work

This work was done within the frame of an extended research program aiming to develop thermoplastic composite materials and technology for the composite industry and to the high voltage industry. So some problems remained unsolved and the following tasks require further investigations:

- Pultrusion technology has to be tested with pCBT and modified matrices. Theoretically modifiers do not change initial viscosity but it has to be studied within a pultruder.
- Dispersion of nanoplatelets should be improved and other exfoliation methods should be tested like high energy ball milling prior to polymerization.
- Study the long-term mechanical property changes of the composites parallel to the effects of higher temperatures – above the glass transition range to see the complete behavior of pCBT as a cable core material
- Mode I interlaminar crack propagation tests would help to understand the failure mechanism of the produced pCBT and modified pCBT matrix composites.

6. Literature

[1] Jones W. D.: More heat, less sag [power cable upgrades]. IEEE Spectrum, **43**, 16-18 (2006).

[2] Central Intelligence Agency: The world factbook. Langley, USA (2011).

[3] MSZ EN 50341-1: Overhead electrical lines exceeding AC 45 kV (in Hungarian)

[4] Varga A.: Grundlage des Elektrosmogs in Bildern. Verlag Umwelt + Medizin, Heidelberg (2002).

[5] Ginsztler J.: Applied materials science (in Hungarian). Műegyetemi Kiadó, Budapest (2005).

[6] Czvikovszky T., Nagy P., Gaál J.: Principles of polymer engineering (in Hungarian). Műegyetemi Kiadó, Budapest (2003).

[7] Geszti P. O.: Electrical power systems 1 (in Hungarian). Tankönyvkiadó, Budapest (1983).

[8] Budnik K., Machczynacuteski W.: Contribution to studies on calculation of the magnetic field under power lines. European Transactions on Electrical Power, **16**, 345-364 (2006).

[9] Beale I. L., Pearce N. E., Conroy D. M., Henning M. A., Murrell K. A.: Psychological effects of chronic exposure to 50 Hz magnetic fields in humans living near extra-high-voltage transmission lines. Bioelectromagnetics, **18**, 584-594 (1997).

[10] Billings M. J., Nellist B. D., Swarbrick P.: Investigation into new designs for h.v. insulators using synthetic materials. Proceedings of the Institution of Electrical Engineers, **113**, 1643-1648 (1966).

[11] Cherney E. A.: Non-ceramic insulators - a simple design that requires careful analysis. IEEE Electrical Insulation Magazine, **12**, 7-15 (1996).

[12] Sarmento M., Lacoursiere B.: A state of the art overview: composite utility poles for distribution and transmission applications. in 'Transmission & Distribution Conference and Exposition: Latin America, 2006. TDC '06. IEEE/PES. 1-4 (2006).

[13] Dutt V., Lacoursiere B.: Composite utility poles: advances in design, materials and manufacturing. in 'Transmission and Distribution Conference and Exhibition, 2005/2006 IEEE PES. Dallas, USA' 1243-1243 (2006).

[14] Alawar A., Bosze E. J., Nutt S. R.: A hybrid numerical method to calculate the sag of composite conductors. Electric Power Systems Research, **76**, 389-394 (2006).

[15] Alawar A., Bosze E. J., Nutt S. R.: A composite core conductor for low sag at high temperatures. IEEE Transactions on Power Delivery, **20**, 2193-2199 (2005).

[16] Murday J. S., Dominguez D. D., Moran J. A., Lee W. D. Eaton R.: An assessment of graphitized carbon fiber use for electrical power transmission. Synthetic Metals, **9**, 397-424 (1984).

[17] Payan S., Le Petitcorps Y., Olive J. M. Saadaoui H.: Experimental procedure to analyse the corrosion mechanisms at the carbon/aluminium interface in composite materials. Composites Part A: Applied Science and Manufacturing, **32**, 585-589 (2001).

[18] VISCAS Corporation: Technical presentation on special conductors. Tokyo (2005).

[19] 3M Corporation: 3M Aluminium Conductor Composite Reinforced^{TM} (ACCR) technical summary. St. Paul, Minnesota, USA (2010).

[20] Beisele C., So S. K. S: Recent developments on epoxy materials for power transmission & distribution applications. in 'INMR 2011 World Congress. Seoul, Korea' 1-15 (2011).

[21] Composite Technology Corporation: Corporate brochure. Composite Technology Corporation, Irvine, California, USA (2004).

[22] Hiel C., Korzeniowski G.: Aluminum conductor composite core reinforced cable and method of manufacture. US. Pat. No.: 7.060.326 (2004).

[23] Hiel C., Korzeniowski G.: Aluminum conductor composite core reinforced cable and method of manufacture. US. Pat. No.: 7.368.162 (2008).

[24] Burks B., Armentrout D. L., Kumosa M.: Failure prediction analysis of an ACCC conductor subjected to thermal and mechanical stresses. IEEE Transactions on Dielectrics and Electrical Insulation, **17**, 588-596 (2010).

[25] Burks B. M., Armentrout D. L. Baldwin M., Buckley J., Kumosa M.: Hybrid composite rods subjected to excessive bending loads. Composites Science and Technology, **69**, 2625-2632 (2009).

[26] Newell J. A.: Carbon fibers. in 'Encyclopedia of polymer science and technology' (ed.: Mark H. F.) John Wiley & Sons, Inc., New York, 91-112 (2004).

[27] Koltai A.: Crimping technology - Project report. Hanford European LLC., Budapest (2011).

[28] Donaldson S. L., Miracle D. B.: ASM Handbook. Volume 21: Composites. ASM International, (2001).

[29] Kollár L. P., Springer G. S.: Mechanics of composite structures. Cambridge University Press, Cambridge (2003).

[30] Cooper W., Daly C., Demarteau M., Fast J., Hanagaki K., Johnson M., Kuykendall W., Lubatti H., Matulik M., Nomerotski A., Quinn B. Wang J.: Electrical properties of carbon fiber support systems. Nuclear Instruments and Methods in Physics Research Section A: Accelerators, Spectrometers, Detectors and Associated Equipment, **550**, 127-138 (2005).

[31] Chung D. D. C.: Carbon fiber composites. Butterworth-Heinemann, Newton, USA (1994).

[32] Morgan P.: Carbon fibers and their composites. Taylor & Francis Group, Boca Raton (2005).

[33] Zoltek Corporation: Panex brochure. (2010).

[34] Mitsui Plastics Inc.: Toray product catalog. White Plains, New York (1998).

[35] Bunsell A. R.: Fibre reinforcements for composite materials. Elsevier, Amsterdam (1988).

[36] Newell J. A., Puzianowski A. A.: Development of a pneumatic spreading system for Kevlar-based SiC-precursor carbon fibre tows. High Performance Polymers, **11**, 197-203 (1999).

[37] Vlasveld D. P. N., Bersee H. E. N., Picken S. J.: Nanocomposite matrix for increased fibre composite strength. Polymer, **46**, 10269-10278 (2005).

[38] Alexandre M., Dubois P.: Polymer-layered silicate nanocomposites: Preparation, properties and uses of a new class of materials. Materials Science and Engineering R: Reports, **28**, 1-63 (2000).

[39] Ebbesen T. W., Lezec H. J., Hiura H., Bennett J. W., Ghaemi H. F., Thio T.: Electrical conductivity of individual carbon nanotubes. Nature, **382**, 54-56 (1996).

[40] Thostenson E. T., Ren Z., Tsu-Wei C.: Advances in the science and technology of carbon nanotubes and their composites: A review. Composites Science and Technology, **61**, 1899-1912 (2001).

[41] Potts J. R., Dreyer D. R., Bielawski C. W., Ruoff R. S.: Graphene-based polymer nanocomposites. Polymer, **52**, 5-25 (2011).

[42] Geim A. K., Novoselov K. S.: The rise of graphene. Nature Materials, **6**, 183-191 (2007).

[43] Novoselov K. S., Geim A. K., Morozov S. V., Jiang D., Zhang Y., Dubonos S. V., Grigorieva I. V., Firsov A. A.: Electric field effect in atomically thin carbon films. Science, **306**, 666-669 (2004).

[44] Kim H., Abdala A. A., Macosko C. W.: Graphene/polymer nanocomposites. Macromolecules, **43**, 6515-6530 (2010).

[45] Gardiner G.: Thermoplastic composites: Primary structure? High Performance Composites, (2011).

[46] Steeg M.: Prozesstechnologie für Cyclic Butylene Terephthalate im Faser-Kunststoff-Verbund. PhD Thesis. Fachbereich Maschinenbau und Verfahrenstechnik, Technische Universität Kaiserslautern, Kaiserslautern (2009).

[47] Dubois P., Coulembier O., Raquez J.M. (eds.): Handbook of ring-opening polymerization. Wiley-VCH, Weinheim (2009).

[48] Brunelle D. J.: Ring-opening polymerization: mechanisms, catalysis, structure, utility. Hanser Publishers, New York (1993).

[49] Semlyen J.A., Semlyen E.R.: Cyclic polymers. Springer, New York (2001).

[50] Czigány T., Karger-Kocsis J.: Textile fabric-reinforced thermoplastic polyester composites. in 'Handbook of thermoplastic polyesters: Homopolymers, copolymers, blends and composites' (ed.: Fakirov S.) Wiley-VCH, Weinheim, 1133-1171 (2002).

[51] Ross S. D., Cobur E. R., Leach W. A., Robinson W. B.: Isolation of a cycle trimer from polyethylene terephthalate film. Journal of Polymer Science, **13**, 406-407 (1954).

[52] Brunelle D. J., Bradt J. E., Serth-Guzzo J., Takekoshi T., Evans T. L., Pearce E. J., Wilson P. R.: Semicrystalline polymers via ring-opening polymerization: Preparation and polymerization of alkylene phthalate cyclic oligomers. Macromolecules, **31**, 4782-4790 (1998).

[53] Brunelle D. J., Takekoshi T.: Process for preparing macrocyclic polyester oligomers. US. Pat. No.: 5.407.984 (1995).

[54] Bryant J. J. L., Semlyen J. A.: Cyclic polyesters: 6. Preparation and characterization of two series of cyclic oligomers from solution ring-chain reactions of poly(ethylene terephthalate). Polymer, **38**, 2475-2482 (1997).

[55] Bryant J. J. L., Semlyen J. A.: Cyclic polyesters: 7. Preparation and characterization of cyclic oligomers from solution ring-chain reactions of poly(butylene terephthalate). Polymer, **38**, 4531-4537 (1997).

[56] Hamilton S. C., Semlyen J. A.: Cyclic polyesters: 5. Cyclics prepared by poly(decamethylene terephthalate) ring-chain reactions. Polymer, **38**, 1685-1691 (1997).

[57] Hamilton S. C., Semlyen J. A., Haddleton D. M.: Cyclic polyesters: Part 8. Preparation and characterization of cyclic oligomers in six aromatic ester and ether-ester systems. Polymer, **39**, 3241-3252 (1998).

[58] Semlyen J. A., Wood B. R., Hodge P.: Cyclic polymers: Past, present and future. Polymers for Advanced Technologies, **5**, 473-478 (1994).

[59] Wood B. R., Hodge P., Semlyen J. A.: Cyclic polyesters: 1. Preparation by a new synthetic method, using polymer-supported reagents. Polymer, **34**, 3052-3058 (1993).

[60] Wood B. R., Joyce S. J., Scrivens G., Semlyen J. A., Hodge P., O'Dell R.: Cyclic polyesters: 2. Topological trapping experiments and theoretical studies. Polymer, **34**, 3059-3063 (1993).

[61] Wood B. R., Semlyen J. A., Hodge P.: Cyclic polyesters: 3. Attempts to prepare catenated polymers using polymer-supported reagents. Polymer, **35**, 1542-1548 (1994).

[62] Wood B. R., Semlyen J. A., Hodge P.: Cyclic polyesters: 4. Cyclics prepared by poly(decamethylene adipate) ring-chain reactions. Polymer, **38**, 191-194 (1997).

[63] Hodge P., Semlyen J. A., Harrison A. G.: Polyesters. US. Pat. No.: 5.756.644 (1998).

[64] Parton H., Baets J., Lipnik P., Goderis B., Devaux J., Verpoest I.: Properties of poly(butylene terephtalate) polymerized from cyclics oligomers and its composites. Polymer, **46**, 9871-9880 (2005).

[65] Wu C-M., Jiang C-W.: Crystallization and morphology of polymerized cyclic butylene terephthalate. Journal of Polymer Science Part B: Polymer Physics, **48**, 1127-1134 (2010).

[66] Pang K., Kotek R., Tonelli A.: Review of conventional and novel polymerization processes for polyesters. Progress in Polymer Science, **31**, 1009-1037 (2006).

[67] Cyclics Corporation: CBT160 - Product information. Cyclics Corporation, Schenectady, NY, USA (2011).

[68] Karger-Kocsis J., Felhős D., Bárány T., Czigány T.: Hybrids of HNBR and in situ polymerizable cyclic butylene terephtalate (CBT) oligomers: Properties and dry sliding behaviour. Express Polymer Letters, **2**, 520-527 (2008).

[69] Wu D., Zhou C., Fan X., Mao D., Bian Z.: Linear rheological behaviour and thermal stability of poly(butylene terephthalate)/epoxy/clay ternary nanocomposites. Polymer Degradation and Stability, **87**, 511-519 (2005).

[70] Moll A., Hildebrandt A., Lenhof H. P.: BALLView: An object-oriented molecular visualization and modeling framework. Journal of Computer-Aided Molecular Design, **19**, 791-800 (2005).

[71] Hakmé C., Stevenson I., Maazouz A., Cassagnau P., Boiteux G., Seytre G.: In situ monitoring of cyclic butylene terephtalate polymerization by dielectric sensing. Journal of Non-Crystalline Solids, **353**, 4362-4365 (2007).

[72] Tripathy A. R., Elmoumni A., Winter H. H., MacKnight W. J.: Effects of catalyst and polymerization temperature on the in-situ polymerization of cyclic poly(butylene terephthalate) oligomers for composite applications. Macromolecules, **38**, 709-715 (2005).

[73] Tripathy A. R., Farris R. J., MacKnight W. J.: Novel fire resistant matrixes for composites from cyclic poly(butylene terephthalate) oligomers. Polymer Engineering & Science, **47**, 1536-1543 (2007).

[74] Harsch M., Karger-Kocsis J., Apostolov A. A.: Crystallization-induced shrinkage, crystalline, and thermomechanical properties of in situ polymerized cyclic butylene terephthalate. Journal of Applied Polymer Science, **108**, 1455-1461 (2008).

[75] Mohd Ishak Z. A., Leong Y. W., Steeg M., Karger-Kocsis J.: Mechanical properies of woven glass fabric reinforced in situ polymerized poly(butylene terephtalate) composites. Composites Science and Technology, **67**, 390-398 (2007).

[76] Mohd Ishak Z. A., Gatos K. G., Karger-Kocsis J.: On the in-situ polymerization of cyclic butylene terephtalate oligomers: DSC and rheological studies. Polymer Engineering and Science, **46**, 743-750 (2006).

[77] Karger-Kocsis J., Shang P. P., Mohd Ishak Z. A., Rösch M.: Melting and crystallization of in-situ polymerized cyclic butylene terephtalates with and without organoclay: A modulated DSC study. Express Polymer Letters, **1**, 60-68 (2007).

[78] Mohd Ishak Z. A., Shang P., Karger-Kocsis J.: A modulated dsc study on the in situ polymerization of cyclic butylene terephthalate oligomers. Journal of Thermal Analysis and Calorimetry, **84**, 637-641 (2006).

[79] Lehmann B., Karger-Kocsis J.: Isothermal and non-isothermal crystallisation kinetics of pCBT and PBT. Journal of Thermal Analysis and Calorimetry, **95**, 221-227 (2009).

[80] Kim T. W., Jun E. J., Um M. K., Lee W. I.: Effect of pressure on the impregnation of thermoplastic resin into a unidirectional fiber bundle. Advances in Polymer Technology, **9**, 275-279 (1989).

[81] Kendall K. N., Rudd C. D.: Flow and cure phenomena in liquid composite molding. Polymer Composites, **15**, 334-348 (1994).

[82] Abt T., Sánchez-Soto M., Illescas S., Aurrekoetxea J., Sarrionandia M.: Toughening of in situ polymerized cyclic butylene terephthalate by addition of tetrahydrofuran. Polymer International, **60**, 549-556 (2010).

[83] Baets J., Godara A., Devaux J., Verpoest I.: Toughening of isothermally polymerized cyclic butylene terephthalate for use in composites. Polymer Degradation and Stability, **95**, 346-352 (2010).

[84] Baets J., Godara A., Devaux J., Verpoest I.: Toughening of polymerized cyclic butylene terephthalate with carbon nanotubes for use in composites. Composites Part A: Applied Science and Manufacturing, **39**, 1756-1761 (2008).

[85] Baets J., Dutoit M., Devaux J., Verpoest I.: Toughening of glass fiber reinforced composites with a cyclic butylene terephthalate matrix by addition of polycaprolactone. Composites Part A: Applied Science and Manufacturing, **39**, 13-18 (2008).

[86] Brunelle D. J.: Method for polymerizing macrocyclic polyester oligomers. US. Pat. No.: 5.498.651 (1996).

[87] Dion R. P., Bank D. H., Beebe M. C., Walia P., LeBaron P. C., Oelberg J. D., Barger M. A., Paquette M. S., Read M. D.: Polymerized macrocyclic oligomer nanocomposite compositions. US. Pat. No.: 7.329.703 (2008).

[88] Bahr S. R., Pawlson J.: Process for making copolymers using macrocyclic oligoesters, and copolymers therefrom. US. Pat. No.: 7.745.651 (2010).

[89] Faler G. R.: Methods for converting linear polyesters to macrocyclic oligoester compositions and macrocyclic oligoesters. US. Pat. No.: 6.855.798 (2008).

[90] Labet M., Thielemans W.: Synthesis of polycaprolactone: a review. Chemical Society Reviews, **38**, 3484-3504 (2009).

[91] Tripathy A. R., MacKnight W. J., Kukureka S. N.: In-situ copolymerization of cyclic poly(butylene terephthalate) oligomers and ε-caprolactone. Macromolecules, **37**, 6793-6800 (2004).

[92] Wu C-M., Huang C-W.: Melting and crystallization behavior of copolymer from cyclic butylene terephthalate and polycaprolactone. Polymer Engineering and Science, **51**, 1004-1013 (2011).

[93] Baets J.: Toughening of in-situ polymerized cyclic butyleneterephthalate for use in continuous fiber reinforced thermoplastic composites. PhD Thesis. Faculteit Ingenieurswetenschappen Department Metaalkunde en Toegepaste Materiaalkunde, Katholieke Universiteit Leuven, Leuven (2008).

[94] Baets J., Devaux J., Verpoest I.: Toughening of basalt fiber-reinforced composites with a cyclic butylene terephthalate matrix by a nonisothermal production method. Advances in Polymer Technology, **29**, 70-79 (2010).

[95] Lanciano G., Greco A., Maffezzoli A., Mascia L.: Effects of thermal history in the ring opening polymerization of CBT and its mixtures with montmorillonite on the crystallization of the resulting poly(butylene terephthalate). Thermochimica Acta, **493**, 61-67 (2009).

[96] Berti C., Binassi E., Colonna M., Fiorini M., Zuccheri T., Karanam S., Brunelle D. J.: Improved dispersion of clay platelets in poly(butylene terephthalate) nanocomposite by ring-opening polymerization of cyclic oligomers: Effect of the processing conditions and comparison with nanocomposites obtained by melt intercalation. Journal of Applied Polymer Science, **114**, 3211-3217 (2009).

[97] Mäder E., Gao S-L., Plonka R., Wang J.: Investigation on adhesion, interphases and failure behaviour of cyclic butylene terephtalate (CBT)/glass fiber composites. Composites Science and Technology, **67**, 3140-3150 (2007).

[98] Parton H., Verpoest I.: In situ polymerization of thermoplastic composites based on cyclic oligomers. Polymer Composites, **26**, 60-65 (2005).

[99] Parton H.: Characterisation of the in-situ polymerisation production process for continuous fibre reinforced thermoplastics. PhD Thesis. Faculteit Ingenieurswetenschappen Department Metaalkunde en Toegepaste Materiaalkunde, Katholieke Universiteit Leuven, Leuven (2006).

[100] Tripathy A. R., Burgaz E., Kukureka S. N. MacKnight W. J.: Poly(butylene terephthalate) nanocomposites prepared by in-situ polymerization. Macromolecules, **36**, 8593-8595 (2003).

[101] Biron M.: Thermoplastics and thermoplastic composites: Technical information for plastics users. Butterworth-Heinemann, Oxford (2007).

[102] Sumerak J. E., Martin D. E.: Pultrusion. in 'ASM Handbook, Volume 21: Composites' (ed.: Donaldson S. L., Miracle D. B) ASM International, Ohio, USA, (2001).

[103] Luisier A.: In-situ polimerisation of lactam 12 for liquid moulding of thermoplastic composites. PhD Thesis. Départment des Matériaux, École Polytechnique Fédérale de Lausanne, Lausanne (2001).

[104] Luisier A., Bourban P-E., Manson J. A. E.: Reaction injection pultrusion of PA12 composites: process and modelling. Composites: Part A, **34**, 583-595 (2003).

[105] www.pultruders.com (November 2011.)

[106] www.substech.com (April 2011.)

[107] Bechtold G., Wiedmer S., Friedrich K.: Pultrusion of thermoplastic composites - New developments and modelling studies. Journal of Thermoplastic Composite Materials, **15**, 443-465 (2002).

[108] Wiedmer S., Manolesos M.: An experimental study of the pultrusion of carbon fiber-polyamide 12 yarn. Journal of Thermoplastic Composite Materials, **19**, 97-112 (2006).

[109] Miller A., Wei C., Gibson A. G.: Manufacture of polyphenylene sulfide (PPS) matrix composites via the powder impregnation route. Composites Part A: Applied Science and Manufacturing, **27**, 49-56 (1996).

[110] Sala G., Cutolo D.: Heated chamber winding of thermoplastic powder-impregnated composites: Part 2. Influence of degree of impregnation on mechanical properties. Composites Part A: Applied Science and Manufacturing, **27**, 393-399 (1996).

[111] Sala G., Cutolo D.: Heated chamber winding of thermoplastic powder-impregnated composites: Part 1. Technology and basic thermochemical aspects. Composites Part A: Applied Science and Manufacturing, **27**, 387-392 (1996).

[112] Sala G., Cutolo D.: The pultrusion of powder-impregnated thermoplastic composites. Composites Part A: Applied Science and Manufacturing, **28**, 637-646 (1997).

[113] Haffner S. M., Friedrich K., Hogg P. J., Busfield J. J. C.: Finite-element-assisted modelling of a thermoplastic pultrusion process for powder-impregnated yarn. Composites Science and Technology, **58**, 1371-1380 (1998).

[114] Parasnis N. C., Ramani K., Borgaonkar H. M.: Ribbonizing of electrostatic powder spray impregnated thermoplastic tows by pultrusion. Composites Part A: Applied Science and Manufacturing, **27**, 567-574 (1996).

[115] Ramani K., Woolard D. E., Duvall M. S.: An electrostatic powder spray process for manufacturing thermoplastic composites. Polymer Composites, **16**, 459-469 (1995).

[116] Woolard D. E., Ramani K.: Electric field modeling for electrostatic powder coating of a continuous fiber bundle. Journal of Electrostatics, **35**, 373-387 (1995).

[117] Luisier A., Bourban P. E., Månson J. A. E.: Initiation mechanisms of an anionic ring-opening polymerization of lactam-12. Journal of Polymer Science Part A: Polymer Chemistry, **40**, 3406-3415 (2002).

[118] Arkema Incoporated: FASCAT 4101 Catalyst - Product Information. (2011).

[119] XG Sciences, Inc: Technical Data Sheet - xGnP Graphene Nanoplatelets - Grade H. (2011).

[120] Yokouchi M., Sakakibara Y., Chatani Y., Tadokoro H., Tanaka T., Yoda K.: Structures of two crystalline forms of poly(butylene terephthalate) and reversible transition between them by mechanical deformation. Macromolecules, **9**, 266-273 (1976).

[121] Bragg W. L.: The Diffraction of Short Electromagnetic Waves by a Crystal. Proceedings of the Cambridge Philosophical Society, **17**, 43-57 (1913).

[122] Szebényi G.: Development of fiber and nanoparticle reinforced hybrid composites. PhD Thesis. Department of Polymer Engineering, Budapest University of Technology and Economics, Budapest (2011).

[123] **Balogh G.**, Czigány T.: Effect of low UD carbon fibre content on mechanical properties of in situ polymerised cyclic butylene terephtalate. Plastics, Rubber and Composites, **40**, 121-124 (2011).

[124] **Balogh G.**: CBT as a novel matrix material and its processing techniques for composites. in 'SPE Eurotec Conference. Barcelona, Spain' p. 1-5, online proceeding (2011).

[125] Radusch H.-J.: Poly(Butylene Terephthalate). in 'Handbook of thermoplastic polyesters: Homopolymers, copolymers, blends and composites' (ed.: Fakirov S.) Wiley-VCH, Weinheim, 389-419 (2002).

[126] Lum R. M.: Thermal decomposition of poly(butylene terephthalate). Journal of Polymer Science: Polymer Chemistry Edition, **17**, 203-213 (1979).

[127] Levchik S. V., Weil E. D.: A review on thermal decomposition and combustion of thermoplastic polyesters. Polymers for Advanced Technologies, **15**, 691-700 (2004).

[128] Park C-S., Lee K-J., Kim S. W., Lee Y. K., Nam J-D.: Crystallinity morphology and dynamic mechanical characteristics of PBT polymer and glass fiber-reinforced composites. Journal of Applied Polymer Science, **86**, 478-488 (2002).

[129] Wunderlich B.: Thermal analysis of polymeric materials. Springer, New York (2005).

[130] Persenaire O., Alexandre M., Degée P., Dubois P.: Mechanisms and Kinetics of Thermal Degradation of Poly(ε-caprolactone). Biomacromolecules, **2**, 288-294 (2001).

[131] Garozzo D., Giuffrida M., Montaudo G.: Primary thermal decomposition processes in aliphatic polyesters investigated by chemical ionization mass spectrometry. Macromolecules, **19**, 1643-1649 (1986).

[132] Li M., Jeong Y. G.: Preparation and characterization of high-performance poly(trimethylene terephthalate) nanocomposites reinforced with exfoliated graphite. Macromolecular Materials and Engineering, **296**, 159-167 (2011).

[133] Kim J. Y.: The effect of carbon nanotube on the physical properties of poly(butylene terephthalate) nanocomposite by simple melt blending. Journal of Applied Polymer Science, **112**, 2589-2600 (2009).

[134] Wu D., Wu L., Yu G., Xu B., Zhang M.: Crystallization and thermal behavior of multiwalled carbon nanotube/poly(butylenes terephthalate) composites. Polymer Engineering & Science, **48**, 1057-1067 (2008).

[135] Kim H., Macosko C. W.: Morphology and Properties of Polyester/Exfoliated Graphite Nanocomposites. Macromolecules, **41**, 3317-3327 (2008).

[136] Romhány G., Vigh J., Thomann R., Karger-Kocsis J., Sajó I. E.: pCBT/MWCNT nanocomposites prepared by in-situ polymerization of CBT after solid-phase high-energy ball milling of CBT with MWCNT. Macromolecular Materials and Engineering, **296**, 544-550 (2011).

[137] **Balogh G.**, Czigány T.: Design of a pultrusion device (in Hungarian). Gép, **60**, 3-6 (2009).

[138] http://www.variopumps.de/ (May 2011.)

[139] Gojny F H., Wichmann M. H. G., Fiedler B., Bauhofer W., Schulte K.: Influence of nano-modification on the mechanical and electrical properties of conventional fibre-reinforced composites. Composites Part A: Applied Science and Manufacturing, **36**, 1525-1535 (2005).

[140] MSZ EN 50189: Conductors for overhead lines - Zinc coated steel wires

[141] **Balogh G.**, Czigány T.: Cyclic butylene terephthalate (CBT) as a novel matrix material and its processing (in Hungarian). Műanyag és Gumi, **48**, 234-240 (2011).

[142] **Balogh G.**, Czigány T.: Effect of air humidity on the mechanical properties of in-situ polymerized cyclic butylene terephtalate matrix composites. Materials Science Forum, **659**, 1-5 (2010).

[143] **Balogh G.**, Hajba S., Czigány T.: Development of cyclic butylene terephtalate matrix graphene and carbon fiber reinforced hybrid composites (in Hungarian). Műanyag és Gumi, (accepted; in press).

[144] Kemény S., Deák A.: Design and evaluation of experiments (in Hungarian). Műszaki Könyvkiadó, Budapest (2002).

7. Appendix

Statistical analyses were performed according to Kemény [144].

Results of the static ILS test (Figure 76) are given in Table 13, and the ANOVA data are given in Table 14.

	Graphene content					
	0	0.1	0.25	0.5	0.75	1
Number of specimen (p_i)	5	5	5	5	5	5
Average result (x_i)	7.47	7.51	8.47	10.36	8.95	8.27
Deviation (s_i)	0.94	1.79	1.55	1.32	1.23	1.25

Table 13. Static ILS results

Similarity of variances was investigated by Cochran analysis. Test statistic value is 0.28 which does not exceed the critical value (0.44) so the variances are considered to be similar at $\alpha = 0.05$ confidence level.

Source of variation	Sum of squares	Degree of freedom	Variance	Trial value (F_0)
Between groups	28.51	5	5.70	3.03
Within groups	45.23	24	1.88	
Total	73.74	29		

Table 14. ANOVA table of the static ILS test

Since the test statistics value ($F_0 = 3.03$) exceeds the critical level of 2.62, the effect of graphene on the static interlaminar shear stress is significant at $\alpha = 0.05$ confidence level.

Results of the dynamic ILS test (Figure 77) are given in Table 15. Dynamic ILS results and the ANOVA data are given in Table 16. ANOVA table of the dynamic ILS test

	Graphene content					
	0	0.1	0.25	0.5	0.75	1
Number of specimen (p_i)	5	5	5	5	5	5
Average result (x_i)	5.96	6.08	6.31	4.98	4.64	4.47
Deviation (s_i)	1.083	0.686	1.54	0.32	0.37	0.31

Table 15. Dynamic ILS results

Similarity of variances was investigated by Cochran analysis. Test statistic value is 0.55 which exceeds the critical value (0.44) so the variances cannot considered to be similar at $\alpha = 0.05$ confidence level.

Source of variation	Sum of squares	Degree of freedom	Variation	Trial value (F_0)
Between groups	11.73	5	2.35	3.23
Within groups	17.40	24	0.73	
Total	29.13	29		

Table 16. ANOVA table of the dynamic ILS test

However, the F_0 value exceeds the critical value (2.62), effect of graphene cannot considered to be significant on the dynamic ILS properties due to the fail in Cochran analysis.